UNIVERSITAT POLITÈCNICA DE VALÈNCIA

UNIVERSITAT POLITÈCNICA DE VALÈNCIA

School of Industrial Engineering

Development of operating and pricing concepts for the V2G provision of an EV aggregator through a bi-level dynamic Stackelberg optimization

Master's Thesis

Master's Degree in Advanced Engineering in Production, Logistics and Supply Chain Management

AUTHOR: Strach, Daniel Maximilian

Tutor: Rodríguez Rodríguez, Raúl

ACADEMIC YEAR: 2023/2024

Diese Arbeit wurde vorgelegt am
Institut für Stromrichtertechnik und Elektrische Antriebe

Development of operating and pricing concepts for the V2G provision of an EV aggregator through a bi-level dynamic Stackelberg optimization

Masterarbeit

von
Daniel Strach

1. Prüfer: Univ.-Prof. Dr. Dirk Uwe Sauer
2. Prüfer: Prof. Dr. rer. nat. Egbert Figgemeier

Aachen, 09.08.2024

Erklärung

Ich, Daniel Strach, versichere, dass ich die vorliegende Arbeit - bis auf die Betreuung durch das Institut für Stromrichtertechnik und Elektrische Antriebe (ISEA) der RWTH Aachen - selbst und ohne fremde Hilfe angefertigt habe. Die benutzten Quellen und Hilfsmittel sind vollständig angegeben, Zitate sind kenntlich gemacht.

Aachen, 09.08.2024 _____

Diese Seite wird nicht mitgebunden und ist als separate Seite bei der Abgabe der Arbeit mit abzugeben.

Development of operating and pricing concepts for the V2G provision of an EV aggregator through a bi-level dynamic Stackelberg optimization

[09.08.2024]
Masterarbeit

Autor: Daniel Strach
Betreuende/r Mitarbeiter/in: Jingyu, Gong
Betreuender Professor: Univ.-Prof. Dr. Dirk Uwe Sauer

Arbeit außerhalb des ISEA angefertigt? - Nein
Wenn ja, wo?

Studienrichtung: Energietechnik M.Sc.

Sprache: Englisch

Vertraulichkeit:
☐ Diese Arbeit fällt unter eine Geheimhaltungsvereinbarung des ISEAs und beinhaltet vertrauliche Daten.
☐ Diese Arbeit steht unter erweiterten Geheimhaltungsvereinbarungen mit Dritten oder zum Schutz von Erfindungsrechten.

Stichworte:
Hier 5 – 10 Stichworte zur Arbeit angeben.

EV Aggregator	pricing concept
Vehicle-to-Grid	power price
Vehicle-to-Home	…….
Bi-level Optimization	…….
Stackelberg game	…….

Zusammenfassung:
Hier 5-8 Zeilen schreiben, die den Inhalt der Arbeit kurz zusammenfassen.
…….

Table of Content

List of Figures

List of Tables

1. Introduction

1.1 Motivation

The ongoing climate change, driven by human consumption of fossil resources, has necessitated a paradigm shift in energy production, distribution and consumption towards sustainable and green solutions. In this context, Germany has made a commitment to combat climate change, aiming to achieve carbon neutrality by 2045 [1]. Consequently, the country's power generation landscape is undergoing rapid transformation, with renewable energy contributing a significant 56 % share in 2023 and an ambitious target of 80 % set for 2030 [2,3]. This high penetration of renewable energy presents substantial challenges in stabilizing the electricity grid, due to the high intermittency and unpredictability of renewable generation profiles. Simultaneously, other sectors such as mobility are advancing at a slower pace. The mobility sector, who is responsible for 20 % of the total greenhouse gas emissions is currently missing their climate targets with only 4 % share of non-fossil-fueled vehicles in Germany [4]. The anticipated electrification is expected to impose additional demands and dynamics on the grid, pushing the urgency for innovative solutions to ensure the success of the energy transition. In this context, the concept of Vehicle-to-Everything (V2X) emerges as a particularly promising solution to leverage bidirectional charging. Just recently, several industry associations submitted together a roadmap for the ramp-up of bi-directional charging technologies to the German government, highlighting the current topicality and importance of that topic [5].

Given these circumstances, electric vehicles (EVs) spend over 96% of their time idle, representing a huge untapped potential to utilize the battery energy storage for flexibility provision [6]. Within V2X, EVs are integrated into the energy ecosystem through bi-directional charging and smart communication, offering rapid and efficient flexibility. Depending on the configuration of the ecosystems, V2X expands the utility of EVs beyond simple transportation, introducing new value streams. Among these, Vehicle-to-Home (V2H) and Vehicle-to-Grid (V2G) are the most prominent concepts. [7]

In the V2H configuration, EVs are connected to smart households, serving as additional home battery storage. This arrangement positions the EV owner as a so-called 'prosumer', capable of producing, storing, and consuming energy through the PV-household-EV setup. This setup enhances household energy self-sufficiency and self-consumption by storing surplus energy from solar photovoltaic (PV) systems during times of high production and low consumption. On the contrary, V2G integrates EVs into the electricity grid, where they serve as flexible asset for frequency stabilization and participation in spot market trading (SMT). Both concepts promote a decentralized grid while enhancing grid stability and thus facilitate the increased incorporation of renewables into the energy mix. Moreover, the additional revenue streams significantly strengthen the attractiveness of EVs and thereby accelerate the current stuttering electrification of the mobility sector. Previous studies indicate that combining both concepts

offers the greatest value for stakeholder including prosumers, encouraging to investigate both concepts in a combined manner [8].

Nevertheless, coordinating these services presents a highly complex task, that involves simultaneously maximizing revenue through value stacking, meeting EV owners' driving needs and minimizing battery degradation while adopting to the gird operational regulations. To accomplish this, specialized trading knowledge, including certificated EPEX trader and advanced bidding and optimization algorithms are needed [9,10]. Moreover, a single EV does not meet the minimum power capacity criteria for participation in the German balancing market [11]. Consequently, there is an inevitable need for an intermediary entity to aggregate multiple vehicles into a pool, thereby facilitating V2G access for single EV owners. This role is fulfilled by the EV aggregator (EVA), which coordinates the bi-directional charging operations and communicates between the energy markets and individual prosumers [10].

In addition to the operational complexities associated with service coordination at the flexibility and energy markets, a continuous competition with the individual prosumers interest takes place. This competition forces the EVA to craft a compelling business model that presents an attractive value proposition to prosumers, encouraging them to participate in the EV pool rather than choosing for individual V2H applications. Depending on the so generated price incentives, the prosumers adapt their consumption behavior and participation choice, which, in turn, impact the EVA's operations and strategy. Hence, it becomes extremely relevant to study the strategic interaction between EVA and prosumers through effective pricing concepts, while optimizing the EVA´s operation, taking into account the competition with V2H.

The Stackelberg game (SBG) theory covers this strategic market interaction and enables an effective investigation. Therefore, SBG describes the dynamics between a leading party, who initiates actions, and a following party, who responds to these initial actions. Both parties aim to optimize their respective objective functions in a selfish and uncooperative environment. Due to its hierarchical structure, a bi-level modeling approach is very promising for investigating this dynamic SBG. [12]

Within this thesis, a mathematical model for a dynamic Stackelberg bi-level optimization is presented. The bi-level model features an upper-level (UL) optimization representing the EV aggregator's profit maximization efforts and a lower-level (LL) optimization reflecting EV owners' cost minimization within individual V2H ecosystems. In doing so, this thesis aims to provide new insights into optimal operating and pricing concepts for the EVA.

1.2 Literature Research

In recent years, V2X topics have drawn significant attention from researchers due to their potential to contribute positively to the energy transition. This is evidenced by the raise of published research articles in this domain. Simultaneously, mathematical optimization models have become an important tool for deeply analyzing the deployment and impacts of V2X concepts. In that sense, [7] presents a mathematical model for maximizing the economic value of EVs through a multi-use value stacking approach, incorporating various applications such as self-consumption increase, peak shaving, frequency regulation, and SMT. The findings

indicate that deploying an EV fleet in multiple value streams significantly enhances the economic benefits, highlighting the flexibility and synergies among different applications. In addition, [8] explores smart charging strategies for EVs, focusing on prosumer systems and the involvement in Germany's balancing market. The outcomes highlight the economic and ecological benefits of integrating EVs with renewable energy sources and grid services, emphasizing the potential of smart charging to optimize energy use and support grid stability.

Although the concept of EVA is not new, it has seen a significant rise in research interest recently, covering areas such as optimal charging and coordination strategies and market participation strategies, bidding strategies, pricing concepts and integration of EVA into energy system [10,13]. The bi-level modeling approach, in particular, has been widely applied in EVA research, due to the relevance of Stackelberg game theory in energy trading and market appearance, which are prevalent topics for EVAs [12]. For instance, [14] examines EVA bidding strategies for optimal day-ahead reserve management, presenting a bi-level optimization model with a novel exact algorithm that aims to benefit all market participants. Regarding pricing strategies, [15] and [16] propose dynamic pricing schemes, including time-of-use (TOU) contracts, to achieve optimal coordination and load management via price incentives. [17] employs a reinforcement learning algorithm for quarter-hourly dynamic pricing models. These studies underscore dynamic pricing's effectiveness in demand management and its benefits for all stakeholders. Furthermore, [18] details a stochastic bi-level optimization model to improve EVA trading strategies across several markets by accounting for uncertainties in market prices and EV fleet characteristics. Similarly, [19] introduces a multi-period joint bidding and pricing strategy that incorporates a stochastic optimization approach to manage uncertainties in baseline load and a robust semi-dynamic traffic assignment model for estimating dynamic EV charging behaviors under variable charging prices. Finally, [20] discusses a bi-level optimization model for EVAs, aiming to develop pricing strategies that consider user response willingness and satisfaction. This approach seeks to minimize decision risks for EVAs in market participation, potentially reducing EVA income but enhancing user satisfaction overall.

Despite these extensive research activities, a significant research gap remains, to which this thesis aims to contribute. There is a need for research into a mathematical approach to explore the leader-follower interactions between the EVA and multiple private prosumers. At the same time, a model for optimizing the value-stacking of multiple value streams for V2G and V2H applications concurrently is missing. This model would provide valuable insights into the operations and pricing concepts of an EVA. To the best of the author's knowledge, no public framework currently exists that addresses the mentioned research objective. By addressing this gap, this thesis contributes an additional piece towards developing a more holistic understanding of the EVA.

1.3 Research Objective

Derived from the previously mentioned research gap, the overarching research target is formulated as follows: This thesis aims to investigate how a reasonable pricing concept for the EVA should be designed in a selfish and non-cooperative environment to create a compelling offer to the prosumer for participating in the V2G service while considering the competition with

individual V2H alternatives. A special focus is put on determining an appropriate dynamic power price the EVA can offer to the prosumer for providing their power. At the same time, this thesis presents an innovative model approach for an EVA with optimized value-stacking, considering energy arbitrage, balancing services, load shifting, and self-consumption increase of the household. In doing so, it will be investigated how the pricing concept influences the operation of the EVA and the behavior of the prosumer within a dynamic SBG. Therefore, an effective bi-level optimization model is developed to quantitatively model and evaluate the given situation within representative scenarios. These scenarios do not only make economic sense for the EVA but also consider the prosumers individual interest under consideration of the current technical and regulatory landscape. This novel approach provides a new perspective in the exploration of the EVA business model, thereby creating new insights in the development of reasonable pricing and operating concepts for the EVA.

To achieve this goal, the mathematical optimization model within this thesis will explore the leader-follower dynamics between EVA and prosumers. Therefore, the model is structured as a bi-level optimization, incorporating a mixed-integer-linear problem (MILP) in both levels. The rationale behind the choice of model comes from the hierarchical characteristics of a bi-level optimization as well as the already given FOCUS-framework by the RWTH Aachen, which serves as framework for the prosumer model [21]. By following this approach, the most efficient method to answer the derived research objective in an accurate and mathematical way is chosen, considering the limited resources of this master thesis.

Overall, this thesis aims to contribute to a more holistic understanding of an EVA and take a further step towards successful implementation in the German market. In the author's view, a comprehensive investigation of the EVA concept is crucial for the ongoing transition of the energy system towards a more flexible, smart, and interconnected system. In that sense, the underlying intention of this thesis is to positively contribute to the global energy transition. However, while the proposed modelling approach is designed to capture the key dynamics of EVA and prosumer interactions effectively, it is based on certain assumptions detailed in Chapter 3. The limitations and implications of these assumptions, as well as other constraints of the model, will be thoroughly examined in the evaluation to provide a balanced view of the study's contributions and areas for future research.

1.4 Outline

The thesis comprises five Chapters and is structured as follows: Chapter 2 provides the necessary theoretical background, covering the electricity market, balancing market, EV and different V2X ecosystems, as well as the basics of mathematical programming. Subsequently, Chapter 3 introduces the proposed bi-level modeling framework, designed to optimize the operation of the EVA and analyze its interaction with prosumers. Then, Chapter 4 evaluates the presented model based on representative scenarios. Based on the results of the scenarios, insights for the development of operating and pricing concepts of the EVA are derived. The work is finalized with a conclusion and outlook in Chapter 5.

2. Theoretical Background

As mentioned before, the EVA can unlock the flexibility potential of EVs, offering significant benefits to our energy system. For a more detailed investigation of the EVA concept, a basic understanding of underlying topics is required. This chapter aims to provide the required theoretical foundation for the subsequent development and evaluation of the bi-level optimization framework in the following Sections. Therefore, in the first Section the German electricity market is introduced and relevant ancillary services in the European balancing market are explained. Afterwards, the second Section discusses the concept of EV as multi-purpose decentralized flexibility assets, focusing on the technical EV battery system, the most important V2X ecosystems, as well as the generic concept of the EVA. Lastly, the third Section introduces the necessary fundamentals in mathematical programming, bi-level optimization, and Stackelberg game theory, which will be applied to build the optimization model.

2.1 German Electricity Market

The ongoing energy transition impacts all domains of the energy industry, including the electricity grid and market. As Germany transitions from fossil fuels to renewable energy sources, it faces a significant increase in volatility and decreased controllability on the production side. Simultaneously, rising electrification across various sectors generates greater electricity demand, thus placing higher loads on the grid. Additionally, the enhanced interconnectedness within the energy sector, through different energy carriers such as hydrogen, positions the electricity grid as a pivotal and central link in the energy transition. These trends greatly amplify the complexity and dynamics within the electricity sector, emphasizing the need for a more robust and flexible grid [22].

To cope with these changes in the energy sector, the traditional centralized grid setup, characterized by inputs from large-scale electricity producers at high voltage levels and outputs at low voltage levels for smaller consumers, is evolving. The grid is becoming more flexible, demand responsive and decentralized, incorporating smart digital solutions to effectively manage short-term fluctuations by exchanging data in real time among all stakeholders, and providing appropriate incentives for participants to adjust their consumption and production profiles by steering flexible assets. An essential part of this evolution are the concepts of V2H and V2G, which integrate the EV battery as a decentralized flexibility resource into the local or central energy system.

Understanding the broader environment and regulatory landscape surrounding these concepts is essential for their thorough investigation within this thesis. This includes acquiring a fundamental knowledge of the specific German electricity market. To comprehend the prosumer perspective, an overview of the mechanisms for price formation and the existing electricity tariffs in Germany is necessary. Furthermore, as an intermediary entity, the EVA operates within the energy market, necessitating a basic understanding of the mechanisms and regulations behind the most prevalent balancing services and trading platforms.

To provide the knowledge foundation, this Chapter is structured as follows: First, a detailed description of the German electricity market and structure is provided in Section 2.1.1, covering key stakeholders, trading and balancing mechanisms, as well as regulatory aspects. Subsequently, in Section 2.1.2, the resultant electricity price structures and tariff options for the prosumer are described, serving as important components for the later development of pricing concepts. Building on this comprehensive introduction, the subsequent Sections focus on the three prevalent value streams for V2G. Hence, SMT, FCR, and aFRR are explored in depth in 2.1.3, 2.1.4, and 2.1.5, respectively. These Sections focus on mechanisms for participation, remuneration schemes, and relevant regulatory considerations essential for the operation of an EVA.

2.1.1 Market Overview & Structure

Germany's electricity market, one of the largest and most dynamic in Europe, operates within a liberalized framework that fosters competitive interactions among various market segments. These segments encompass generation, wholesale trading, transmission, distribution. balancing and retail supply. All segments' functions are under the regulatory oversight of the Federal Network Agency (Bundesnetzagentur). [22,23] Figure 1 shows the structure of the Electricity market. The four German Transmission System Operator (TSO) and over 900 German Distribution System Operator (DSO) are responsible for operating the grid while ensuring the realization of the demand. Before realization of the demand, the energy is contractualized or traded through either the retail market or wholesale market. In this structured environment, the retail market serves residential, commercial, and industrial consumers, offering them the autonomy to select their electricity suppliers with customized agreements. Conversely, the wholesale market facilitates transactions among generators, traders, and retailers through a trading platform. [24]

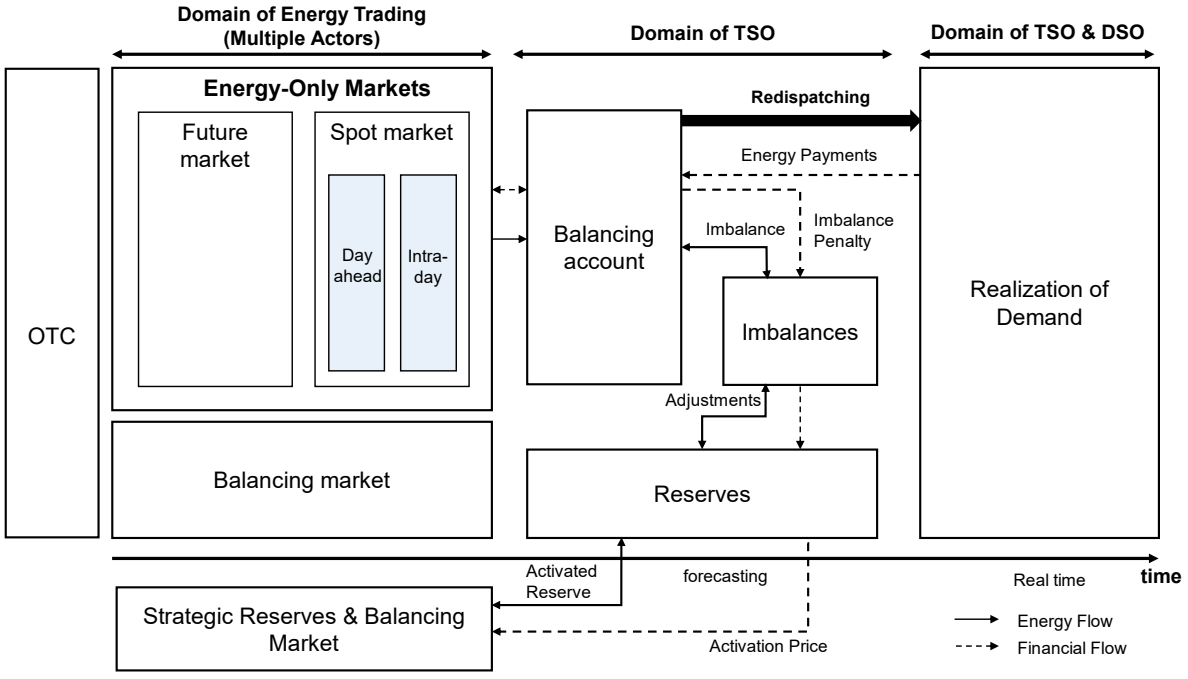

Figure 1: German electricity market structure and redispatch mechanism adapted from [25]

Within the wholesale market, two primary trading platforms exist: the Over-The-Counter (OTC) market and the exchange market. The OTC market is characterized by direct negotiations and trades between participants, bypassing a centralized exchange. This setup allows for greater flexibility in terms of pricing, contracts, and volume. On the other hand, the exchange market operates through a structured process where multiple participants submit bids and transactions are executed in a transparent and immediate manner. The exchange market can be divided into the futures market and the spot market. Futures market involve electricity being bought and sold from a few days up to six years ahead of delivery, while the spot market is where short-term transactions are immediately delivered. [24] The spot market trading mechanisms will be explained more detailed in Section 2.1.3. Germany hosts significant electricity exchanges such as the European Power Exchange (EPEX) SPOT, the European Energy Exchange (EEX), and Nord Pool, each playing a crucial role in the market's liquidity and efficiency [26].

To maintain the electricity grid´s operational integrity, the TSO implement grid balancing and redispatch measures. These actions are essential for stabilizing the grid frequency and thus avoiding system failures. Triggered by deviations between consumption and production, the reserved power capacity is activated by the TSOs. The deviations can occur due to fluctuations in consumption, unexpected changes in generation, bad forecasts and the failure of power plants or transmission lines. These balancing services are offered in a competitive marketplace for Balancing Service Providers (BSP), realized by the TSO´s public platform. There each BSP has a balancing account, which can generate imbalances, which in turn will trigger the reserves in the balancing services encounter the deviation in generation and consumption. [25]

The ancillary services are divided in five different types of balancing services as visualize in Figure 2. These differ mainly in terms of activation time and duration of use and are gradually replaced by each other to restore and maintain grid stability after a deviation. The instantaneous reserve (IR) is an inherent characteristic of the electricity supply system. The inertial from synchronous machines and thermal power plants prevents power differences from directly leading to critical frequency deviations [27].

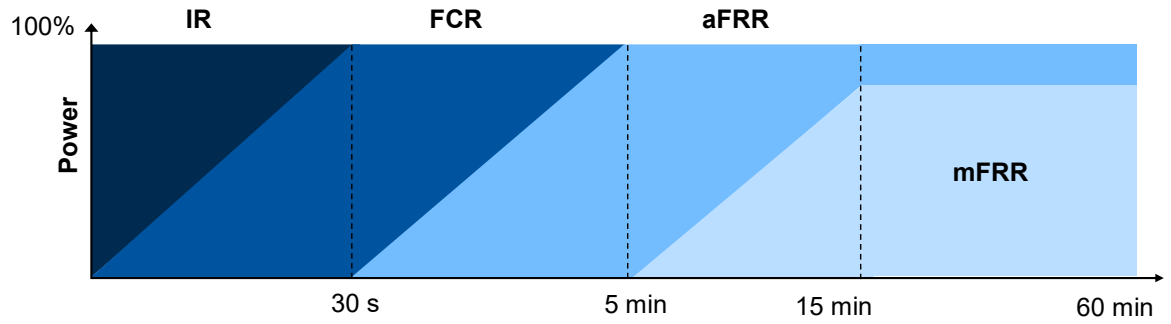

Figure 2: German balancing services by activation time adapted from [28]

Further, Frequency containment reserve (FCR), also known as primary reserve, is the fastest active compensation measurement, which needs to be in place after 30s. FCR is then gradually replaced by automatic frequency restoration reserve (aFRR), which in turn is then replaced by

manual frequency restoration reserve (mFRR) to stabilize the grid. [24] At the very last, depending on the TSO, restoration reserve can be activated to maintain grid frequency for long term. However, each of them has individual technical requirements defined by the Network Code on Load-Frequency Control of ENTSO-E [29].

Due to the rapid response capability of EV battery systems in adjusting their charging behavior, the most promising ancillary services for V2G are FCR and aFRR, as indicated in [7]. Therefore, this thesis will focus exclusively on these ancillary services for modeling purposes. They will be described in more detail in Sections 2.1.4 and 2.1.5.

2.1.2 Electricity Price & Tariffs

Between a customer and a supplier, several contract types may exist. For small-scale customers, the usual arrangement is a static tariff, setting a fixed price per energy unit consumed. In private households, energy consumption is often recorded by an analog meter, which the supplier checks annually. The customer's bill is then determined by their yearly energy consumption. However, if a household has a metering system that can track consumption in 15-minute intervals, known as a Smart Meter, it opens the possibility for more adaptive pricing models.

With a Time-of-Use (TOU) scheme, the price for energy usage varies over time, providing incentives to use energy during periods that are beneficial both for the grid and economically advantageous for the customer [30]. This price variation usually depends on the time of day and season, constituting a static TOU tariff. Days are segmented into different periods, each assigned a specific rate. Conversely, a dynamic TOU tariff adjusts prices for every 15-minute interval, reflecting wholesale market rates [31]. Although dynamic tariffs are standard for large industrial consumers, they are rarer for smaller consumers, also due to the absence of the necessary smart metering infrastructure. Smart meters facilitate the measurement of energy consumption in high temporal resolution, allowing suppliers to create a detailed consumption profile over time for each customer [31]. This also creates new tariff options for charging electric cars. So-called "car power" tariffs measure consumption using a separate smart meter and allow the DSO to throttle the power supply in the event of peak loads in the grid. In exchange, the DSO charges lower grid fees for charging the electric car. [32] However, smart metering systems are not yet widely deployed among private consumers in Germany, but their adoption is gradually increasing [5]. Consequently, it's plausible to anticipate that private households will be equipped with smart meters in future scenarios, especially in the assumed ecosystem of V2X.

Regardless of the tariff scheme, every electricity user must pay additional charges that depend on the supplier and regulatory expenses, such as taxes and levies. Table 1 outlines these components, providing average values for a private household in 2023. It's important to note that the actual costs may vary among different DSOs, consumer behaviors, household setups and from year to year. Given the current volatility in electricity prices, all values should be treated with caution.

Table 1: Composition of average electricity costs in Germany 2023 [33]

Component	Costs
Electricity procurement, sales and profit margin	23.59 ct/kWh
Grid fee (Netzentgelt) incl. measurements fee	9.35 ct/kWh
Other Levies and duties	2.985 ct/kWh
Electricity taxes	2.050 ct/kWh
VAT	19 % of the total price

The component of the electricity bill that suppliers can adjust encompasses charges for energy procurement, sales and their profit margin. On average, this accounts for 23.59 ct/kWh, representing 52 % of the total electricity price in 2023 [33]. These costs are further broken down into capacity and energy prices. However, for private households, the capacity price is of less significance, allowing it to be aggregated into an average overall price [34]. Depending on the specific TOU contract details, this portion may partially reflect the wholesale market electricity prices. Additionally, the TSO and DSO levies a net grid fee for grid operation and maintenance, amounting to 9.35 ct/kWh. Other charges and duties amount to 2.985 ct/kWh, covering Concession fees, the Combined Heat and Power Act (KWKG), Electricity Grid Charges Ordinance, offshore grid fees, and charges for disconnectable loads. [33]

Furthermore, the German government imposes an electricity tax of 2.05 ct/kWh, eligible for a refund on self-consumed electricity. Laslty, the German Value Added Tax (VAT) is applied at a rate of 19 % on the total summed costs. Consequently, the average electricity price for a private household in Germany in 2023 is calculated to be 45.19 ct/kWh. [33]

For prosumers, the feed-in tariff for solar PV-generated electricity is of great importance for the design and operation of the energy management of the smart house. With the abolition of the EEG surcharge as of 01.07.2022, the surcharge for the feed-in tariff for decentral generated electricity from solar PV was also reduced. For the partial feed-in of solar PV electricity, the average remuneration price in 2023 was 8.6 ct/kWh and 7.5 ct/kWh for peak power until 10 kWp and 40kW, respectively. [35]

2.1.3 Spot Market Trading

The concept of SMT or also known as arbitrage trading refers within this thesis to the systematical utilization of price spreads between buying and selling energy in the spot market. With a flexible storage asset, such as an EV battery system, these trades help to adjust power balances in the market and thus grid stability, while generating revenue or mitigating costs for traders. [7] At present, mobile energy storage systems used for V2G applications are systematically disadvantaged by double taxation of the stored energy. The recently submitted recommendation for action on bi-directional charging from the National Centre for Charging

Infrastructure called for mobile energy storage systems to be exempt from double taxation in the same way that stationary energy storage systems are currently exempt. [36] In this scenario, only the end consumer will have to pay the taxes and levies once. That change in regulations enables the possible participation of EVs in SMT. Therefore, in the following the market environment and mechanism for SMT are explained.

The spot market consists of the day-ahead and intraday markets, each serving unique functions and playing vital roles within the energy value chain. The day-ahead market primarily facilitates the secure trading of the majority of the produced or required electricity, while the intraday market allows for minor, short-term adjustments. [37] The Day-Ahead Market operates via a blind auction conducted daily throughout the year. In this auction, traders submit bids and offers for quarter, half, and full-hour segments for the following day, expressing their intent to buy or sell. Orders are accepted from 10:00 CET on the day preceding delivery, with all bids required to be consolidated in the shared order book before the Gate Closure Time at 12:00 CET. This includes specifying the delivery period, volume, and all price levels from the auction's minimum to maximum prices. [38]

The auction adheres to the principle of Market Clearing Price (MCP). Based on the ascending buy-orders, the Power Exchange constructs a demand curve, while the sell-orders form a descending supply curve, generating curves for each hour of the subsequent day, as shown in Figure 3. The MCP lies at the intersection of these curves. As a result of this order matching, the Power Exchange determines trades to purchase or sell a determined quantity of electricity to a defined delivery area for the matched MCP. The auction has the advantage of gathering liquidity at one point in time while offering full transparency on the traded Market Clearing Volumes. [38]

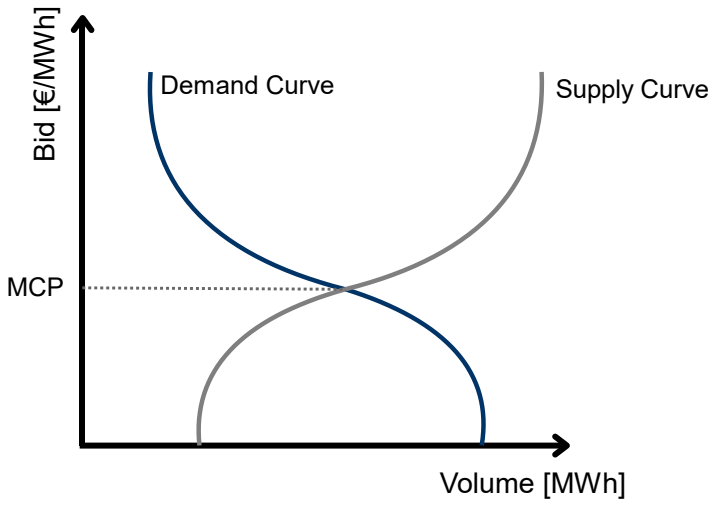

Figure 3: MCP principle

On the intraday market, market participants engage in continuous trading 24 hours a day, with delivery occurring on the same day. When a buyer and a seller match on a price, the trade is immediately executed. In Germany, electricity trading is possible until 5 minutes before delivery. Like in the day-ahead market, trading can be done using hourly, half-hourly, and

quarter-hourly contracts, along with block products. As mentioned, this market provides more flexibility, enabling traders to adjust their positions almost in real-time. During periods of low demand, prices can fall, potentially even below zero, on both the Day-ahead and Intraday markets. In such cases, producers must weigh the cost of shutting down plants against selling energy at a negative price. [38] This scenario happened in 2023 for over 300 hours on the day-ahead market and 1729 quarter-hours in the intraday market, offering a valuable opportunity for other traders. [39]

2.1.4 Frequency Containment Reserve

To ensure the proper functioning of electrical devices, the grid's frequency must remain stable around 50 Hz. A deviation exceeding 0.01 Hz triggers the deployment of the required balancing power. FCR is the fastest reacting frequency reserve in the balancing mechanism and thus is activated first. As of April 2024, Germany has reserved 564 MW of FCR power [40]. With the anticipated increase in volatile renewable energy generation, the demand for reserve power is expected to rise [7,41,42]. The transition to shorter service time slots in 2020 has made it possible for more flexible assets, including those with underlying multi-purpose concepts such as EVs, to participate in FCR provision [43].

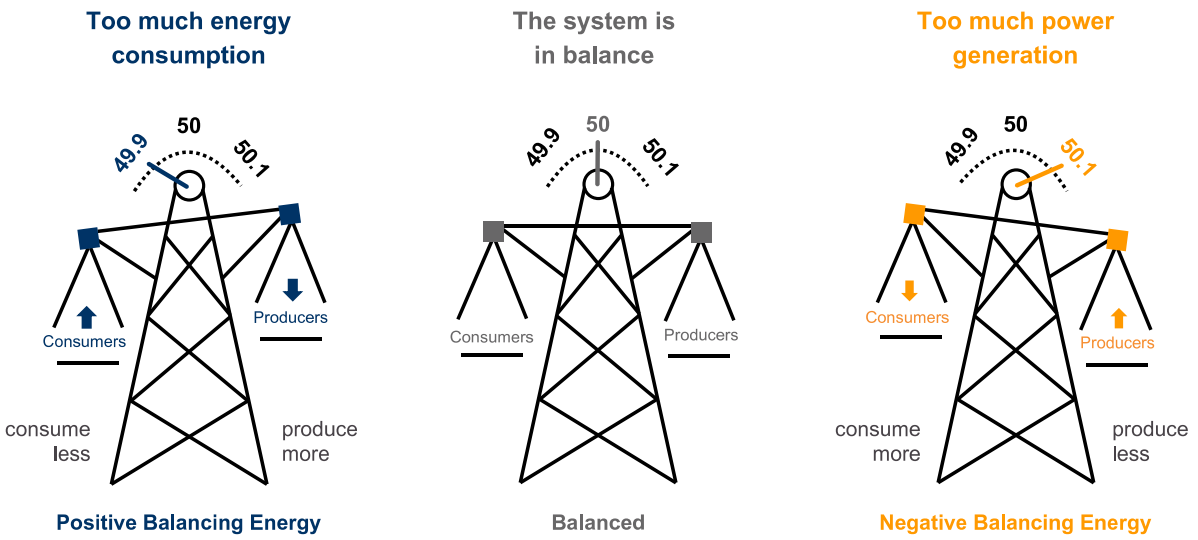

Figure 4: Grid frequency balancing principal adapted from [44]

FCR needs to be fully activated within 30 seconds and covers a period of 15 minutes. In the central European FCR market, ENTSO-E dictates a 4-hour product duration, adjusted for daylight saving time, requiring bids to reserve power in 4-hour intervals. The day is segmented into six 4-hour slots, starting from 00:00 to 04:00. TSOs allow a minimum bid size and resolution of 1 MW from BSPs. TSOs systematically procure the necessary FCR volume daily, initiating the bidding window seven days prior at 11:00 CET and concluding it a day before implementation at 08:00 CET. BSP bids are organized in ascending price order to form a merit-order list (MOL), prioritizing those that meet the demand at the lowest marginal costs. This process employs a marginal pricing mechanism, awarding all chosen bids at the MCP for their power reservation commitment. [45] If a BSP fails to deliver its reserved power, this is

considered as a breach of contract and penalties are imposed, depending on the severity of the non-delivery, the duration of the failure, and the current market conditions. [43]

FCR, being a symmetric product, allows for the simultaneous provision of both negative and positive power adjustments through the activation or deactivation of resources for BSPs. The compensation within FCR schemes is provided for the reserved power, rather than for the actual energy delivered as the power provided is equalized on average. [43] FCR resources often include assets like hydroelectric plants, gas turbines, and energy storage systems, due to their rapid response capabilities [46]. The emergence of aggregators as intermediaries between EVs and grid operators has facilitated the participation of EV owners in the ancillary services market by pooling resources to meet minimum bid sizes and compliance requirements.

2.1.5 Automatic Frequency Restoration Reserve

The aFRR belongs to the secondary frequency control activated by automated systems to address more significant frequency deviations when FCR capacity is insufficient. Unlike FCR, which responds almost instantaneously, aFRR has a maximum full activation time of 5 minutes and is designed to sustain its response for at least 15 minutes. This staged approach ensures a gradual restoration of grid frequency. [47]

In the aFRR market, the selection of bids is conducted via the MOL method. Different from FCR, in aFRR a pay-as-bid principle is applied for the power price where bids are compensated at their submission price if selected, while the energy bidding stays pay-as-cleared [48]. Also, power capacity and energy are traded distinctly with an additional separation in negative and positive bids for each. Thus, a participant can submit up to 4 bids for each 4-hour block. Power capacity bidding enables BSPs to commit a certain power capacity for durations specified in 4-hour blocks, with market gates opening seven days ahead at 00:00 and closing the day before delivery at 09:00. Thereby, the selection is based on the Merit-Order List of the bided price in €/MW, independent of the energy prices. Therefore, TSOs use historical data to forecast the expected power consumption and determine the required amount of capacity bids. Energy bids reflect the actual power delivery in case of activation. The minimum activation period is set at 15 minutes, with bids submitted from 12:00 CET the day before and closing 25 minutes before activation. Energy bids, priced in €/MWh, are compensated based on the actual delivery against the setpoint - a predetermined reference reflecting real-time frequency deviations. The bided energy price determines the selection of providers for delivering the energy. [49]

The demand of aFRR depends on the product type and time slot and can vary roughly between 1,600 MW and 2,000 MW in Germany on an exemplary week in April 2024. In addition the compensation price varies strongly even within a day. [40] This increases the complexity of aFRR market and shows the importance of advanced bidding strategies for optimized participation.

2.2 EV as Multi-Purpose Flexibility Asset

Over time the charging of EVs evolved from unidirectional uncontrolled charging to smart charging, and lastly to bi-directional intelligent charging, owning to technological advances [50]. Controlling the bi-directional charging of EVs unlocks the full flexibility potential of EV batteries. In [51], decentralized flexibility is described as "the ability of distribution-grid connected assets to shift or change their expected consumption or generation pattern in response to a signal".

To properly utilize this potential, it is essential to integrate the EV into an energy ecosystem and allow for smart data exchange to ensure a high degree of interconnectivity between all energy assets and participants within a favorable regulatory framework. This general concept is known as V2X, where X stands for any arbitrary configuration where the EV serves as mobile and decentralized flexibility within an energy ecosystem. Consequently, the EV is able to be integrated into multiple different energy ecosystems, such as vehicle-to-vehicle, vehicle-to-load, vehicle-to-home, vehicle-to-grid, etc. [52] The most prevalent concepts are V2H and V2G, as they will be described in more detail below.

All these concepts differ in individual system configuration and added value streams the flexibility of the EV is serving. However, the main purpose of the EV maintains the mobility provision. Additional value streams, where the EV owner benefits directly include the reduction of charging costs through increase in storing surplus energy, peak shaving, energy arbitrage or load shifting, and remuneration through participation in the balancing services. In addition, there are further non-financial value streams, such as stabilizing the grid, reducing grid congestion, emergency power supply, peer-to-peer energy trading, carbon-dioxide intensity reduction and mobile power supply for machinery & tools. [7]

For a comprehensive understanding of the concepts previously mentioned, a basic technical understanding of the EV battery system is essential. This brief elaboration is presented in the subsequent Sections 2.2.1. Following this, the two most promising concepts, V2H and V2G, are explained in more detail in the Sections 2.2.2 and 2.2.3, respectively. The focus is set on the configuration of the energy ecosystem and the additional value streams they offer. Finally, Section 2.2.4 describes the concept of an EVA as a pivotal entity for enabling the V2G concept to single EVs.

2.2.1 Electric Vehicle Battery System

The battery system is the core component of the EV, which enables the decentralized flexibility for the emerging concepts of V2X by storing and releasing electrical energy through chemical reactions. At the same time, the battery represents the most cost-intensive, sensitive, and complex component of the EV [53]. The operational management and system integration is predominant for an optimized usage of the battery over the whole lifecycle and applications.

To facilitate the effective implementation of V2X services, it is essential to equip EVs with durable batteries capable of sustaining many charging and discharging cycles [54]. Therefore, lithium-ion batteries are regarded as the most suitable for EVs due to its high energy density

and reliable stability, achieving the significant adoption in the individual automobile market [55]. Nonetheless, imperfections in the battery cause degradation thereby diminishing the lifecycle and available capacity over time [56]. This presents a significant challenge and serves as a crucial counterargument for V2X applications since additional cycles introduced by extra value streams can reduce the availability for the EV's primary mobility purpose. Main factors influencing battery lifespan include temperature, charge and discharge rates, state-of-charge (SOC) dwelling, and retention time [56]. However, [57] have demonstrated that strategically coordinated smart charging can maintain battery life near optimal levels despite the introduction of V2G services.

To integrate the EV battery in a V2X system, several systems for controlling the battery operations, chare and discharge flows and facilitate communication within the system are needed. The Battery Management System (BMS), serving as the "brain" of the EV battery system, is a control unit designed to maximize battery performance efficiently while ensuring system safety. The BMS interact with the batteries and the Energy Management System (EMS), maintaining battery operation within predefined voltage, temperature, and current ranges. Further, the EMS is a control system that is responsible for monitoring and controlling energy flow while charging and discharging. During charging, the EMS controls the power conversion system (PCS), which is an electrical power unit integrated in the electric vehicle charger (EVC) responsible for converting the voltage level of the current flow. Given the relatively low operation voltage of batteries due to the chemical characteristics of the cells, a PCS is essential for adjusting the voltage from charging stations to the battery's required level. [53]

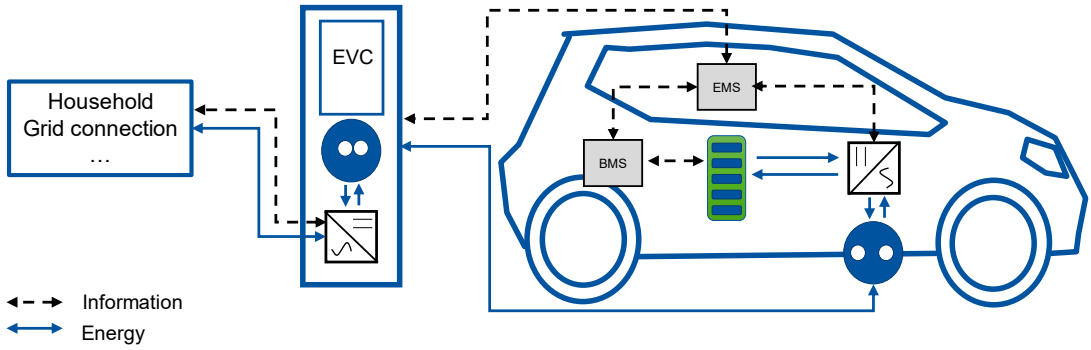

Figure 5: Simplified EV charging infrastructure

Lastly, bi-directional charging infrastructure is necessary to connect the EV with the grid, facilitating fast and efficient energy flow in both directions [54]. This infrastructure includes a bi-directional EVC for converting grid electricity to the appropriate voltage level for efficient charging and discharging. During converting and transporting the electricity, energy losses due to imperfections of the technical components need to be considered. Today charging efficiency range goes up to 95 %, depending on the technical component and power level [53]. The charging infrastructure spans an Alternating Current (AC) spectrum from Level-1 (up to 1.9 kW) and Level-2 (up to 19 kW) to Level-3 (up to 90 kW), and Direct Current (DC) fast

charging stations, each distinguished by its power output [58]. In a private household setup, the most common power outputs are 3.7 kW, 7.4 kW or 11 kW AC, due to the power connection of the household and obligation to register higher power outputs at the grid operator [59].

2.2.2 Vehicle-to-Home

V2H represents a forward-looking approach to decentralized energy management, integrating the capabilities of EVs with residential power systems to create a more sustainable, efficient, and resilient local energy ecosystem. At its core, V2H technology enables bi-directional energy flow between EVs and the home, transforming EVs into mobile energy storage units during idle times. This technology leverages the flexibility potential in EV batteries, which specially create value in combination with dynamic electricity tariffs, high purchase and feed-in price spread and energy surplus from power generation unit, such as solar PV. To realize this, an EMS in the smart home manages the energy flow between the power units in the household and allow constant communication through data exchange between the assets to control their operation.

While V2H supports a decentralized and flexible grid, it mitigates the load and intermittency to which the grid is exposed. However, from prosumer perspective there are primarily three value streams he benefits financially from [7]:

Load shifting. As the EV acts as a mobile energy storage unit, energy costs can be reduced through coordinated charging of the EV in combination with dynamic electricity tariffs. During periods of low energy prices, the EV stores energy which can be later released to meet the demand of household during times of high energy prices. This strategy diminishes exposure to high electricity prices, thereby lowering energy costs for the household.

Increasing self-sufficiency. In scenarios where energy production exceeds consumption, surplus energy, which would otherwise be fed back to the grid at minimal compensation, can be stored in the EV and discharged later to cover the consumption needs with the self-sourced energy. In doing so the self-sufficiency is enhanced. Here, self-sufficiency is defined as the ratio of self-produced and consumed energy to the total consumed energy [60]. Given that electricity feed-in tariffs are generally lower than supply prices, storing surplus energy in the EV represents the more cost-efficient and sustainable option. This assumes the absence of other home battery storage solutions.

Peak power shaving. Lastly, for households incur costs based on the maximum power demand within the billing period. To reduce these peak power costs, the EV can supplement the energy supply during periods of extremely high load, thereby lowering the peak power demand. This concept, known as peak power shaving, leads to savings on electricity bills for the owner. However, since these effects are relatively low in a private household setting, this aspect is not considered in this thesis.

Despite the numerous benefits for the EV owner and other stakeholders in the grid, a widespread adoption of this technology has not yet realized. This is primarily due to infrastructure and regulatory challenges that need to be addressed. [36] From infrastructure

perspective, a smart meter, bi-directional EVC and EMS of the household is required to enable V2H. This infrastructure remains prohibitively expensive for private applications, such that the financial benefits do currently often not offset the high investment costs associated with setting up a single EV [61].

2.2.3 Vehicle-to-Grid

With the raising share of renewables, the electricity grid becomes more volatile, necessitating flexibilities to compensate for these fluctuations and maintain stable grid frequency. Within the concept of V2G, the EV is connected via a bi-directional charging station to the grid, functioning as a decentralized flexibility for storing and releasing of energy in a smart manner. Thereby, V2G supports the system operators to stabilize the grid and promote a more sustainable electricity mix. Unlike V2H, where the EV is connected to a microgrid and serves as flexibility solely for the local energy system, V2G integrates the EV into the broader electricity grid, enabling direct communication and interaction with the system operators, who are responsible for balancing the grid.

In the literature, the V2G concept is often referred to as the evolutionary step following V2H, as it can extend the functionalities of V2H [50]. Therefore, it can be considered a complementary technology to V2H, enabling participation in the electricity market through SMT and ancillary services such as FCR and aFRR. From a utility perspective, there are numerous economic benefits from V2G. These include ancillary services such as energy balancing, active and reactive power support, valley filling, peak shaving and load following for stabilizing and increasing resilience of the grid. Further, V2G can replace large-scale energy storage systems for balancing services, provide integration support for renewable energy sources and reduce electricity transport losses in grids with promotion of decentralized generation. Additionally, the savings in utility operations will minimize the overall service cost to customers, which will be reflected in energy prices. [54] From EV owner perspective, additional financial or energy-based remuneration can be generated through energy arbitrage and participation ancillary services.

These different value streams create competition among these, especially for balancing services that require the reservation of power output and input, precluding the service of other value streams during this reservation period. A reasoned assessment of each value stream at every moment becomes crucial to optimize operation and maximize cost savings. [18] This underscores the need for an intermediary entity, which will be explained in more detailed in the next Section.

However, several system requirements are needed for a seamless operation of V2G services. An EMS is required for allowing effective load management, distinguishing between critical and non-critical loads and ensuring energy prioritization. Further, a robust communication network is required that facilitate data exchange between EVs, charging stations, and the grid [62]. Real-time monitoring and management of energy flows is essential by smart metering infrastructure, which supports dynamic pricing and demand response strategies. Lastly, the entire V2G ecosystem's interoperability, security, and safety are underpinned by clear

regulatory guidelines and standardized protocols. More details for the technical requirements can be found in [54].

While the potential benefits of V2G transition have been widely recognized, they may not come without significant challenges. One significant concern is battery degradation, as the frequent charging and discharging cycles with large depth of discharge (DOD) required by V2G operations can accelerate degradation on EV batteries, potentially shortening their lifespan and necessitating more frequent replacements [57]. Energy conversion losses also present a hurdle, with efficiency losses occurring at various stages of energy transfer between the grid and the EVs, leading to less effective use of the stored energy. Additionally, the impact on the distribution system cannot be overlooked; the integration of EVs into the grid introduces complexities in load management and requires upgrades to existing infrastructure to handle new patterns of energy demand and supply. [54]

2.2.4 Electric Vehicle Aggregator

A single EV faces two major hurdles in participating in V2G services on its own. First, the minimum bid size of 1 MW power capacity does not allow a single EV to participate in ancillary services [11]. Second, a single EV lacks the necessary capabilities to participate in the electricity market profitably [10]. Complex forecasting and mathematical optimization models are required, along with constant real-time communication with the TSO [10]. Because of this, an aggregation agent is needed to simplify the interactions between the EV owner and the electricity system, making it accessible for the private EV owner. Thus, the concept of an EVA emerges as an intermediary entity between the EV owners and the energy market, who aggregates multiple EVs into a pool and manages their operations. Thereby, the EV pool aggregation can enable significant benefits by compensating for individual weaknesses.

Figure 6 illustrates the EVA's interaction with the EV owner and energy market, visualizing data, financial, and energy flow. The main responsibility of the EVA is to manage market participation and commercialization, schedule charging and discharging, and purchase electricity for vehicles. For the EV owner, the EVA acts as a service provider, taking responsibility for the flexibility potential of the EV and, therefore, financially and energy wise compensating them. From the energy market perspective, the EVA is considered as a virtual power plant, aggregating and managing decentralized flexibilities and participating as one in the energy market.

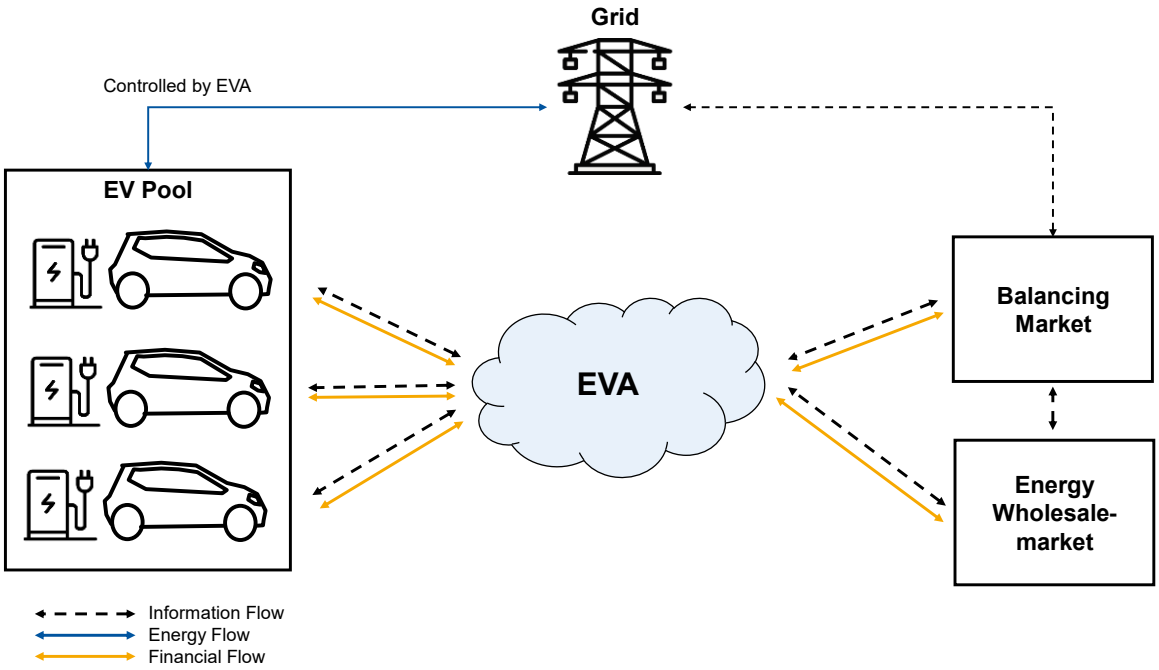

Figure 6: The concept of EVA as intermediary entity between EV pool and energy markets

The operations of the EVA include managing the fleet to meet the customers' driving demands while optimizing revenue through V2G services in the electricity market. In a household setup, this can also include consideration of V2H services for cost reduction. Assessing the different value streams is a highly complex task, due to future reservations for balancing services and energy trading. Therefore, the EVA needs to forecast market prices as well as the driving profiles of its fleet. However, the EVA faces high level of uncertainty when performing in highly uncertain market conditions and due to the uncertain nature of fleet characteristics. Hence, the EVA is motivated to become more involved in intraday and balancing markets that are closer to real-time. [18] Optimizing the fleet composition can also have significant positive effects on the behavior and forecasting reliability of the fleet [63].

The underlying business model of the EVA is to exploits its EV fleet to maximize profits. The EVA's profit model is based on the revenue generated from energy trading and balancing services, subtracting the costs incurred for compensating EV owners for the use of their assets, and covering personnel and infrastructure expenses. [64] To enter in such a relationship, a compelling V2G tariff needs to be offered to the EV owner to accept the EV pool participation. The V2G tariff should lower the charging costs for the EV owner and include compensation for the utility loss of their batteries due to degradation when participating in V2G services [65]. For the services from EVs to be economically viable, the revenues must outweigh the cost compensation for the degradation of EV batteries. If this is not the case, then using EV batteries beyond supplying their motion needs does not make economic sense. [64]

2.3 Mathematical Programming

Mathematical programming plays a pivotal role in addressing large and complex problems within the energy sector and other engineering domains. This Chapter briefly dives into the underlying theories and methods of computational optimization that enable effective quantitative investigation within this thesis. The focus is on introducing only the important aspects of mathematical programming, which form the core foundation for understanding the issue and choice of solving approach of the problem.

Therefore, this Chapters sets the stage for the later in-depth description of the developed optimization model. The structure of the Chapter is as follows: after this first general introduction to mathematical programming, Section 2.3.1 describes the Stackelberg game theory and application for the real problem of an EVA. Afterwards, Section 2.3.2 provides all necessary theoretical background foundation needed for understanding the technical modelling approach of this thesis.

2.3.1 Stackelberg Game Theory

Stackelberg game theory (SBG), named after the German economist Heinrich Freiherr von Stackelberg [66], is a branch of non-cooperative game theory, extensively used in the literature due to its significance for investigating market participants interactions. It is a leader-follower game, in which there is a leader who sets his strategy first, and other players of the game become his followers, who adjust their strategies based on the strategies announced by the leader. [12] In this hierarchical setup, the leader has a strategic advantage by being the first mover, also called the Stackelberg leader [67]. SBG plays a crucial role in environments where individuals involved are rational and aim to optimize their individual payoff function. This model becomes particularly relevant in economics and decision-making scenarios where the actions of one entity preemptively influence the reactions of others.

Like non-cooperative games, SBG can also be classified as static and dynamic situations. In static SBG, players choose their strategies once, either simultaneously or in sequence, without any knowledge of the other player's strategies. Conversely, dynamic SBG allows players to refine their strategies over multiple instances. [12] This variation is often referred as stage-wise or sequential SBG, in which all players have full awareness of each other's strategies, with decisions made based on a comprehensive set of given information [68].

The theory’s applicability extends to various domains in science where participants interact. In the context of V2G services, Stackelberg game theory provides a framework for modeling the interaction between an EVA and EV owners, where participants act selfishly and rationally, aiming to optimize their own payoff functions. The EVA, acting as the leader, formulates strategic actions regarding energy pricing, charging, and discharging schedules. EV owners, as followers, adjust their behavior based on the aggregator’s offer, aiming to optimize their own benefits. This leader-follower dynamic facilitates an efficient distribution of energy resources and effective positioning of the EVA in the competitive market. Thereby, the EVAs objective is to maximize profits, while the EV owners’ goal is to minimize charging costs, all within the constraints of the electrical grid’s operational requirements.

The SBG solution allows the player to analyze their counterparts' outcomes and then optimize their payoffs in a non-cooperative environment. In other words, SBG provides hierarchical support in which complex problems are broken down into layers of sequential problems to find optimal solutions at each layer. As all the participants optimize their actions by considering the actions of other players, there exists a point when no one can further improve their actions; this point is called the equilibrium point. In non-cooperative games, it is referred to as the Nash equilibrium [69]. To reach a SBG solution, the optimization problem for the follower, corresponding to the decision announced by the leader, is determined using the backward induction method. Then, the optimization problem for the leader is solved considering the response function of the follower. [12]

2.3.2 Proposed Bi-level Optimization Method

Bi-level optimization is a sophisticated area of mathematical programming that involves a nested structure where one optimization problem (the "upper level") directly contains another optimization problem (the "lower level") as a constraint [70]. This method effectively captures hierarchical decision-making processes and is often incorporated in SBG. Both optimization problems can generally be characterized as either a linear problem or a non-linear problem. The latter requires exponentially more computation time and cannot guarantee a solution since traditional linear solving methods, such as the Simplex algorithm, cannot be applied. Especially for large-scale problems like those discussed in this thesis, it is highly recommended to design them not as NLPs to limit computation time. Additionally, an optimization problem can be designed as a continuous or discrete problem, with the latter involving binary or integer decision variables. These so-called Mixed-Integer Linear Problems (MILP) also require additional computation time typically using branch-and-bound solving methods. However, in this case, the computation time grows linearly, and finding a solution is still guaranteed. In this thesis, a bi-level optimization method is chosen to model the interaction between EV owners and EVAs, incorporating a MILP at both levels. Generally, an optimization problem consists of an objective function to minimize or maximize and a set of constraints, both including decision variables and constant parameters [70]. Certain variables from the UL are also the subject to the LL, which creates the nested structure. The generic mathematical formulation is as follows, with u notated variables for UL-Model and l notated variables for LL-Model: [70,71]

$$\max_{x_u \in X_U, x_l \in X_L} \quad F(x_u, x_l)$$

$$subject\ to$$

$$G_k(x_u, x_l) \leq 0,\ k \in \{1, \dots, K\}$$

$$x_l \in min(f(x_l): g_j(x_l) \leq 0, j \in \{1, \dots, J\})$$

$$with\ x_u, x_l \in \mathbb{Z}^p, \mathbb{R}^q$$

Solving bi-level optimization problems is generally challenging due to characteristics like non-convexity and the NP-hard nature of these problems. Solving approaches can be divided into

traditional methods and advanced metaheuristics. Traditional solving approaches typically address mathematically well-behaved bi-level problems, which assume linear or convex functions along with continuous differentiability and lower semi-continuity.[70] Common analytical solving methods for these include single-level reduction with Karush-Kuhn-Tucker (KKT) conditions, descent methods, penalty function methods, and trust-region methods [71]. However, due to the not well-behaved characteristics of the given optimization problem in this thesis, these approaches are not applicable. Especially, the large size and mixed integer variables do not allow most traditional solving approaches. However, more challenging bi-level problems are often addressed by applying metaheuristics, which effectively combine exploration and exploitation within the solution area. These approaches cannot guarantee the discovery of a global optimum and generally require intensive computational effort, but they can be very effective in finding a quick solution for complex problems.[71,72]

Due to the high complexity and unique characteristics of the bi-level optimization problem in this thesis, an individual solving approach is chosen. Here, the bi-level problem is reformulated as a single-level problem by replacing the LL-problem with its first-order condition results [71]. This results in a single-level mathematical program with equilibrium constraints, which is then iteratively solved by exploring the space of sensible solutions using the method of exhaustion. This approach guarantees to find the best applicable solution with reduced computational effort. The detailed solving approach is described applied to the model in Chapter 3.

Both levels of the bi-level problems are designed as single-level MILP problems, which are modeled in the Python programming language using the programming software VSCode [73]. Python is renowned for its simplicity and readability, featuring object-oriented programming that emphasizes code readability with its clean syntax [74]. The open-source software package Pyomo is used to formulate and solve the optimization problem within the model [75]. For solving these problems, the Gurobi-optimizer is taken, a state-of-the-art solver for mathematical programming. Gurobi is designed to exploit modern architectures and multi-core processors, utilizing the most advanced implementations of the latest algorithms.[76]

To further reduce the computational efforts for large-scale, time-dependent optimization problems, a commonly applied method is time decomposition. This technique involves splitting the large original model into smaller sub-problems that can be solved more efficiently. The method applied within this thesis is known as the rolling-horizon (RH) approach, a very common approach in energy modelling. Figure 7 illustrates the schematic process of an optimization problem decomposed by the RH approach. In the RH method, the total simulation horizon is divided into several sub-problems, each then solved sequentially over a smaller timescale of the horizon. After solving every small-scale horizon, only a part of the subsequent solutions is retained to ensure the accuracy of the decomposed solution. The left overlap secures the continuity and sufficient accuracy of the overall solution. [77]

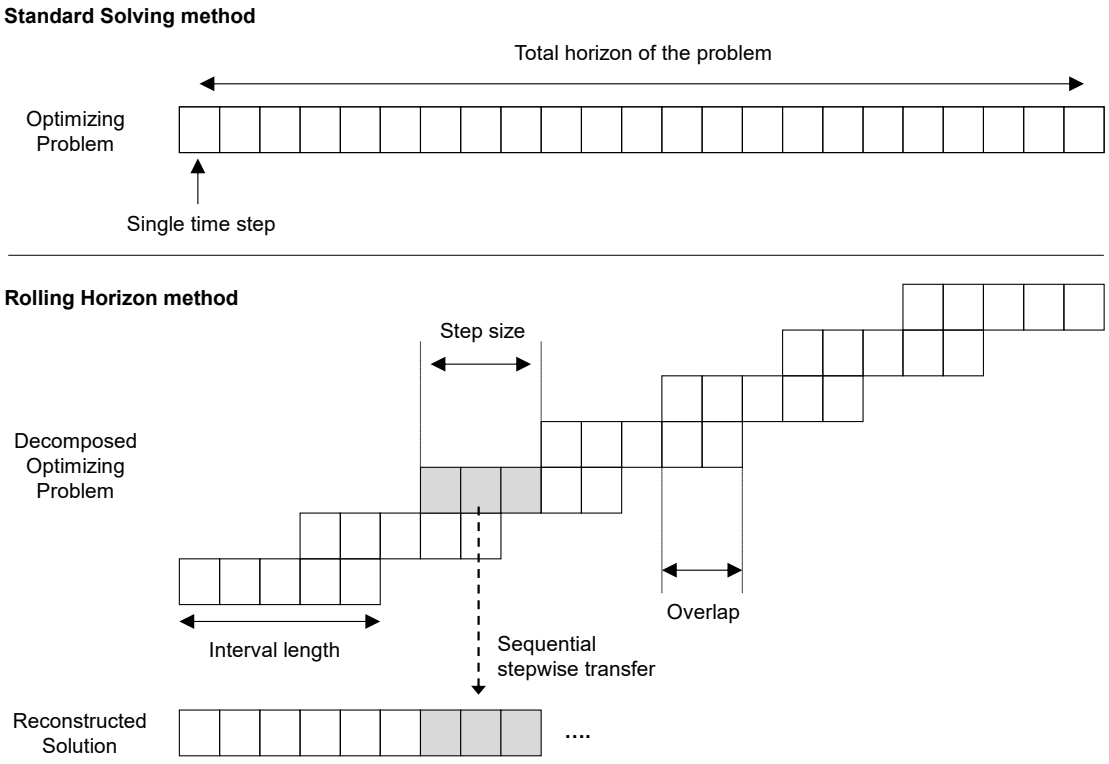

Figure 7: RH method adapted from [77]

3. Bi-level EVA Optimization Framework

This Chapter introduces the bi-level EVA optimization framework for modeling the operations of an EVA by managing a pool of EVs from private prosumers. The framework enables users to aggregate multiple EVs into a pool and participate in V2G services in the energy market, while considering complementary V2H applications for the prosumer. In addition, the bi-level structure of the framework simulates the recurring interaction between the EVA and the prosumer in a dynamic SBG to determine a reasonable compensation within a defined pricing concept. The evaluation of the model, which investigates the pricing and operating concepts of the EVA, will be conducted in Chapter 4.

First, the developed model design based on the facing problem situation as well as the solving approach is introduced in Section 3.1. Building on that, the model structure and class architecture are described in Section 3.2, followed by the program flow in Section 3.3. Chapter 0 describes then the framework configuration, the user is able to modify according to his needs. With these four Chapters in place, the necessary foundation is given to deep dive into the mathematical model description in Section 3.5. Here, the newly developed model equations and underlying model assumptions for the LL-Model, UL-Model and bi-level interaction are explained in detail. Lastly, a validation of the modelling method is conducted in Section 3.6 to verify the solving approach and modelling techniques used.

3.1 Framework Concept

The following Section 3.1.1 provides a detailed discourse into the problem situation of an EVA facing while approaching possible EV pool participants and planning its operations. Based on this, the model design is derived and rationale behind the choice of solving approach is explained in Section 3.1.2.

3.1.1 Problem Situation

To establish its EV pool, the EVA needs to present a compelling offer to prosumers to encourage their participation in the EV pool for V2G services. The decision of the prosumer has then a direct influence on the operations of the EVA, through the change in the EV pool configuration, which in turn, effects the offer. A decline of the offer may lead to a regeneration of the offer. This iterative negotiation process continues until both parties reach convergence in their respective objective functions, resulting in an accepted offer. If accepted, the prosumer will provide the EVC power and the EVA will compensate him accordingly. Figure 8 illustrates the given problem situation and the entanglement between pricing and operating concept.

First, several assumptions are made, when analyzing this situation. It is assumed that a prosumer registers once to be available for selection. Subsequently, both parties can dynamically decide at every decision time step, set at 4 hours to correspond with the reservation time for balancing services, whether to participate based on the current offer and conditions. The 4-hour period represents the smallest decision time step, facilitating the highest dynamics in the SBG framework. Both actors act in a selfish and uncooperative

manner, as part of the SBG. Hence, both actors aim for their highest benefits in this 4-hour decision period. It cannot be guaranteed how each actor will act in later time steps, since the decision is always made according to the current circumstances. Also, it is assumed to divide the power of the EVC to serve for V2H and V2G simultaneously and even allowing opposed energy flow. Further, the EVC is connected to the EVA through a dedicated grid connection and meter point. Thus, the EV battery represents the only flexibility in the system to which the EVA has access.

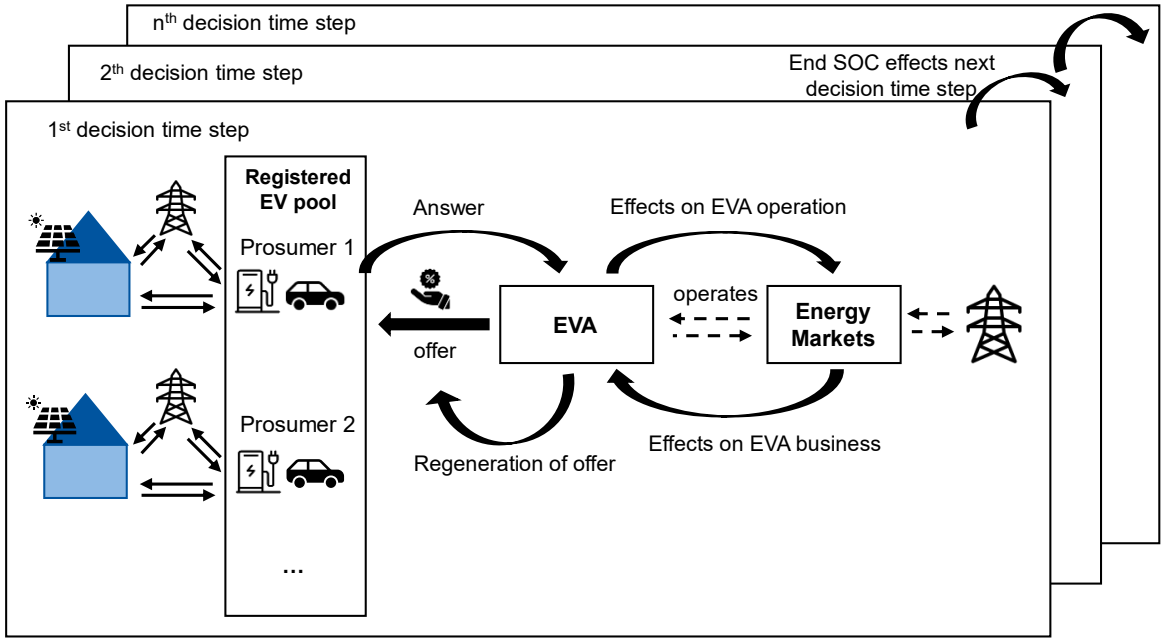

Figure 8: EVA offer generation process and entanglement with EVA operations

The pricing concept is a decisive component for the interaction process, which sets the rules and form of the offered V2G tariff. The offer includes the required power share from the EV charger together with a compensation according to the V2G tariff. Therefore, the compensation needs to be based on the power provided by the prosumer. Since the EVA does not own assets to store energy the pricing concept inevitably features an energy valuation for the energy exchange between EVA and prosumer. This is an essential component, which is decisive for the decision in EV pool participation and energy distribution. In addition, the agreement features that the EVA complies with the SOC requirements of the EV, set by the EV owner. This typically includes a limited SOC range for V2X usage as well as a minimum SOC at departure. It is assumed that the EVA is informed about the current SOC and SOC requirements as well as the availability of the EV.

Based on this situation, the deep entanglement between pricing and operational concepts of the EVA is revealed: First, the prosumer's decision has a direct influence on the available configuration, and thus on the operations of the EVA. Second, the V2G tariff inevitably includes an energy-based compensation component, which is directly tied to energy distribution and, consequently, the operations of the EVA. These interconnections result in a non-linear term in the objective function when attempting to solve it in a single-level model. This is caused by the generated profit is directly correlated with the power reserved for V2G multiplied by the

specified power price. A conventional non-linear single level model design would not be feasible given the size of the problem and the technical resources available. To address this challenge, a bi-level structure of the framework is chosen, which is going to be explained in the next Section. Through splitting the problem into multiple dedicated MILP problems, each problem can then be solved with less computational effort.

3.1.2 Model Design and Solving Approach

Figure 9 illustrates the design of the developed bi-level model. For each prosumer, a LL-Model is created, enabling V2H-only to reduce the electricity costs. The UL model builds around the EVA, incorporating the energy markets and the entire pool of prosumers. The rationale behind incorporating the entire pool of prosumers in the UL model, rather than just the EVs, is to enable an exact assessment of both technologies V2H and V2G at every moment. It is assumed that the prosumer must split the EVC power for every decision period to provide power for V2G and V2H services accordingly. This split is binding for the whole period of 4 hours. With this model setup the optimal operational plan, combining V2H and V2G is achieved. By doing so, the need for an outer loop to determine the optimal power division between V2H and V2G is avoided.

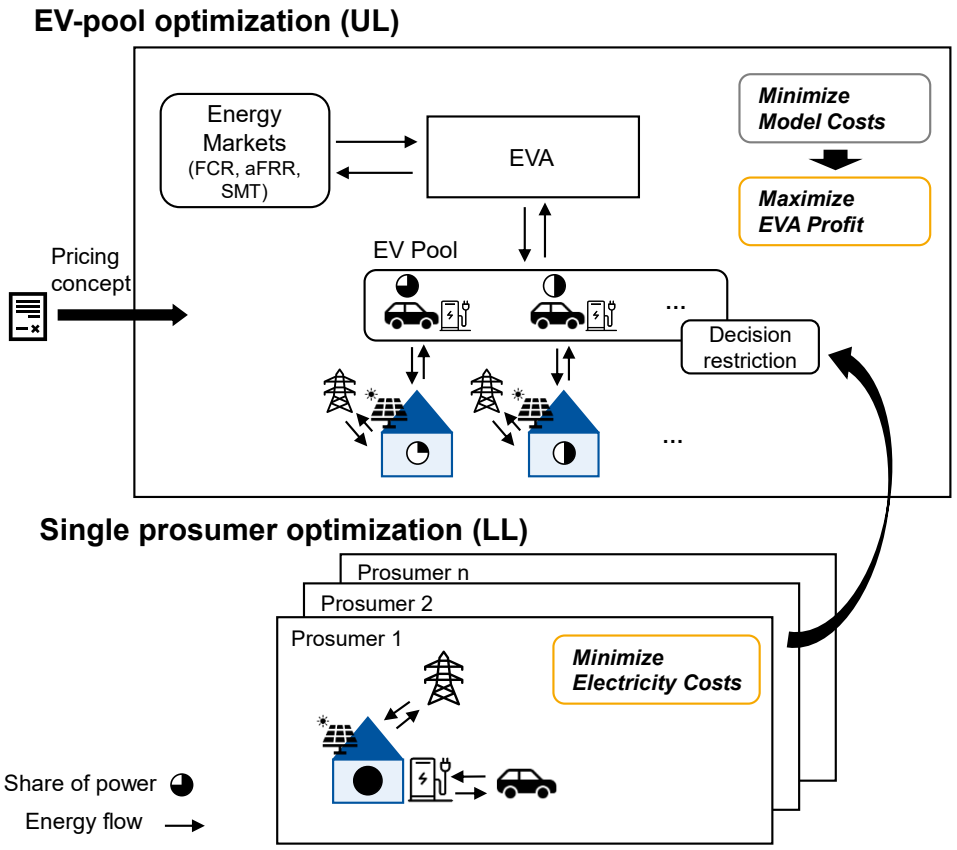

Figure 9: Bi-level optimization model design

This saves significant amount of computation time. As a result of this setup, the EVA will never reserve more power for V2G, than it would incur costs for the prosumer through less power

available for V2H. As this action would entail paying the prosumer more than what could be gained from such an action. This idea can be applied to a real-world scenario, where the EVA is aware of the prosumer detailed situation through advanced models and predictions.

However, the described model design calculates the optimal operation plan for a fixed pricing concept rather than optimizing the pricing concept itself. To analyze the pricing concept while optimizing operations, an additional external logic in the bi-level model is required to modify the pricing concept. Within this thesis, a self-developed method based on the reformulation method and an iterative solving approach is applied.

A widely known method for solving bi-level optimization models are the KKT conditions, as mentioned in Chapter 2.3.2. However, due to the complexity and size of the given optimization problem, these are not applicable. But the method works on the general principle of reformulating the bi-level problem into a single-level problem by solving one problem and transforming it into a constraint for the other problem [78]. This approach is known as reformulation method. Applying this method requires individual analysis and adaptation to the model, considering the problem design, restrictions, and limitations. Since the pricing concept for V2G is inherently multi-dimensional, only one parameter of the pricing concept can be optimized at a time through this method. Given the scope of this thesis, the focus will be on an exhaustive analysis of the power price, while analyzing certain designs of the energy exchange valorization, as described in more detail in Chapter 4.1.

The solving approach includes the reformulation of the bi-level model and iterative increase of the input power price parameter. Therefore, the reformulation separates the LL-Model from the UL-Model by putting the outcome of the LL-Model as a restriction for the UL-Model. More precisely, a cost-value function for each prosumer is defined and determined in the LL-Model for the V2H-only case for every decision period, as it will be described mathematically in Chapter 3.5. This cost-value serves as a threshold within the UL-Model for the internal decision function of each prosumer. The decision function decides whether the prosumer accepts or declines the offer. The assumption behind that is, that the prosumer will accept the offer as soon as it is more economical beneficial for him than the V2H stand-alone case. Incorporating this decision logic as a restriction within the UL-model avoids the need for an external determination process of whom to choose for pool participation, which combination of values streams is the best and how to distribute the energy as part of the compensation. These decisions will be done within the model calculation as part to optimize the objective goal. Therefore, this integration significantly reduces computational time.

By doing so, the optimal operation plan for a fixed power price can be calculated, considering the competition between V2H and V2G in the EV pool. When incrementally increasing the power price and recalculating the UL-Model, the results yielding the highest profit for the EVA are selected, and the process moves to the next timestep. The detailed program-flow for the solving process is explained in Chapter 3.3.

However, this approach achieves only a solution that is nearly optimal for determining the power price dimension of the pricing concept, due to the discrete steps of the power price. Consequently, the solution's quality primarily depends on the chosen step size and the maximum number of increments, as explained below.

Figure 10 shows an illustration of the relation between profit and V2G power price during piecewise increase. Point 1 on the graph shows the profit of the EVA when setting no power price and relying solely on compensation through energy. As the power price increases, the profit gradually declines. Bend points may occur, such as at Point 2, indicating a shift in the operational plan due to the higher power price. An upward jump in profit occurs when a prosumer is convinced to join the EV pool, signaling a positive reply from the decision function in the model. This increase in the pool's power capacity can cause a significant rise in profit when the bid size limit for balancing services is reached, as shown at Point 3. By endlessly raising the power price, the profit will reach zero, meaning no V2G services are provided anymore. The power prices c_1 and c_2 represent two discrete power price steps. It is observed, that these steps do not achieve the maximum possible profit, indicated at Point 4. Although this deviation from the optimal solution is unavoidable, it is considered sufficiently minor compared to the total profit achieved by the EVA. Hence, a step size of 0.01 €/kW*h with a maximum of 9 increments up to 0.09 €/kW*h is recommended in order to not compromise the quality of the solution.

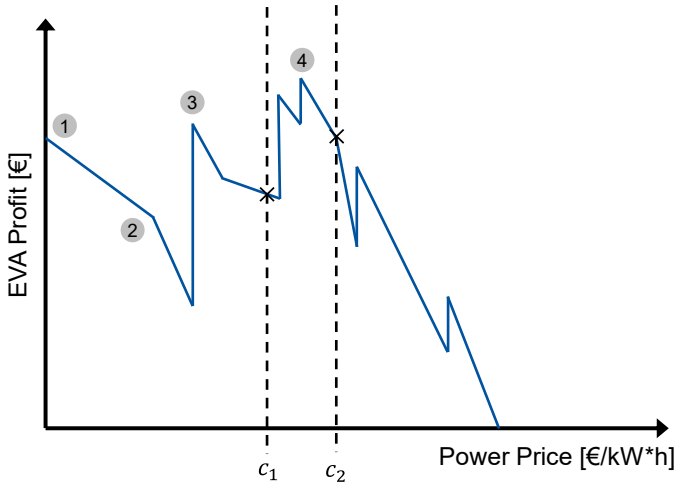

Figure 10: Relation of EVA profit and discrete power price increases

3.2 Framework Structure

Building upon the previously described framework concept, this Section provides an overview of the layout design and architecture developed within the framework. Therefore, Section 3.2.1 presents the technical model layout, including relevant components and energy flows. Then, Section 3.2.2 explains the class architecture used for building the python model.

3.2.1 Model Layout

Figure 11 shows the layout design of the UL-Model, visualizing the physical energy flow between the components in the Model. The UL-Model incorporates multiple single prosumer models as indicated in the figure. One prosumer model is exemplary shown in detail. The

prosumer model corresponds to each LL-Model of the framework, leaving out the connection to the VirtualAggregator and inserting an individual EMS.

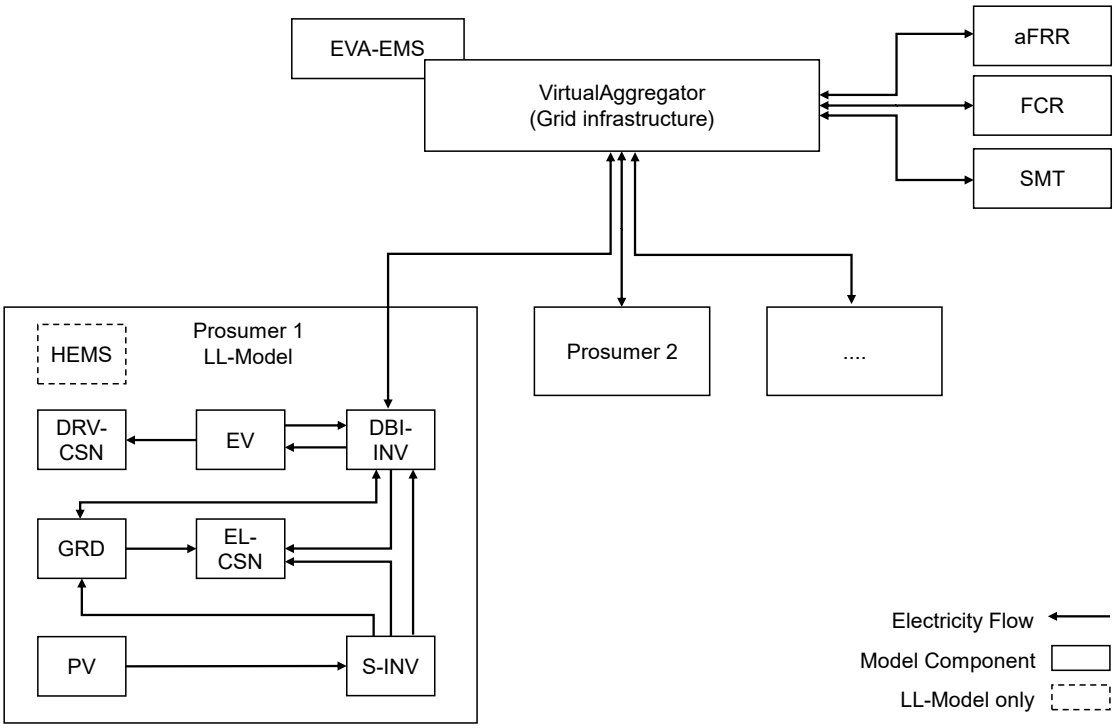

Figure 11: Overview model components and energy flow

In the LL-Model each prosumer is containing an individual Household-EMS (HEMS). Characterized by no energy flow connections, the HEMS component serves as superior component to implement the respective strategy and optimization goal. This contains defining the objective function and implementing general restrictions to comply with the model assumptions. Within the single prosumer the energy flow between the components is generally unidirectional, expect for the dynamic bi-directional inverter (DBI-INV), representing the EVC. Notably, that the driving consumption (DRV-CSN) and electrical consumption (EL-CSN) can just receive energy, since they represent the demand of electricity for the household or for the EV to be served. The component PV system is connected through a static unidirectional inverter (S-INV) to the EVC, electrical consumption and to the grid. The grid is designed as external source for electricity, able to purchase and sell electricity to.

Further, the UL-Model contains also a single EVA-EMS component, serving for the EVA to implement its strategy. The detailed functionalities of the EVA-EMS will be discussed in 3.5.2. In the UL-Model the prosumer´s have no HEMS but the rest of the structure remains identical as shown in Figure 11. Through the VirtualAggregator component, each individual prosumer is connected to the energy markets. This component allows simultaneous bi-directional energy flow from and to all connected components.

Thereby, it serves the model purpose to aggregator multiple prosumers into an EV pool. However, this component does not represent a real physical component since this would be

done by the existing grid infrastructure, as indicated in the model. On the other side of the VirtualAggregator are the energy market components connected, consisting of each a component for aFRR, FCR and SMT.

3.2.2 Class-Architecture

The model is built up on the existing FOCUS-Framework from the RWTH Aachen for modelling energy systems of prosumer, communities and cities [21]. Thus, the fundamental class structure and component design were adopted from the FOCUS framework for the purpose of this thesis. Figure 12 shows the underlying class architecture of the model. The implemented object-oriented class structure enables each object within a class to perform individual operations, providing an ideal environment for representing architectures with multiple individual actors as seen in the UL-Model. The EMS component, which is central to the prosumer, incorporates most logical implementations for the model objective and was thus mostly redesigned. Other components used in the model, have been extended and modified to meet the specific requirements of this model.

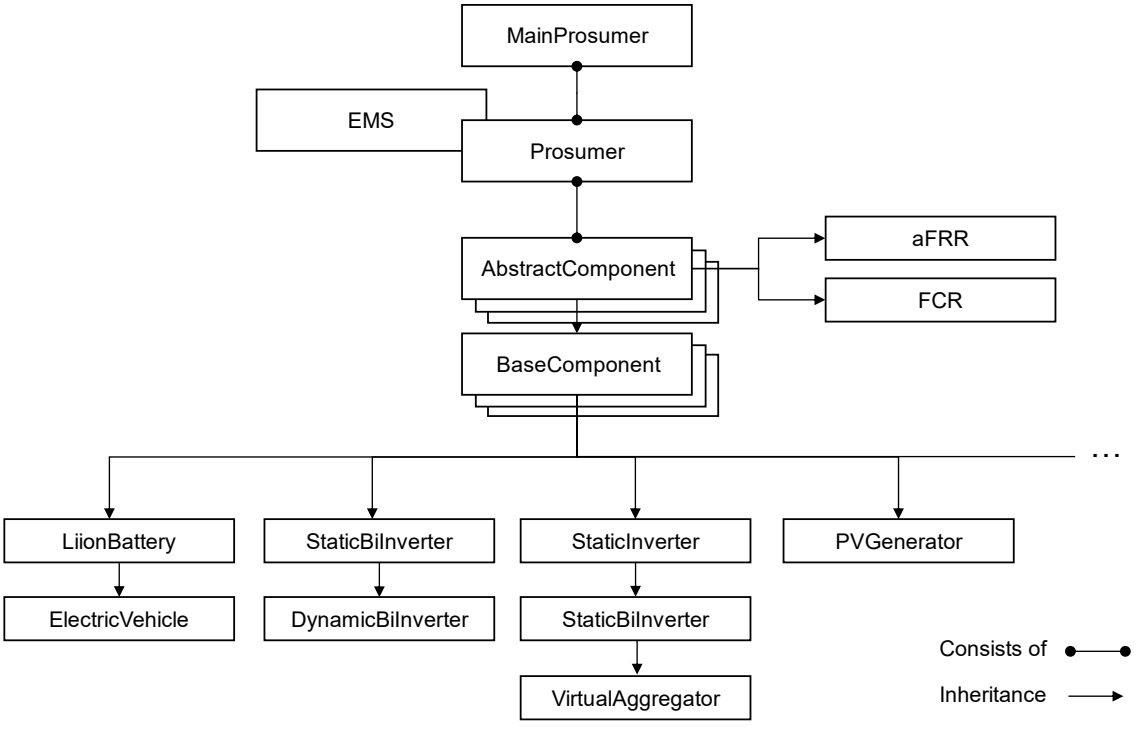

Figure 12: Class Architecture of the bi-level Model

The overarching class, `MainProsumer`, comprise one or multiple `Prosumer` classes and is responsible for optimizing the created prosumer model. The `Prosumer` class is the core of the optimization model, linking the components and energy flows in the model layout, and activating the EMS to achieve its individual objectives. In that sense, the EVA in the UL-Model is modeled by using a single `Prosumer` class but adapted component configuration, including all prosumers components. However, to efficiently model these components, an inheritance

structure is utilized. The class `AbstractComponent` forms the fundament for several basic component's classes, such as `BaseComponent`, `BaseGrid`, `BaseStorage`, `BaseGeneration`, and `BaseConsumption`. These components inherit standard functions primarily for modeling purposes, but also already first logical constraints for the respective component type. Then the basic component classes serve for advanced component classes such as `ElectricVehicle` or `DynamicBiInverter`.

3.3 Program Flow

For incorporating the dynamic interaction between the EVA and prosumers for price negotiations, while the EVA operations, a bi-level model design was developed, as outlined in Chapter 3.1. These two dedicated models are sequentially solved through a specified approach and interact within the simulation run via the exchange of input and output data. The RH method assists in decomposing an extremely large and complex energy modelling problem into serval smaller problems, while simultaneously enabling the dynamic decision steps for SBG. These aspects are integral parts of the framework and program flow as explained below. Figure 13 illustrates the program flow of the presented bi-level optimization framework.

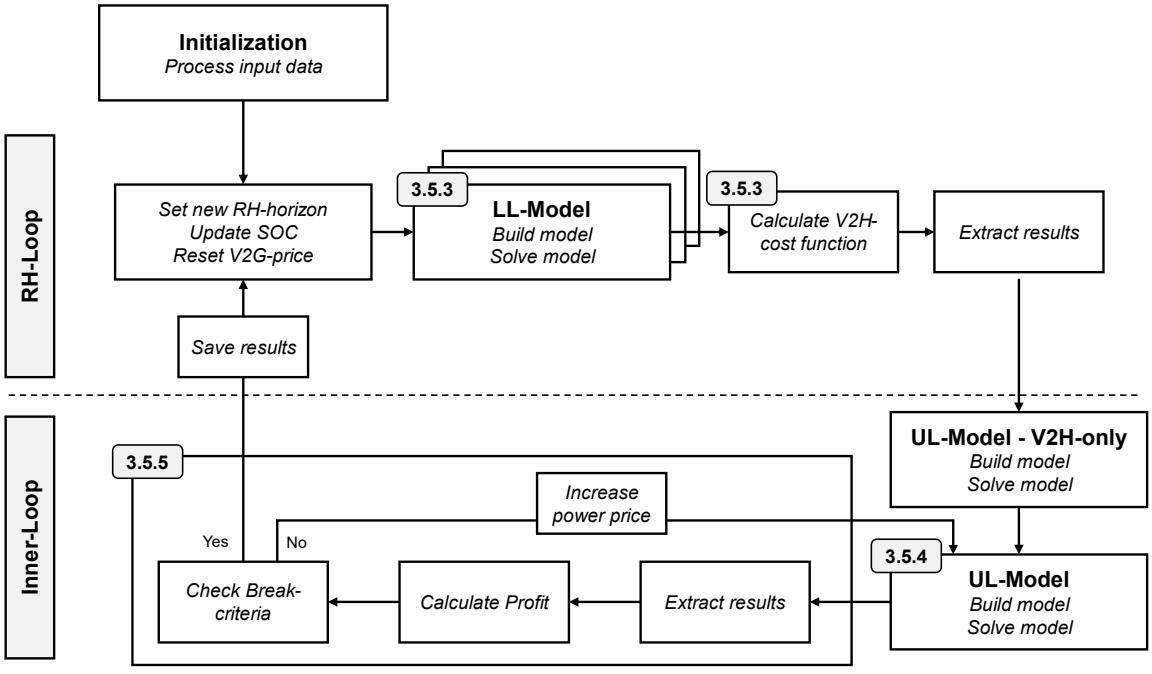

Figure 13: Program flow of the bi-level optimization

The program flow can be separated into two loops. The outer loop is responsible for implementing the RH method and establishing the dynamic decision process, while the inner loop determines the optimal power price within one decision time step. But before, an initialization step processes the input data and sets up the necessary variables for the bi-level interaction. Each iteration of the RH loop begins by setting the new time horizon, updating the input data as well as the SOC, and resetting the power price to zero. Subsequently, the LL-

Model is constructed and solved for each prosumer within the EV pool, serving as reference case. The V2H cost-value function is calculated to determine the economic value of the V2H-only case for the prosumer. Afterwards the inner loop starts to determine the optimal power price.

The inner loop starts by calculating the UL-Model in a V2H-only case. Due to the model design and RH method, some decision periods can result in an operation plan, which results in negative profit for this decision period. In that case, the model will take the V2H-only operation plan. Afterwards, the V2H cost value is given as input to the UL-Model, serving as a threshold for the internal decision restriction. With the fixed pricing concept and V2H cost-value function, the UL Model calculates the optimal operation plan for the EVA, considering the complementary use of V2H and V2G and the prosumer's decision to decline the offer. The results are then extracted, and the EVA's profit is calculated. During exhaustive search, the break criteria are assessed; if not met, the power price is incrementally increased, and the UL Model is resolved with the updated power price. The break criteria analyze the profit of the EVA, the availability and acceptance rate of the EV pool in order to prevent unnecessary iterations when no improvement in profit is expected anymore. The break criteria will be described in more detail in Chapter 3.5.3. When a break criterium is met, the optimal results are stored and selected for the next rolling horizon loop to update the SOC accordingly. A more detailed examination of the workflow within the individual models can be found in the appendix.

3.4 Framework Configuration

The framework is designed to be highly dynamic, allowing users to adjust a wide range of configurations. These can be accessed directly from the 'runme' script or be modified through the input data. Below, the key configurations essential for both general use and specifically for defining the EV pool are outlined.

Initially, it is crucial to establish the simulation's temporal parameters. This involves setting five key values:

- t_{start} specifies the start date of the simulation.
- t_{step} sets the smallest unit of time - resolution in hours - used for calculations.
- t_{total} determine the total number of time steps, defining the simulation's end date.
- $t_{horizon}$ defines the time steps for each RH calculation to implement the RH method.
- t_{roll} defines the overlap used for progressing through the simulation timeline.

In addition, a set of variables must be defined to adjust the solving approach and certain model assumptions. These variables are directly inserted into the 'runme' file. $Iter_{max}$ specifies the maximum number of iterations and, consequently, the maximum price increases undertaken by the solving approach. c_{price_add} represents the step size for increasing the power price per iteration. Further, the variable b defines the minimum bid size and bid size resolution for FCR and aFRR. Lastly, the value for c_{cycle} need to be defined. This value determines the costs

caused by additional cyclical aging of the battery for non-mobility applications, such as V2H and V2G.

Next, the configuration of the EV pool must be defined. Therefore, JSON files are required as input for each prosumer for the LL-Model and for the EVA in the UL-Model. These files specify the components, their sizing parameters, cost parameters, and connections between the components. Table 2 provides an overview of the relevant input parameters for defining the EV pool configuration for each prosumer n in the JSON file.

Table 2: Input parameters of the JSON file for model configuration

Parameter	***Sign***
Power Capacity EVC	$P_n^{EVC,max}$
Power Capacity PV	$P_n^{PV,max}$
Power Capacity PV Inverter	$P_n^{PINV,max}$
Battery Capacity	E_n^{max}
Electricity Procurement Price	c_p
Levy	c_l
VAT	c_{vat}
Electricity Injection Price	c_{inj}

For the initialization step of the program, input data must be defined. This data is typically provided as time-series data in CSV files. The necessary input files include:

Electricity demand: This includes all electrical loads within each prosumer's household, excluding EV charging. To accurately model EVA operations, it is advisable to use distinct profiles for each prosumer. The electricity demand time series may be sourced directly from existing data or generated artificially using the `DemandGenerator` tool within the framework. This tool generates representative profiles based on the standard load from the German Association of Energy and Water Industries (BDEW) [79]. The generator requires the annual demand for generating the time series data.

Driving profiles: The driving profiles contain the time-series data of the electricity consumption of the EV due to driving and specify the departure and arrival times. Such data can be generated artificially to ensure representative simulation, as detailed in Section 4.2.2. Besides the power load time series, this data should include an additional column marked '1' when the car is departing.

Weather data: This includes temperature and irradiance time-series data, which are essential for calculating the PV solar generation profile. It is important to use representative weather data in order to see accurate correlations between PV generation and electricity prices on the spot market.

Electricity prices: For the prosumer, time series data for electricity prices must be provided if a dynamic or TOU electricity tariff is used. Additionally, for the UL-Model the intra-day spot market data is required for enabling SMT. This dataset should contain only the raw procurement prices, as levies and taxes are automatically added in the model.

aFRR and FCR data: For modelling the participation in balancing services, input data of the according balancing market is required. This includes time series data for the FCR price, grid frequency, aFRR power price, aFRR energy price, and aFRR set point. While this data can be sourced online from [40], the aFRR set point is a specially developed dataset for modeling the participation in balancing services. Further details on this and the necessary data and processing steps are described in [21].

3.5 Mathematical Model Description

This Chapter dives into the mathematical model description, structured by first explaining the LL-Model in Section 3.5.1, followed by the UL-Model in Section 3.5.2, and finalizing with the bi-level interaction in Section 3.5.3. The focus is on explaining newly developed functionalities and components, which were created to serve the model's purpose. For more detailed information on the underlying FOCUS-Framework, please refer to [21] and [80]. To formulate the mathematical optimization model in the subsequent Sections, it is necessary to define the following sets:

- T: The time series with all time steps t over the total optimization horizon t_{total}.
- T_h: The time series for the current RH-step $t_{horizon}$. This results to $T_h \subset T$.
- T_r: The time series of the rolling horizon t_{roll}, which are taken into the next RH-step. This results to $T_r \subset T_h$.
- T_d: The set of decision time points of a RH-step $t_{horizon}$. For every t_{roll} in $t_{horizon}$ exists a t_d as decision point. The following equation (3.1) indicates this correlation. Consequently, the time points 00:00, 04:00, 08:00, etc. for each day are respective decision time points.

$$\boldsymbol{T_d = \frac{T_{horizon}}{T_{roll}}} \tag{3.1}$$

- $T_{out,n}$: The time series when the EV of the prosumer n is driving and thus not connected to the EVC.
- $T_{dep,n}$: The time series when the EV of the prosumer n is departing from the household.
- N: Containing all prosumers n of the EV Pool.

3.5.1 LL-Model

The LL-Model encompasses the single prosumer set-up with his household and at the same time builds a fundamental part of the UL-Model. A visualization of the components and flows was showed in Figure 11. The chosen prosumer setup reflects the minimum required setup for modeling consumption and production capabilities, combined with flexibility and driving constraints in the form of an EV. The model's challenge lies in managing both driving consumption and electrical consumption while minimizing total costs within the given constraints.

The `Energymanagementsystem` acts as the core component to define the model strategy. The objective function, aimed at minimizing the total costs $\mathbb{C}$, is defined as follows:

$$\boldsymbol{Min}\ \mathbb{C} = \mathbb{C}^{\boldsymbol{op}} + \mathbb{C}^{\boldsymbol{cycle}} + \mathbb{C}^{\boldsymbol{penalty}} - \mathbb{C}^{\boldsymbol{energy}} \tag{3.2}$$

The operating costs $\mathbb{C}^{op}$ in general cost caused by a component. In the LL-Model this applies only to the component `ElectricalGrid` for buying and selling electricity to the grid. The power drawn from the grid and power fed back into the grid is multiplied by the corresponding price of the electricity tariff with levies and taxes added on top. The operating costs are summed over the total time period T.

$$\mathbb{C}^{\boldsymbol{op}} = \mathbb{C}^{\boldsymbol{grd}} \tag{3.3}$$

$$\mathbb{C}^{\boldsymbol{grd}} = \sum_{\boldsymbol{t \in T}} (\boldsymbol{P}^{\boldsymbol{grd}}_{\boldsymbol{output,t}} * (\boldsymbol{c_p} + \boldsymbol{c_l}) * (\boldsymbol{1} + \boldsymbol{c_{VAT}}) - \boldsymbol{P}^{\boldsymbol{grd}}_{\boldsymbol{input,t}} * \boldsymbol{c_{inj}}) * \Delta \boldsymbol{t_{step}} \tag{3.4}$$

The cycle cost $\mathbb{C}^{cycle}$ refers to costs compensating for battery degradation caused by additional cycling due to applications other than mobility. This cost is calculated by multiplying the power input from the EV charger on the battery side, which is detailed in equation (3.6). The cycle costs enable a careful consideration value added through additional cycle and battery degradation. When calculating the cycle costs in the model, only the discharge direction is considered. Here, a simplified calculation of cycle costs is shown in equation (3.5):

$$\boldsymbol{Cycle\ Cost} = \frac{\boldsymbol{Cost\ Battery}}{\boldsymbol{Life\ Cycles} * \boldsymbol{Capacity}} \tag{3.5}$$

$$\mathbb{C}^{\boldsymbol{cycle}} = \sum_{\boldsymbol{t \in T}} \boldsymbol{P}^{\boldsymbol{EVC,input_2}}_{\boldsymbol{t}} * \boldsymbol{c_{cycle}} * \Delta \boldsymbol{t_{step}} \tag{3.6}$$

The penalty costs $\mathbb{C}^{\boldsymbol{penalty}}$ are costs added to lower battery degradation due to calendric aging. Staying in high SOC regimes, the calendric degradation in lithium-ion batteries is increased significantly [57]. To prevent the EV battery staying too long in these high SOC regimes, the penalty costs correlate with the duration of stay. A binary variable indicates whether the SOC status of the battery exceeds the threshold of 80 % SOC:

$$\boldsymbol{z_t^{above}} \in (\mathbf{1}, \mathbf{0}) \tag{3.7}$$

$$\mathbb{C}^{\boldsymbol{penatly}} = \sum_{\boldsymbol{t} \in \boldsymbol{T} \setminus \boldsymbol{T_{out}}} \boldsymbol{z_t^{above}} * \boldsymbol{c_{penalty}} * \Delta \boldsymbol{t_{step}} \tag{3.8}$$

The energy costs $\mathbb{C}^{energy}$ are introduced to prevent selling of the EV battery energy at the end of the calculation horizon T_h. In the LL-Model the grid injection with the price c_{inj} represents the only option to sell energy for the prosumer. Thus, taking this price for the final state of energy in the battery, does prevent the model sells the energy at the end of the calculation period:

$$\mathbb{C}^{\boldsymbol{energy}} = \mathbf{E}_{\mathbf{t_{end}}} * \boldsymbol{c_{inj}} \tag{3.9}$$

After defining the objective function, the `Energymanagementsystem` executes the function `calculate_V2H_cost_function` to calculate and store the value in the results, and pass it as part of the solving approach to the UL-Model for every prosumer n. The V2H cost-value function represents the actual costs for the prosumer for every decision time step t_d.

$$\boldsymbol{\xi_{n,t_d}^{V2H}} = \mathbb{C}_{\boldsymbol{t}}^{\boldsymbol{op}} + \mathbb{C}_{\boldsymbol{t}}^{\boldsymbol{cycle}} \quad \forall \boldsymbol{n} \in \boldsymbol{N}, \boldsymbol{t} \in \boldsymbol{T_r}, \boldsymbol{t_d} \in \boldsymbol{T_d} \tag{3.10}$$

Modifications to the `ElecVehicle` component were necessary to implement driving constraints essential for modeling the use of the EV. This component inherits from the `Li-ion Battery`, which in turn inherits from `BaseStorage`, as seen in Figure 7. This arrangement includes functions and restrictions defined in the superior components. Further details are available in [21]. The restrictions (3.11) and (3.12) ensure that no power flows through the EVC in either direction when the EV is absent due to driving.

$$\boldsymbol{P_{t,n}^{EVC,input_1}} = \mathbf{0} \quad \forall \boldsymbol{n} \in \boldsymbol{N}, \boldsymbol{t} \in \boldsymbol{T_{out,n}} \tag{3.11}$$

$$\boldsymbol{P_{t,n}^{EVC,input_2}} = \mathbf{0} \quad \forall \boldsymbol{n} \in \boldsymbol{N}, \boldsymbol{t} \in \boldsymbol{T_{out,n}} \tag{3.12}$$

To better model the uncertainty the EVA faces in managing the EV pool, a restriction sets the minimum SOC of the EV to 70 % upon departure. This addresses the unpredictability of travel duration and distance. Therefore, the EV driving profile is analyzed again, and a list, $T_{dep,n}$ is created for each prosumer, indicating the time steps for departing:

$$\frac{\boldsymbol{E_{t,n}}}{\boldsymbol{E^{max}}} \geq \mathbf{0.7} \quad \forall \boldsymbol{n} \in \boldsymbol{N}, \boldsymbol{t} \in \boldsymbol{T_{dep,n}} \tag{3.13}$$

Furthermore, the minimum SOC of the EV battery is set to 30 % to mitigate enhanced cyclic and calendric aging associated with very low SOC levels [57]. Setting the SOC to 30 % also

accommodates the unpredictability of departure needs, ensuring the EV can always undertake short trips:

$$\frac{\boldsymbol{E_{t,n}}}{\boldsymbol{E^{max}}} \geq \boldsymbol{0.3} \quad \forall \boldsymbol{n} \in \boldsymbol{N}, \boldsymbol{t} \in \boldsymbol{T} \tag{3.14}$$

With these formulas, the LL optimization model is comprehensively described. After building the model and solving the respective pyomo model for each prosumer, as outlined in the workflow in Figure 35 in the appendix, the results are systematically stored. Each component has the function `get_base_variable_names` to identify and store base variables in the result dataset. Moreover, the `OptimizationModel` class specifies which additional variables should be recorded. Settings are optimally chosen to ensure all critical model variables are documented in an Excel file. Adjustments can be tailored to user needs.

3.5.2 UL-Model

The UL-Model encompasses all prosumer models in the EV pool along with the `VirtualAggregator`, its own `Energymanagementsystem`, and components for `FCR`, `aFRR` and `SMT` as outlined in Figure 11. Details on the components and functions shared between both models are available in previous Section 3.5.1.

A newly added component, the `VirtualAggregator`, inheriting from `BaseComponent`, facilitates bi-directional energy flow without capacity limits. Modeled without energy losses, it is serving as an ideal electrical conductor, which allows only two directions of energy flow. Thereby, preventing energy exchange between individual prosumers or different energy market components. To realize this component, four power variables are defined and interconnected through restrictions:

$$\boldsymbol{P_t^{VC,input_1}}, \boldsymbol{P_t^{VC,input_2}}, \boldsymbol{P_t^{VC,output_1}}, \boldsymbol{P_t^{VC,output_2}} \in (\boldsymbol{0}, \infty), \quad \forall \boldsymbol{t} \in \boldsymbol{T} \tag{3.15}$$

$$\begin{aligned} \boldsymbol{P_t^{VC,input_1}} &= \boldsymbol{P_t^{VC,output_1}} \quad \forall \boldsymbol{t} \in \boldsymbol{T} \\ \boldsymbol{P_t^{VC,input_2}} &= \boldsymbol{P_t^{VC,output_2}} \quad \forall \boldsymbol{t} \in \boldsymbol{T} \end{aligned} \tag{3.16}$$

Modifications to the `DynamicBiInverter` class are necessary to enable the splitting of EVC power for V2H and V2G. The constraint `constraint_bi_flow` is deactivated to permit simultaneous energy flow in both directions without suppressing any flow due to opposing demands from V2H and V2G.

Adjustments to the `FCR` and `aFRR` classes are required to adapt them for the EV pool. These modifications include implementing a fixed bid size b (3.18). Therefore, three integer variables are defined (3.17) to ensure that offered powers are multiples of the bid size b:

$$\boldsymbol{z_t^{aFRR_{pos},int}}, \boldsymbol{z_t^{aFRR_{neg},int}}, \boldsymbol{z_t^{FCR,int}} \in \mathbb{N}, \quad \forall \boldsymbol{t} \in \boldsymbol{T} \tag{3.17}$$

$$\begin{aligned} \boldsymbol{P_t^{aFRR_{pos},offer}} &= \boldsymbol{b} * \boldsymbol{z_t^{aFRR_{pos},int}} \quad \forall \boldsymbol{t} \in \boldsymbol{T} \\ \boldsymbol{P_t^{aFRR_{neg},offer}} &= \boldsymbol{b} * \boldsymbol{z_t^{aFRR_{neg},int}} \quad \forall \boldsymbol{t} \in \boldsymbol{T} \\ \boldsymbol{P_t^{FCR,offer}} &= \boldsymbol{b} * \boldsymbol{z_t^{FCR,int}} \quad \forall \boldsymbol{t} \in \boldsymbol{T} \end{aligned} \tag{3.18}$$

The optimization model's goal is to minimize the total costs of the entire EV pool through accessing V2H and V2G in an optimal combination. Thereby, the profit is implicitly maximized through the selected optimization approach. The objective function, implemented in the `EnergyManagementSystem`, is:

$$\boldsymbol{Min}\ \mathbb{C} = \mathbb{C}^{\boldsymbol{op}} + \mathbb{C}^{\boldsymbol{cycle}} + \mathbb{C}^{\boldsymbol{penalty}} - \mathbb{C}^{\boldsymbol{energy}} + \mathbb{C}^{\boldsymbol{compensation}} \tag{3.19}$$

Where $\mathbb{C}^{op}$ includes operational costs caused by the grid summed over all prosumers N and operating costs for FCR, aFRR, and SMT:

$$\mathbb{C}^{\boldsymbol{op}} = \left(\sum_{\boldsymbol{n}\in\boldsymbol{N}} \mathbb{C}_{\boldsymbol{n}}^{\boldsymbol{grd}}\right) + \mathbb{C}^{\boldsymbol{FCR}} + \mathbb{C}^{\boldsymbol{aFRR}} + \mathbb{C}^{\boldsymbol{SMT}} \tag{3.20}$$

The calculation of $\mathbb{C}_{\boldsymbol{n}}^{\boldsymbol{grd}}$ is explained in (3.3) and is here summed up for the EV pool. The calculation of $\mathbb{C}^{\boldsymbol{FCR}}$ and $\mathbb{C}^{\boldsymbol{aFRR}}$ is explained in previous work in [80]. $\mathbb{C}^{\boldsymbol{SMT}}$ corresponds to the operating costs caused by buying and selling energy at the spot market, which is exclusively available for the EVA. Therefore, the `SMT` component inherits from `BaseGrid` and uses the spot market prices c_t^{id} to calculate the operating costs:

$$\mathbb{C}^{\boldsymbol{SMT}} = \sum_{\boldsymbol{t}\in\boldsymbol{T}} (\boldsymbol{P_{output,t}^{SMT}} * \left(\boldsymbol{c_t^{id}} + \boldsymbol{c_l}\right) * (\mathbf{1} + \boldsymbol{c_{VAT}}) - \boldsymbol{P_{input,t}^{SMT}} * \boldsymbol{c_t^{id}}) * \Delta \boldsymbol{t_{step}} \tag{3.21}$$

The terms for $\mathbb{C}^{\boldsymbol{cycle}}$ and $\mathbb{C}^{\boldsymbol{penalty}}$are defined for a single EV in (3.4), (3.6) and (3.7) respectively and are in the UL-Model aggregated over the EV pool. The term $\mathbb{C}^{\boldsymbol{energy}}$ is changed to comply with the access to the spot market. Therefore, the end energy is multiplied with lower value of the average spot market price in that period and the lowest purchase price for the prosumer in that period. The average of the spot market price $c_{SMT,avg}$ indicates the model to buy or sell energy from the EV, if the current spot market price is respectively below or above $c_{SMT,avg}$. Further, to prevent the model from buying energy at the prosumers grid and selling it at the spot market, the value can maximum be as high as the cheapest purchase price c_n^{el} in the prosumer's electricity tariff.

$$\mathbb{C}^{\boldsymbol{energy}} = \sum_{\boldsymbol{n}\in\boldsymbol{N}} \mathbf{E}_{\mathbf{t_{end},}\boldsymbol{n}} * \mathbf{min}\ (\boldsymbol{c_{SMT,avg}}, \boldsymbol{c_n^{el}}) \tag{3.22}$$

The newly added term $\mathbb{C}^{\boldsymbol{compensation}}$ accounts to the compensation payments made by the EVA to prosumers. This term consists of two parts (3.23): one for the power compensation in T_r (3.24) and another for an individual compensation in subsequent time steps (3.25). The variable for provided power for V2G $\boldsymbol{P_{n,t}^{V2G}}$ is introduced below in (3.27). The variable for

individual compensation is defined in (3.26). This set up allows an optimistic operations planning post T_r. Optimistic operation planning enables the EVA to provide tailored compensations to prosumers—rather than uniform power price adjustments—to achieve the desired power levels in the EV pool for optimized operations:

$$\mathbb{C}^{\boldsymbol{Compensation}} = \mathbb{C}^{\boldsymbol{CompPower}} + \mathbb{C}^{\boldsymbol{Ind}} \tag{3.23}$$

$$\mathbb{C}^{\boldsymbol{CompPower}} = \sum_{\boldsymbol{n \in N, t \in T_r}} \boldsymbol{P_{n,t}^{V2G}} * \boldsymbol{c_{power,i}} * \Delta \boldsymbol{t_{step}} \tag{3.24}$$

$$\mathbb{C}^{\boldsymbol{Ind}} = \sum_{\boldsymbol{n \in N, t \in T_d}} \boldsymbol{C_{n,t}^{Ind}} \tag{3.25}$$

$$\boldsymbol{0 \leq C_{n,t_d}^{Ind} \leq \infty \quad \forall n \in N, t_d \in T_d} \tag{3.26}$$

A series of constraints is implemented to facilitate the internal decision-making process for EV pool participation by each prosumer. A new variable $\boldsymbol{P_{n,t}^{V2G}}$ is introduced to account for the power reserved for V2G by each prosumer n.

$$\boldsymbol{0 \leq P_{n,t}^{V2G} \leq P_{n}^{EVC,max} \quad \forall t \in T} \tag{3.27}$$

Once power is reserved for pool participation, the offer cannot be varied for the current decision period T_r, excluding the time steps in T_{out} when the vehicle is unavailable due to driving:

$$\boldsymbol{P_{n,t}^{V2G} = P_{n,t+1}^{V2G} \quad \forall t \in (T_r \setminus (\{last(T_r)\} \setminus T_{out}))} \tag{3.28}$$

The provided power for V2G of each prosumer is restricted by the driving pattern (3.29), the V2H energy flow (3.30) and V2G energy flow (3.31). The energy flows from the EVC to meet electrical consumption (ELCSN), from the PV inverter to the EVC to store surplus energy, and from the EVC to the `VirtualAggregator` are decisive for the V2H and V2G usage and thus built in the constraints:

$$\boldsymbol{P_{n,t}^{V2G} = 0 \quad \forall n \in N, t \in T_{out}} \tag{3.29}$$

$$\boldsymbol{P_{n,t}^{V2G} \leq P_{n}^{EVC,max} - P_{n,t}^{EVC-ELCSN} - P_{n,t}^{PV-EVC} \quad \forall n \in N, t \in T} \tag{3.30}$$

$$\boldsymbol{P_{n,t}^{V2G} \geq P_{n,t}^{EVC-VC} \quad \forall n \in N, t \in T} \tag{3.31}$$

To integrate the available power from the EV pool with the power reserved for FCR and aFRR as well as utilized for SMT, the method `add_multi_V2G_constraint` is modified, according to the EV pool. This method implements three restrictions to manage the power (3.32), the energy input (3.33) and the energy output (3.34). Restriction (3.32) implicitly contains energy flow for SMT through including both inputs of the `VirtualAggregator`. $t_{reserve}$ corresponds to the reservation time for balancing services, which is defined as four hours:

$$\boldsymbol{P_t^{aFRR_{pos},offer} + P_t^{aFRR_{neg},offer} + P_t^{FCR,offer} + P_t^{VC,input_1} + P_t^{VC,input_2} - P_t^{aFRR,input} - P_t^{aFRR,output} - P_t^{FCR,input} - P_t^{FCR,output} \leq \sum_{n \in N} P_{n,t}^{V2G} \quad \forall t \in T} \tag{3.32}$$

$$\boldsymbol{\left(P_t^{aFRR_{pos},offer} + P_t^{FCR,offer}\right) * t_{reserve} \leq \sum_{n \in N} (E_{n,t} - 0.3 * E_{n,t}^{max}) \quad \forall t \in T} \tag{3.33}$$

$$\boldsymbol{\left(P_t^{aFRR_{neg},offer} + P_t^{FCR,offer}\right) * t_{reserve} \leq \sum_{n \in N} (E_{n,t}^{max} - E_{n,t}) \quad \forall t \in T} \tag{3.34}$$

Finally, the decision function is formulated for implementing the internal decision process where the prosumer chooses whether to accept or decline an offer. This function integrates the financial and energy compensation aspects of the pricing concept. Analogous to the V2H cost-value function in the LL-model, the V2G cost-value function for the UL-Model is calculated. Here, additional terms for energy compensation (3.36) and financial compensation (3.37) are added. $\mathbb{C}_{n,t}^{CompEnergy}$ accounts for the difference of the energy at the beginning and end of the respective decision period, multiplied with a fixed cost value according to the pricing concept. This term puts a price for a deviation in SOC, which leads to a consideration between energy exchange and financial compensation.

The term $\mathbb{C}_{n,t_d}^{Comp}$ covers the financial compensation for the provided power within the decision time step and the individual compensation term for each t_d in the RH-step. Since the individual compensation is only for optimistic operation planning in the time steps after the taken rolling time step, it is being restricted to zero (3.38) the first decision time step.

$$\boldsymbol{\xi_{n,t_d}^{V2G} = \mathbb{C}_{n,t_d}^{GRD} + \mathbb{C}_{n,t_d}^{cycle} + \mathbb{C}_{n,t_d}^{CompEnergy} - \mathbb{C}_{n,t_d}^{Comp}} \tag{3.35}$$

$$\boldsymbol{\forall n \in N, t_d \in T_d}$$

$$\boldsymbol{\mathbb{C}_{n,t_d}^{CompEnergy} = \left(E_{n,t_{r,last}} - E_{n,1}\right) * c_{energy}} \tag{3.36}$$

$$\boldsymbol{\mathbb{C}_{n,t_d}^{Comp} = \sum_{t \in T_r} P_{n,t}^{V2G} * c_{power} * \Delta t_{step} + C_{n,t_d}^{Ind}} \tag{3.37}$$

$$\boldsymbol{C_{n,t_d}^{Ind} = 0 \; \forall t_d = 1} \tag{3.38}$$

The underlying assumption for the decision logic is that, as soon as the V2G cost-value function ξ_{n,t_d}^{V2G} is lower than the V2H cost-value function ξ_{n,t_d}^{V2H}, indicating a higher value gained for the prosumer from participating in the EV pool to the defined conditions, the prosumer will accept the offer. The constant e accounts for a minimum benefit the prosumer requires to accept the offer, which is set to almost zero within this thesis to represent the highest EVA profit potential. The costs functions capture the value for the prosumer for the respective operation plan and allows so the EVA to adapt the operation plan to achieve added value for each prosumer and thus an acceptance of the offer. The choice of value stream as well as the energy distribution within the EV pool adapts according to the decision function and individual needs of each prosumer. To implement this logic, a binary variable is defined (3.39), which is then bounded by two constraints (3.40) to model the decision logic using the 'big M' method, where 'M' represents a large number [81]. The binary variable equals to one when accepting the offer and zero if not. Lastly, the binary variable is connected to the provided power for V2G in (3.41).

$$\boldsymbol{z_{n,t_d}^{V2G}} \in (\mathbf{0},\mathbf{1}) \quad \forall \boldsymbol{n} \in \boldsymbol{N}, \boldsymbol{t_d} \in \boldsymbol{T_d} \tag{3.39}$$

$$\begin{aligned} \boldsymbol{\xi_{n,t_d}^{V2G}} - \boldsymbol{\xi_{n,t_d}^{V2H}} &\leq \boldsymbol{M} * \boldsymbol{z_{n,t_d}^{V2G}} \\ \boldsymbol{\xi_{n,t_d}^{V2G}} - \boldsymbol{\xi_{n,t_d}^{V2H}} &\geq \left(\mathbf{1} - \boldsymbol{z_{n,t_d}^{V2G}}\right) * \boldsymbol{M} + \boldsymbol{e} \end{aligned} \tag{3.40}$$

$$\begin{aligned} \boldsymbol{z_{n,t_d}^{V2G}} * \boldsymbol{P_{n,t}^{V2G}} &= \mathbf{0} \\ \forall \boldsymbol{n} \in \boldsymbol{N}, \boldsymbol{t} \in \boldsymbol{t_r}, \boldsymbol{t_d} &\in \boldsymbol{T_d} \end{aligned} \tag{3.41}$$

3.5.3 Bi-Level Interaction

After detailing the two models in previous Sections, the mathematical description of their interaction within the ‘runme’ file is now presented. As illustrated in Figure 8, the interaction involves two loops: one implements the RH method and the other addresses the solving approach, previously explained in Section 3.3.

The EVA profit is calculated from the results extracted from the UL-Model for the first decision period $t_d = 1$, containing all time steps in T_r. All terms are multiplied by minus one to convert negative costs into profit. The terms $\mathbb{C}^{\boldsymbol{aFRR}}$, $\mathbb{C}^{\boldsymbol{FCR}}$ and $\mathbb{C}^{\boldsymbol{SMT}}$ remain as defined in (3.20), and $\mathbb{C}^{\boldsymbol{PowerComp}}$ from (3.24) represents the financial compensation for power provision. Additionally, a term for cycle cost payments from EVA to the prosumer compensates for battery aging from V2G applications, as specified in (3.43):

$$\mathbb{P}_{t_{d,i}} = (-\mathbf{1}) * \left(\mathbb{C}^{\boldsymbol{aFRR}} + \mathbb{C}^{\boldsymbol{FCR}} + \mathbb{C}^{\boldsymbol{SMT}} - \mathbb{C}^{\boldsymbol{V2G,cycle}} - \mathbb{C}^{\boldsymbol{PowerComp}}\right) \tag{3.42}$$

$$\mathbb{C}^{V2G,cycle} = \sum_{n \in N, t \in T_r} P_{n,t}^{EVC-VC} * c_{cycle} * \Delta t_{step} \quad (3.43)$$

The power price for V2G services is incrementally increased with each iteration i by the minimum price addition, set at 0.01 €/kW*h. This procedure continues until one of the four break-criteria is met, as outlined below. These break-criteria are derived from logical constraints of the model or experience from test runs to minimize the computation time:

- The first break criterion is met when the maximum iteration is reached, corresponding to the highest allowed power price increase.
- The second break criterion is reached when the power provided by the EV pool exceeds the maximum possible bid sizes, and the operating costs from SMT are less than 0.10 €. When this applies, no significant improvements through participation in balancing services are possible, and profit improvement through raising the power price and thus reducing the compensation by energy exchange has already been exhausted.
- The third break-criterion considers the maximum available power of the EV pool, which is the minimum continuous power available from EVs in the pool at that decision step. The available power is limited through the absence of EVs due to driving demands. If this available power falls below the minimum bid size and the amount of operating costs from SMT are less than 0.10 €, no significant profit improvement is expected.
- The fourth break-criterion is met when the EVA profit remains zero or negative after two consecutive power price increases. This condition is based on experience gained from test and is employed to prevent unnecessary additional iterations.

When a break criterion is met, the iteration yielding the highest profit for the EVA for the first decision period of this calculation is selected as the best result and carried over to the next RH-step by updating the SOC accordingly. Results from all iterations and RH-steps are systematically stored in an Excel file for convenient evaluation of the simulation run.

3.6 Method Validation

After the model was extensively described in the last Sections, it is required to validate the applied modelling methods according to the intended purpose. According to several institutions, mathematical model validation is described as “process of determining the degree to which a computer model is an accurate representation of the real world from the perspective of the intended model applications” [82]. However, an experimental validation of the model cannot be conducted. Instead, a validation of different aspects of the modelling method is discussed in the following Sections. Since computation time is a major hurdle for solving such large-scale bi-level optimization problems, special focus is placed on computation time reduction techniques and their impact on accuracy. Therefore, Section 3.6.1discusses the impact on the solving approach. Then, Section 3.6.2 validates the modelling techniques applied to solve the model, such as RH method, parallel computing and solver settings.

3.6.1 Solving Approach

For the solving the bi-level problem the reformulation method is applied. This method iteratively tests all steps within the defined solution space until a break criterion is met. The step size is set to 0.01 €/kW*h with a maximum of 9 increases per decision period, resulting in a maximum price of 0.09 €/kW*h for the provided power. As described in 3.1.2, with this method it is very unlikely to achieve the exact optimal value.

However, the resulting error from this step size is relatively small. Firstly, it can be seen that the most profitable power price was zero in 77 % of the decision periods. These periods are unaffected by the solving approach are thus optimally resolved. Secondly, in only 0.7 % of the decision periods, the maximum power price led to the highest profit. Allowing to assume that the maximum number of price increases is sufficient high. Thirdly, an infinite small step size could only increase the EVA profit within one decision period by 2.64 € given the total power of 66 kW and reservation time of 4 h, which are the chosen configuration for the EV pool in this thesis. This is calculated by multiplying the highest EV pool participation with the power price step size and reservation time. Thus, half the step size would lead in the best case to an increase of the EVA profit of 1.32 €, while roughly doubling the computation time. Still this increase in profit is only excepted for very few decision periods. For all decision periods, where a power price of zero is the optimum, no improvement will be achieved. Considering the increased computation time, the caused error due to the step size of 0.01 € is acceptably low.

3.6.2 Modelling Techniques

Different modelling techniques, including RH method, parallel computing and solver settings for solving the model are discussed below.

Rolling-Horizon

The RH method is a crucial part of the model for two primary reasons. First, considering the size of a complete yearly optimization problem, it is unsolvable with the computational resources available. So temporal decomposition is urgently required. Second, to properly model the dynamic decision-making process, recalculating after each decision period is essential to incorporate the updated SOC requirements. This highlights the unavoidable need for implementing this technique, despite its inherent trade-off: a deviation from the global optimum due to the reduced calculation horizon.

However, the selected time horizon and rolling horizon can influence the accuracy of the results and the utilization of different value streams. This is because the model lacks foresight beyond the horizon. Value streams over a large time scale, such as SMT and load shifting, will be disadvantaged through a too small choice of the horizon step. This prevents the model from considering trades beyond the scale of the horizon. Since the highest dynamic for decision taking in the model is aimed, the rolling horizon is not modified. But it is essential to validate the chosen horizon step of 1 day. To assess this, a comparison of EVA profit and computation time was performed across five daily simulations with 0.5-, 1-, 3- and 7-day horizons. Figure 14 visualizes the resulting computation time for an exemplary daily simulation. The

computation time raises significantly with increasing time horizon, while the EVA profit remains almost the same for all time horizons.

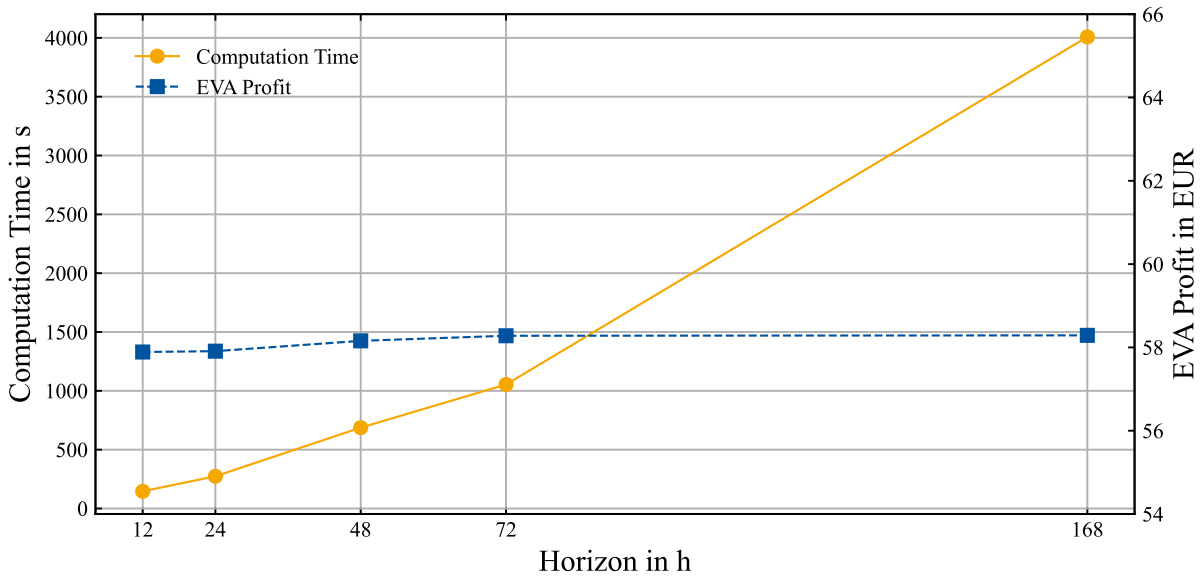

Figure 14: Computation time and EVA profit for different time horizons

Consequently, extending the time horizon alone does not significantly affect the quality of the results. Instead, the combined choice of time horizon and rolling horizon is assumed to have a more substantial impact on the model. The rolling horizon is the period of each calculated time horizon, which is taken as final result, as previously explained for the RH method in Section 2.3.2. The choice of rolling horizon is determined by the length of the decision period, set to four hours in this thesis. Additionally, choosing a short horizon of 1 day replicates the unpredictability and limited foresight of real-world actors during the planning of EVA operations. Within the calculated horizon, the model operates with deterministic knowledge. In a real-world application, this could be approximated through advanced prediction models and collaboration with the prosumers. For horizons beyond 1 day, this assumption is not valid as predictions lose their accuracy and reliability over time. Furthermore, the prosumer can usually plan their current day well, knowing when to depart and for how long. However, the further this planning horizon extends, the more unreliable it becomes. Hence, the chosen horizon of 1 day provides a good balance between computation time, accuracy, and replication of real-world conditions.

Parallel Computing

High computation time is a significant challenge when dealing with large-scale and complex optimization models, such as the developed bi-level model. To efficiently manage yearly simulations within the available computational resources, the problem was temporally divided into four segments, each covering approximately three months. These segments were then processed simultaneously on the ISEA RWTH super-computer, which utilizes 256 CPU cores with a frequency of 3.28 GHz and 2 TB of available RAM, to maximize computational power.

To facilitate the simultaneous calculation of each model part, the EV profiles were artificially modified, and a model constraint was introduced to ensure that the end-of-simulation SOC values for the three segments were approximately known. At the three overlapping points of the simulation segments, the EV profiles were modified, so that all EVs departure at 8 am for varied distances. This setup represents an unlikely but possible scenario where the availability of EVs is too low for V2G to be conducted. Moreover, a constraint was implemented to maintain the SOC within a tight range of 10 % at the exact departure times of the EVs. This constraint ensures that the error in terms of SOC remains below 5 %, when joining the four model parts. The modification in the EV profile effects only 3 days out of 365, which is acceptable considering a shorten computation time by a quarter.

Solver settings

Lastly, a strategy was implemented to ensure reliable results within a reasonable computation time. Initially, for the UL-Model, a relative solution gap of 0.02 and an absolute solution gap of 1 € were set. Setting an absolute gap is crucial for the model, since the resulting objective function can be very close to zero. In that case the accepted absolute error with only setting a relative gap is unnecessarily low, resulting in very long calculation times.

However, for the LL-Model, a more stringent relative gap of 0.001 was applied, considering its minimal impact on the bi-level optimization's computational demands. If a solution is not achieved within 600 seconds, the calculation is restarted with a relaxed relative gap of 0.06 and an absolute gap of 4 €. These deviations from the model objective to the global objective refer to the entire UL-Model settings. Since the UL-model does not directly optimize the EVA profit and through the RH method only a short part of the calculation is taken as solution, the estimated error from using this logic is comparably small. Also, experiences from test runs show, that certain decision steps and configurations are increasing the computation time immensely and can possibly lead to unsolvable time steps, which would stop the simulation. To overcome this, a logic was implemented, that if no solution after a certain time with increased gap is obtained, the program moves to the next decision step, if already a solution was obtained before.

Nevertheless, it is important to validate how the solver settings, specifically the relative solution gap, influence the quality of the results. For this, daily test runs comparing computation time and EVA profit with different relative gap settings were conducted. Figure 15 visualizes the outcomes. For these test runs, the break criteria were disabled to ensure all runs performed the same number of iterations. It was observed that a decrease in relative gap values led to an exponential increase in computation time. Moreover, a lower relative gap does not always result in higher EVA profitability for two reasons. First, the objective value in the UL-Model

does not directly optimize EVA profit. Second, due to the RH method, only a small part of the solution is considered, which might remain unaffected by further optimization.

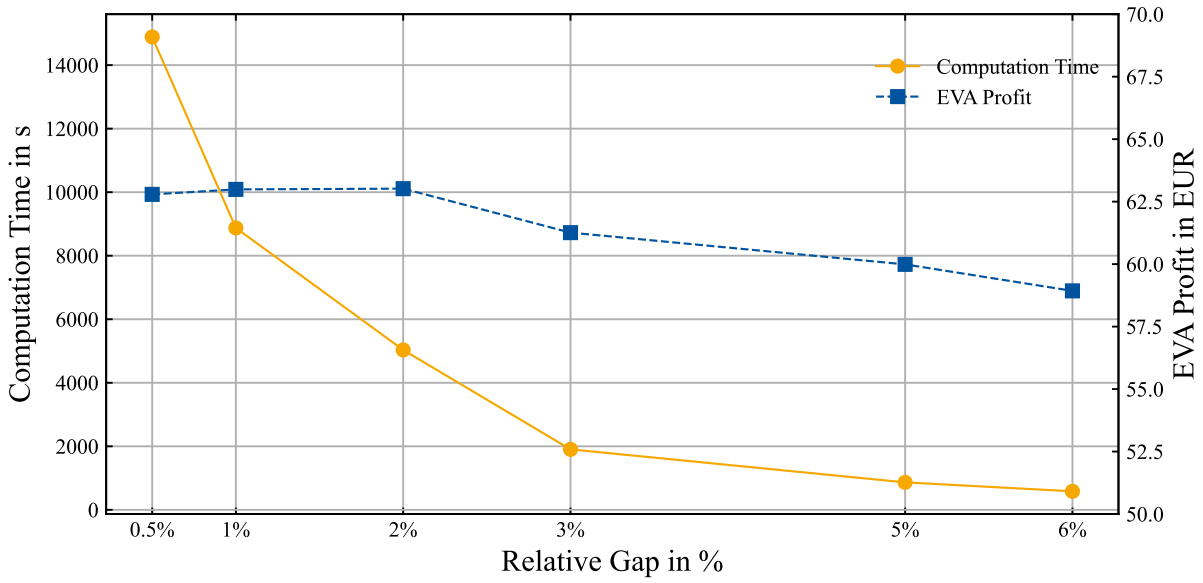

Figure 15: Computation time and profit over different relative gap values

Although a lower relative gap reduces the total electricity costs of the EV pool for that calculation horizon, it was noted that a 2 % relative gap setting yielded the highest EVA profit in the test run. However, this observation is based on a single exemplary day and does not constitute an exhaustive analysis. It can be assumed, that generally a lower relative gap does improve the quality of results. But more importantly, the results indicate a necessary trade-off between a lower gap setting and computation time. Based on experience from this and further test runs, a 2 % relative gap setting demonstrates sufficient performance with acceptable computation time.

4. Model Evaluation

In this Chapter, the developed bi-level optimization model is evaluated by examining results from yearly simulations across three different scenarios. This evaluation pursues two primary objectives. First, to assess whether the bi-level model effectively models the interactions and operations of an EVA, thereby facilitating an investigation into EVA pricing concepts. Second, to derive insights from the outcomes of these scenarios to understand the design principles of EVA pricing concepts. These insights are discussed in regard to a more holistic view of the EVA in real-world conditions.

Therefore, this Chapter is structured as follows: In Chapter 4.1 the evaluation approach for the subsequent Sections is presented. This includes, explaining the design of the chosen pricing concept and the rationale behind the design for the scenarios. Then in Section 4.2 the model configuration used for the yearly simulations, including parametrization and input data, is described. Lastly, Section 4.3 discusses the results from yearly simulations according to the three scenarios from the perspective of the EVA and EV owner. Therefore, a special emphasize is put on the business and operational aspects.

4.1 Evaluation Approach

The evaluation pursues to explore the pricing concepts employed by the EVA and their effects on operations and the business model. Through this evaluation, design directions for the pricing concept are identified, a reasonable power price for a TOU pricing scheme is developed, and the main factors influencing EVA operations and profitability are discussed. To accomplish these objectives, three scenarios are derived in the following.

First, it is essential to examine the design of the pricing concept for the EVA. Figure 16 below visualizes the chosen pricing concept in this thesis. On one side, the EV owner is compensated through financial payments for providing their flexibility. These financial payments are based on battery aging incurred through V2G, priced through static cycle costs, and on the power provided, priced through the dynamic power price of each decision period.

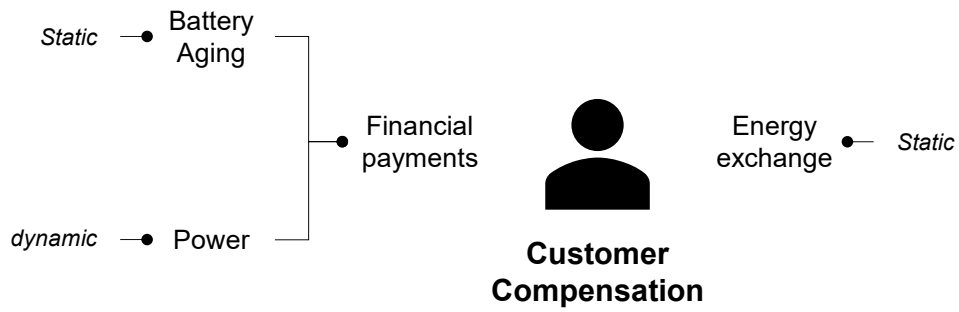

Figure 16: Pricing concept design in this thesis

On the other side, the EV owner is compensated through energy exchange. Since the EVA does not own assets and therefore cannot store energy themselves, the energy exchange between the EV owner and energy markets becomes an essential part of the compensation. In this thesis, no financial payments for the energy received or delivered between the prosumer and EVA are considered. This would represent an additional component of the pricing concept. However, the energy exchanged is valorized by a static price, equal for both directions of the energy exchange, as detailed in (3.36). The valorization of energy could potentially differ for delivering and receiving. Additionally, several temporal pricing schemes are possible for each component of the pricing concept, such as static, TOU, seasonal, and dynamic.

Each component of a pricing concept influences each other's, making it impossible to investigate all parts simultaneously with the developed linear model. In order to optimally investigate the power price, other components of the pricing concept are kept fix, while determining the optimal dynamic power price in the model. The static valorization for the energy exchanged is changed within three scenarios to examine the intercorrelation of both power and energy pricing design components.

Since there is no known common design for the pricing concept of an EVA, several design possibilities for the energy exchange compensation are reasonable. The underlying question is: "What is the current value of the energy for each actor?". A simple determination of a static value in form of a price does not seem senseful, due to dynamic electricity prices and volatile production conditions of the solar PV. In addition, the availability and need of energy does change significantly for the prosumer. A more in-depth calculation would need to consider factors such as spot market prices, PV production, consumption needs and storage capacity of the prosumer. However, a deep investigation of the energy exchange compensation design while investigating the power price is beyond the scope of this thesis. But to understand the interplay between power price and energy valorisation, three scenarios are defined, which differ in the value for the energy exchanged. These values are derived, based on logical constraints, as explained in the following.

Figure 17 visualizes the energy compensation structure with a price for receiving energy and delivering energy from the prosumer´s perspective. The upper limit for positive energy pricing is set at 0.38 €/kWh, which is the maximum rate of the applied electricity tariff, including taxes and levies. This rate represents the highest price a prosumer would pay for receiving energy from the EVA. Conversely, the lower limit is set at 0 €/kWh. Since the EVA lacks storage assets, it relies on prosumers to take energy when conducting V2G services. Similarly, for the negative energy price, the logical boundaries are derived by the prosumer's electricity tariff. The highest price at which energy could possibly be purchased from the grid, ignoring energy conversion and storage losses, represents the upper limit at 0.38 €/kWh. The lower limit is set by the prosumer's injection price at 0.08 €/kWh, as injecting the energy into the grid would otherwise be a more lucrative option. Based on these boundaries, three scenarios are derived, varying in their valuation of energy. As a simplification to make prices uniform the lower bound is set to 0.08 €/kWh for positive energy exchange. The resulting energy prices are 0.08 €/kWh, 0.23 €/kWh, and 0.38 €/kWh for the Low Energy (LE), Mid Energy (ME), and High Energy (HE) scenarios, respectively.

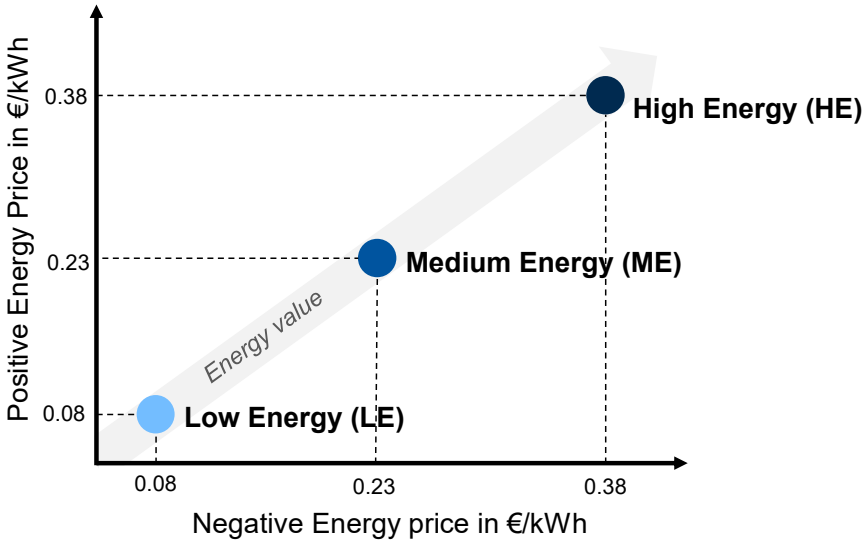

Figure 17: Energy exchange compensation design for the three scenarios

4.2 Simulation Configuration

The input data and parametrization do play a crucial role for the accuracy and reliability of a mathematical model. With reasonable sorted and processed input data, the model gets capable of replicating the real-world scenario, that it is accurate and representative enough to investigate the research target effectively. Therefore, the following two Sections provide an overview of the chosen parametrization and input data.

4.2.1 Parameterization

Parameterization describes the set of fixed values which are being used within the model. The choice of the parameters can either be done with the reason of corresponding to a real-world scenario or allowing effective and time efficient modelling. The following Table 3 gives an overview of general parameters defined within the model, while Table 4 shows the parameters of the prosumers in the EV pool.

Table 3: Overview of simulation setup

Parameter		
Simulation time	t_{total}	1 [year]
Horizon	$t_{horizon}$	24 [h]
Rolling horizon & decision period	t_{roll}	4 [h]
Time step size	t	15 [min]
Cycle cost	c_{cycle}	0.10 [€/kWh]
Bid size	b	30 [kW]

Table 4: Overview of EV pool composition

Parameter		
Number of prosumers	n	9
Battery capacity	E_{max}	60 [kWh]
EVC power	$P_{inv,max}$	3.7 / 7.4 / 11 [kW]
PV peak power	$P_{PV,max}$	3 / 7 / 10 [kWp]

The step size of 15 minutes is chosen to balance computational efficiency with the ability to accurately replicate dynamics in the energy markets, where the intra-day spot market price is traded in this interval. Cycle cost calculations are based on assumptions regarding battery costs and lifespan, as detailed in [83]. However, these values are slightly reduced to reflect underutilization of the battery over its assumed 10-year lifespan and to match with the SOC restriction applied in the model. Further, a simplified bid size of 30 kW is adopted for the model, as simulating a realistic EV pool size matching the 1 MW bid size is impractical. It is therefore assumed that the simulated EV pool represents a fraction of a larger EV pool with a total size of 2.2 MW. This assumption allows to replicate the hurdle of reaching the bid size threshold with a smaller-scale mathematical model.

The EV pool represents three types of prosumers with common power sizes for the EVC an PV generator in the regulatory framework of Germany. The explanation behind the EVC power was given in Section 2.2.1. Further, it is regulatory and economically more attractive to install a maximum PV system of 10kWp for private households. The prosumer benefits from less registration work and higher injection remunerations [84]. As a consequence, this represents in most cases the highest adapted power size in the market for private households. However, generally when installing a larger PV system in a V2H ecosystem, it is natural to also install an EVC with sufficient charging power to exploit the benefits completely. Because of this, each prosumer type in the model (S, M, L) combines the respective size of PV system and EVC.

4.2.2 Input Data

The EVA operations are typically characterized by a high degree of unpredictability and randomness, stemming from the inherent unpredictability of private person choices and market dynamics. For representative modeling of EVA operations, variance and randomness in the input data among the EV pool participants is essential. The techniques applied to account for this are described in the following. The input data was sourced from the year 2022, except for the temperature and irradiance data used for solar PV generation.

Electrical Consumption: A representative electrical consumption profile for a single-family house, including typical user patterns was used and modified for each prosumer. Figure 18 shows the electricity consumption and PV generation profiles for a sample week in July 2022. Typical profiles characteristics for the electrical consumption with peaks in the morning and afternoon can be observed for the weekdays. At weekend days there are multiple peaks during

the day. To account for the variance in prosumer usage patterns, the electrical consumption profiles were randomly shifted by ±0-60 minutes and scaled by ±10 % in power load for every time step. This introduces a certain degree of variability, which better reflects real-world consumption patterns. In this thesis, the electrical consumption profiles do not correlate with the departure and arriving times of the driving profiles.

Solar PV profile: Seasonal changes, climate, and weather have a significant influence on the actual production of solar PV. To account for this, real measured data for temperature and irradiance from 2006 at the Lindenberg station in Germany is utilized and converted into a PV generation profile. This data ensures that the model reflects realistic variations in solar production, typical for the seasonal and climatic changes in Germany. Figure 18 shows the PV production of a panel in July with 3 KWp peak power in addition to the electrical consumption pattern. Factors such as panel orientation, shading, and soiling were not considered.

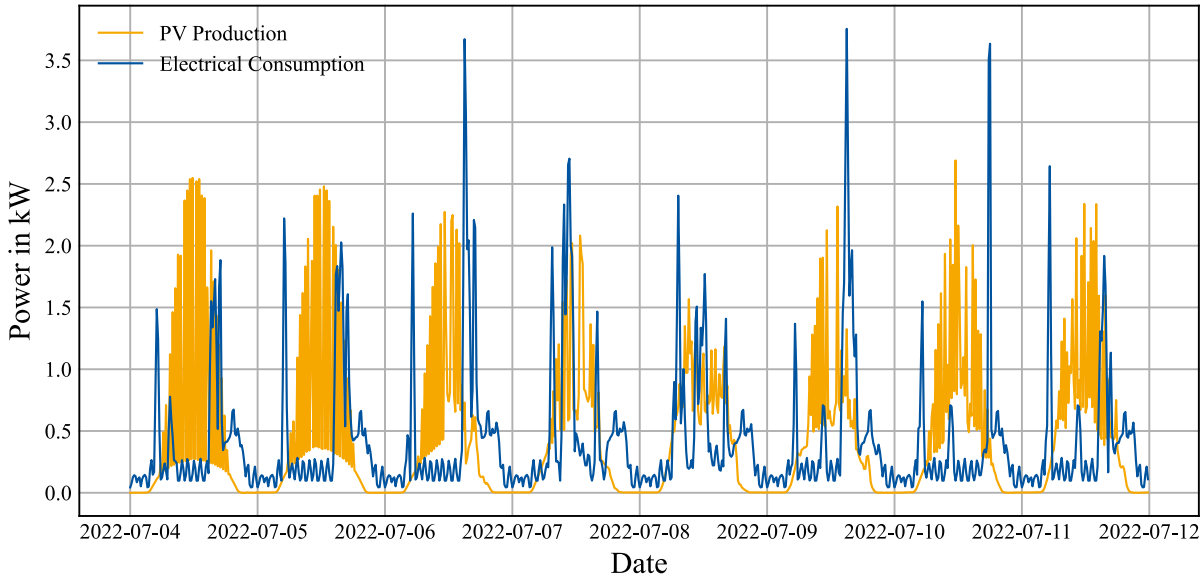

Figure 18: PV production and electricity consumption of a sunny week in July

In addition to the typical daily production profile of solar PV panels, these systems also exhibit a typical production profile throughout the year. Figure 19 visualizes the monthly energy production of the PV system with 10 kWp and electrical consumption. The electrical load remains nearly constant throughout the year, as no electrical heating system is installed, resulting in only minor seasonal variations. The PV production profile increases during the year until it peaks in June and then declines thereafter.

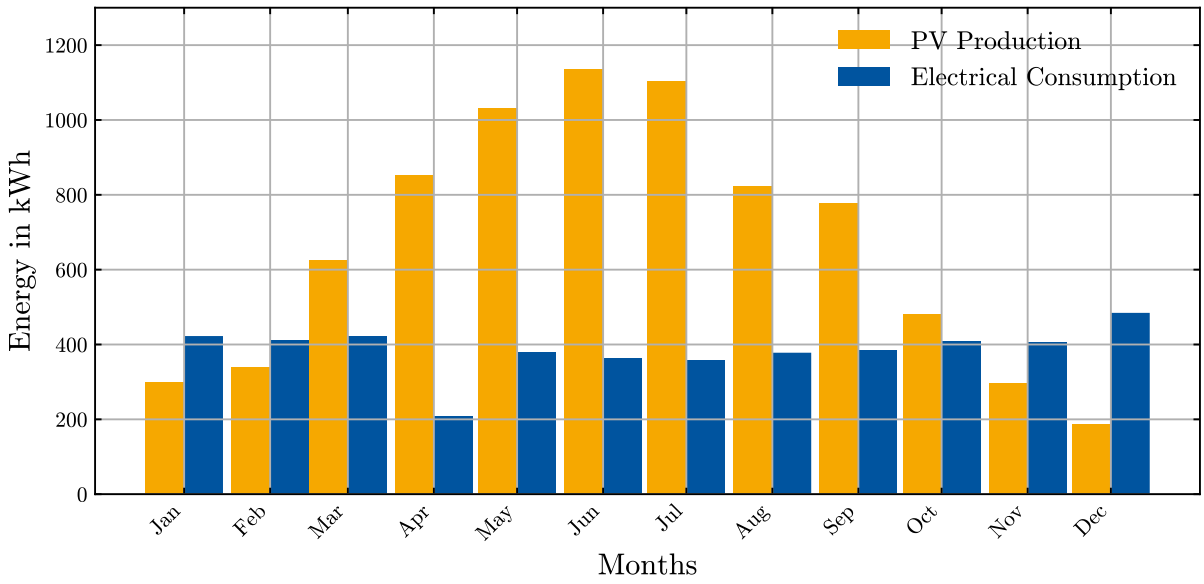

Figure 19: Monthly PV production and Electrical consumption in the Simulation

Electricity tariff: As mentioned in Section 2.1.2, electricity tariffs can vary based on different contractual designs and frequently change due to fluctuating energy prices. To enable the more potential of V2H with load-shifting, a current available two-shift TOU contract is used [85]. An energy consumption split of approximately 1:2 is assumed for night and day. Therefore, the energy consumed during the night (from 22:00 to 06:00) is billed at 0.2793 €/kWh, while the energy consumed during the day (from 06:00 to 22:00) is billed at 0.3867 €/kWh. The monthly fixed costs of the contract are already included in the kWh price, as well as levies and taxes. For grid injection, the prosumers are remunerated with a fix price of 0.08 €/kWh, independent from day and time.

Energy market data: To model the operations of the EVA within the spot market and balancing services, realistic pricing data needs to be obtained and processed. In Germany, such data is publicly available, provided by the TSOs and stock markets for reasons of transparency. Intra-day and day-ahead pricing data, aFRR power and energy prices and bids, as well as FCR prices and bids, can be found in [40] For the EPEX spot market price, the average traded price within the 15-minute interval is used. For the FCR power prices, an aggressive bidding strategy is assumed, where bids are always lower than the MCP, resulting in a 100 % participation rate. Regarding aFRR, a bidding strategy of 20 % is applied, meaning a relative position of 20 % of all bids in the merit-order list is selected to determine the participation rate. This bidding strategy is also considered as aggressive as it results in a very high participation rate. Before using the data in the model, it must be processed by applying filters and time aggregation. More details regarding the input data processing for the energy markets can be found in [80].

Figure 20 visualizes the intra-day spot market price at the EPEX power exchange for 2022, while Figure 21 visualizes the monthly average EPEX spot market price and positive and negative aFRR power and energy price for 2022. It can be observed that the prices and volatility at the EPEX spot market and for aFRR extremely raised in late summer 2022. The simulation year 2022 represents an abnormal year at the energy markets due to an energy

crises [86]. As it can be observed, the pricing data are pretty volatile and unsteady. The average price increases extremely in late summer with peak in August to October.

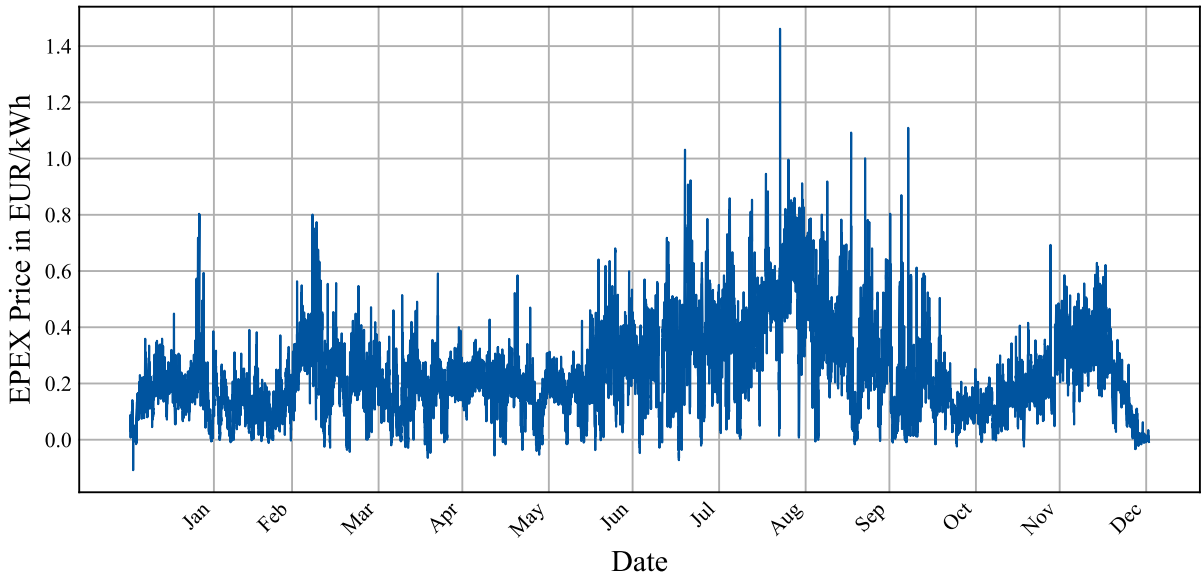

Figure 20: Average traded 15-min intra-day spot market price at the EPEX for 2022

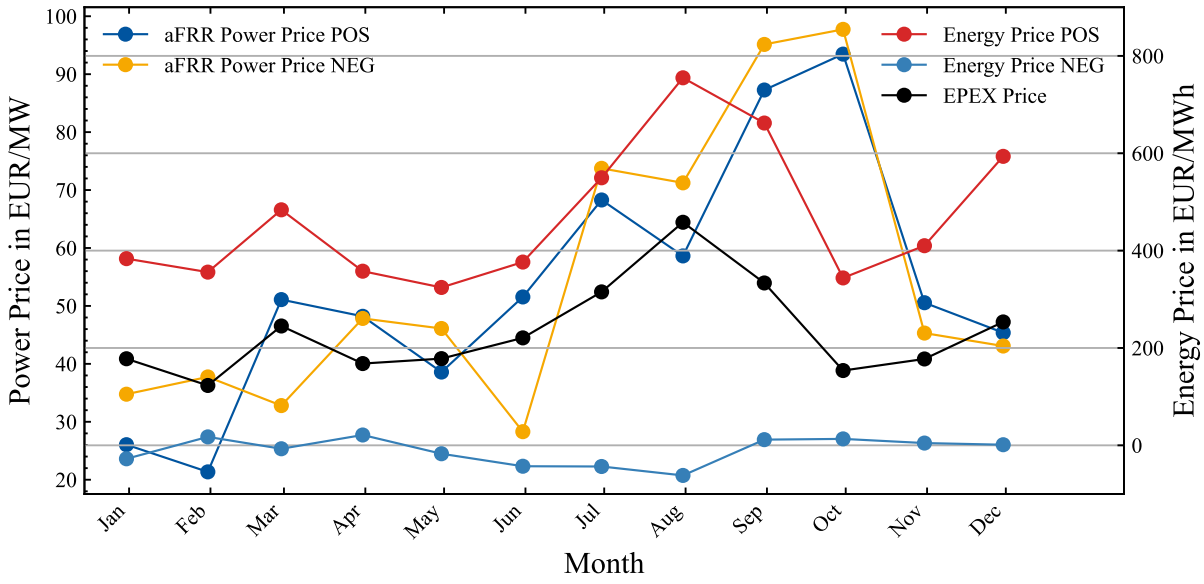

Figure 21: Average monthly aFRR power and energy and EPEX price for 2022

EV driving profiles: To generate representative and varied driving profiles for EVs, Probability Density Functions (PDFs) in form of a normal function were employed [87]. These PDFs define the probability for departure times, travel absence, and energy consumption through with defined mean values and standard deviations of the normal function. This probabilistic approach models the inherent variability and randomness in driving patterns to ensure they closely correspond to real-world behaviors, which is essential for effective modeling of the EVA operations.

The generated profiles replicate the driving patterns of a family car following a hybrid working model. The EV owner works in average two out of five days from home. On home office days, the car is not used, represented by a 60 % probability of departure for each day. The yearly driving consumption of the cars cumulates to roughly 12,000 km, assuming 20 kWh consumption per 100 km. The driving profiles were sampled from PDFs with different parameters for weekdays and weekends. Figure 22 visualizes the PDF characteristics of the generated EV driving profiles for weekday and weekend. Weekdays, representing more structured days with longer trips due to office times and less deviation than weekend trips. For weekdays, the mean departure time was set at 08:00 with a standard deviation of 60 minutes, while weekends had a mean of 13:00 with a standard deviation of 120 minutes. Weekday EV absence durations had a mean of 7 hours with a standard deviation of 60 minutes. For weekends, a shorter absence duration of 4 hours was set with a higher deviation of 120 minutes. Energy consumption per trip was modeled with a mean of 10 kWh and a standard deviation of 2 kWh for weekdays, and 20 kWh with a standard deviation of 5 kWh for weekends. After generating these profiles and ensuring the data remained within logical and realistic ranges, the data was saved as CSV files to serve as input for the model.

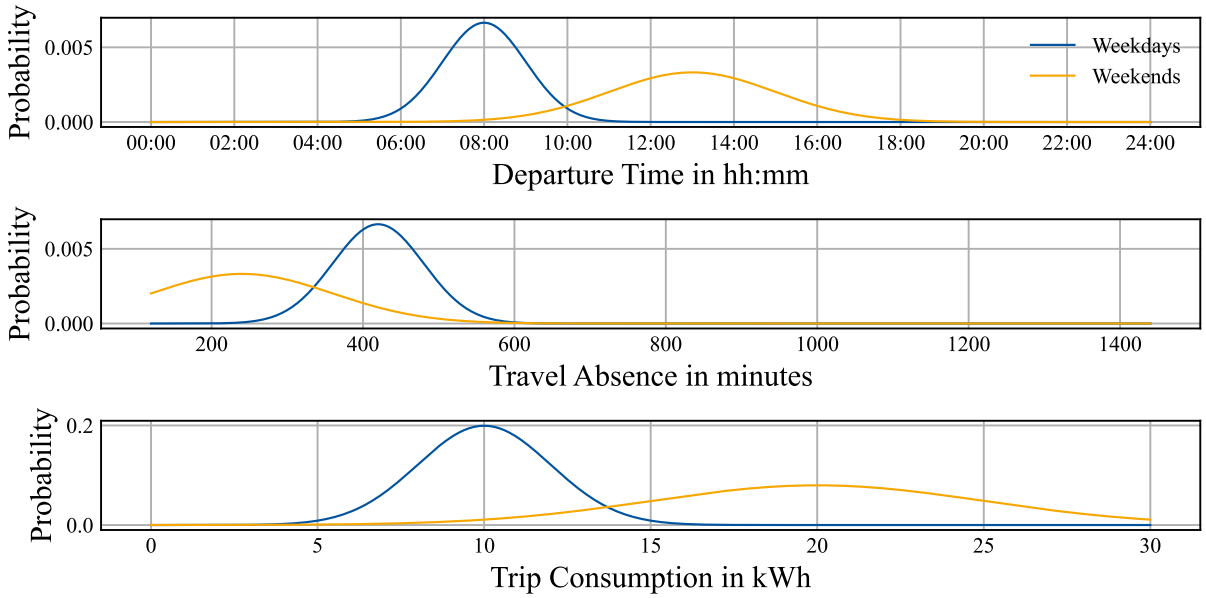

Figure 22: PDF for characteristics of generated EV driving profiles

4.3 Analysis of Simulation Results

This Chapter examines the functionality of the presented framework by analyzing the results from yearly simulations. First, a closer look into the EVA business aspects and operations is taken in Section 4.3.1. Afterwards, in Section 4.3.2 the prosumers perspective during the EV pool participation is examined. The analysis focus on comparing the three scenarios, prosumer types as well as revealing temporal patterns in the operations.

For all three scenarios an identical EV pool configuration is being used as detailed in Section 4.2. Table 5 below lists the most important characteristics of the EV pool. The annual electrical consumption does not include electricity for electrical charging. The availability of the

EV is calculated by the idle time divided through the total simulation time. It represents the share of time the EV is connected to the EVC and thus available for V2X services.

Table 5: EV pool prosumer characteristics

Prosumer	*Annual Driving Need [km]*	*Availability EV [%]*	*Annual Electrical Consumption without EV Charging [kWh]*	*Annual PV Production [kWh]*	*EVC Power [kW]*
S1	14,300	84.93	3,995	2,385	3.7
S2	13,367	85.76	4,359	2,385	3.7
S3	12,702	85.56	4,138	2,385	3.7
M1	13,415	85.76	3,849	5,565	7.4
M2	14,687	85.01	4,675	5,565	7.4
M3	13,738	85.23	4,074	5,565	7.4
L1	13,044	85.56	4,627	7,950	11
L2	13,299	85.56	4,698	7,950	11
L3	13,976	84.45	4,169	7,950	11

Due to the very high and volatile spot market prices in the third quarter of the year, the simulation for this period required significantly more computation time. This led to a more frequent increase in the relative gap, occurring in 8.3 % of the total decision periods. In 3.1 % of the decision periods, the V2H-only results were taken due to excessively long computation times for the EV pool calculation. The volatility in August, particularly for the HE scenario, made it challenging to find solutions within the given time. Consequently, the results for three weeks in August for the HE scenario were substituted with the data from the ME scenario.

Figure 23 below shows the distribution of break criteria met and their respective average iteration during the simulations. The first iteration is always the V2H-only calculation. The applied break criteria significantly reduce the computation time, while the chances of missing a significantly better result are comparably low, as this could mostly occur with break criterion 2 only. But the average iteration for this criterion is already very high at 6.9, letting assume that no improvement is expected by then.

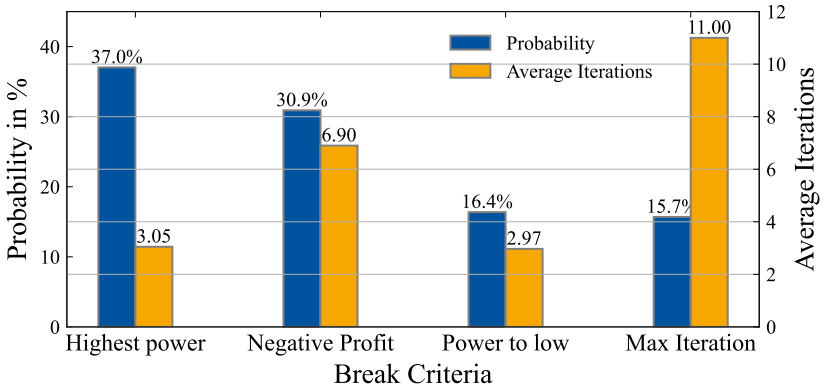

Figure 23: Analysis of break criteria met during annual simulations

4.3.1 EV Aggregator

The following analysis examines the simulation results from the EVA's perspective, focusing on profitability, operations, and pricing concepts. The EVA aggregates multiple prosumers' flexibility within an EV pool and participates in the energy market as a unified flexibility to generate revenue and lower charging costs for the EV owners. Since the EVA does not own flexibilities, they need to adapt their operations to meet the requirements of each individual prosumer. Due to this, the simulated operations will not achieve the optimal potential for utilizing EV flexibility for V2G. This potential for a single EV was analyzed extensively with the FOCUS-framework in [80]. Although, the added restrictions for minimum bid size and SOC requirements reduce profitability but therefore do replicate the EV pool behavior in a more realistic environment.

Figure 24 shows the power rates, power offered, and SOC of the EV pool managed by the EVA for a sample week in July, starting on 04.07.2022, for the ME scenario. Positive power rates represent the charge of the EV pool, visible by an increase in the EV pool SOC. High power rates due to positive aFRR are predominantly used in the afternoon hours. Bids for positive aFRR are raised significantly more often than for negative aFRR or FCR. During this summer week, the high PV production results in an abundance of surplus energy available for positive aFRR. Bids for negative aFRR and FCR are comparatively few but tend to occur during the night hours. Regarding power rates, positive aFRR causes high discharge power rates for the EV pool of up to 45 kW. The power rates for FCR and SMT are comparatively low up to 15 kW. Lastly, it can be seen that the aggregated EV pool SOC does not vary strongly and remains mostly within the 60 % to 80 % SOC window. The EV pool SOC does fall during the weekend, due to longer driving trips and thus more driving consumption.

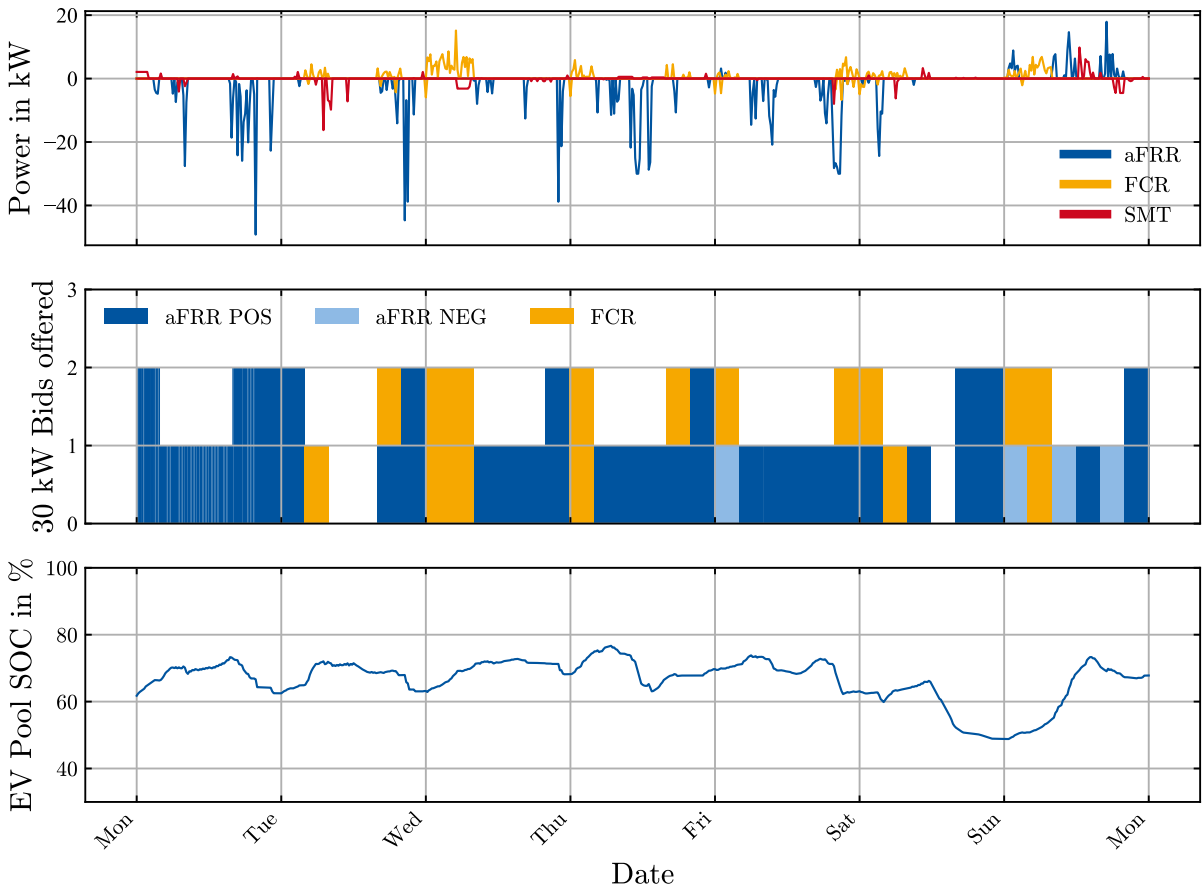

Figure 24: Power rates, offered power and SOC of the EV pool for a sample week in July

A comparison of the EVA's revenue streams for the different scenarios is shown in Figure 25 below. The EVA generates income through participation in aFRR, FCR, and SMT, while losses occur due to compensation to the prosumers for using their EV flexibility. The highest annual profit is 19,951 € for the HE scenario, followed by 19,632 € and 18,113 € for the LE and ME scenarios, respectively. As outlined in [63], the EV pool composition does strongly influence the revenue potential for the EVA. The calculated profit could possibly be improved, when optimizing the EV pool composition

Notably, aFRR is the major income source for all three scenarios, contributing over 85 % of the revenue. It can be assumed, that the higher profitability in the HE and LE scenario is mainly due to better exploitation of extremely low or high energy valuation in the model. Although the compensation for battery cycling is the highest in the HE scenario compared to the other scenarios, indicating that slightly more energy is being transferred, more compensation is done through energy exchange rather than financial payments. In the ME scenario, the highest costs for power compensation occurred, suggesting that the energy valuation of 0.23 €/kWh provides the most fair and appropriate value. Thereby the ME scenario results in more benefits for the prosumer as it will be shown later.

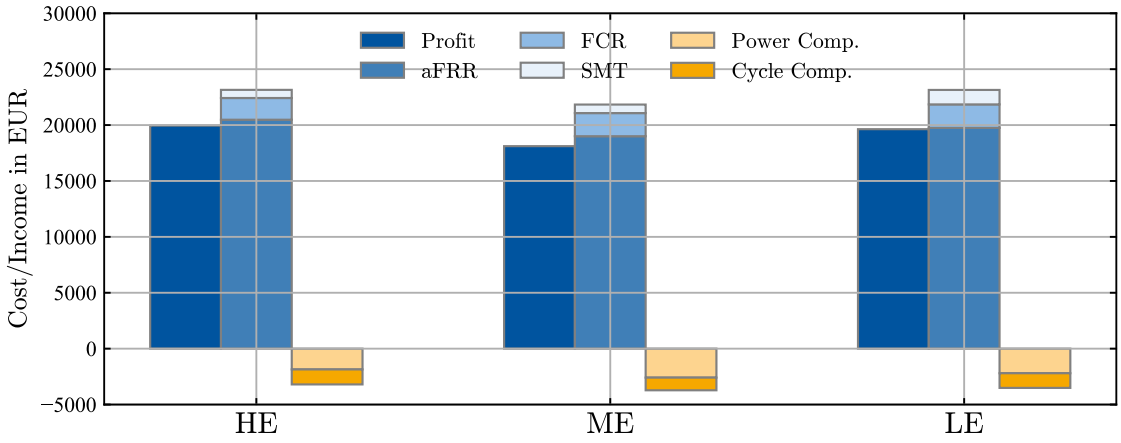

Profit	19951	18113	19632
aFRR	20478	19003	19749
FCR	1943	2070	2100
SMT	728	763	1294
Power Comp.	-1857	-2590	-2198
Cycle Comp.	-1342	-1134	-1312

Figure 25: Profitability analysis of the EVA for all scenarios

However, FCR does only contribute with a minor share to the EVA revenue, which aligns with the results from [42]. FCR is characterized by a very high fluctuation with small energy flows in both directions. In means these fluctuations does cancel out each other, so that there is no net energy exchange and thus no energy price for participating in FCR. Generally, FCR activities do still result in a slightly loss of energy due to high conversion losses of the EVC at very low power rates [88]. Although the EVA can partially counter this by utilizing the aggregation of the EV pool to concentrate the power drain on only few participants, the high rate of energy exchange causes significant battery degradation, penalized by cycle costs. Additionally, a major advantage of V2X services lies in shifting energy in time according to consumption needs. However, participating in FCR neither helps reduce surplus energy nor achieve SOC requirements for driving. Thus, the EVA in the model clearly prefers participating in aFRR over FCR most of the time.

Similar, SMT contributes only very little to the EVA revenue in every scenario. This can be attributed to several reasons. First, the applied pricing concept does not allow transferring money from the prosumer to the EVA, disadvantaging buying energy at the spot market to charge the prosumer's EV. Second, SMT is disadvantaged by the short rolling horizon of 4 hours applied in the model to replicate the dynamic decision process. As a result, trades longer than the 4-hour period, which do not yield the highest profit for the current 4-hour period are not taken. Third, the applied day-night electricity tariff for the prosumers already notably lowers the costs for electricity during the night, raising the barrier for buying electricity at the SMT, as it competes with the cheap night tariff price. It is expected, that in the case of a static electricity price, the potential of SMT would be higher.

Table 6 compares the total power offered and energy traded for the three scenarios. Further examining of the EVA operations reveals that positive aFRR was roughly used three times more than negative aFRR across all scenarios. The higher utilization of positive aFRR can be explained by several factors: First, the power and energy price for positive aFRR is significantly higher than for negative aFRR, as shown in Figure 21. This price gap is much greater than the difference for buying and injecting energy for the prosumer, considering the night tariff. Therefore, the prosumer has always the option to buy energy at a stable medium price through their local electricity tariff to directly serve their consumption needs, avoiding conversion losses. This option competes strongly with negative aFRR for receiving energy. However, selling surplus energy through grid injection is not very economical, leaving positive aFRR or direct marketing at the spot market as only economical options. Secondly, the pricing concept design allows compensating the prosumer for providing their energy for positive aFRR participation. But giving energy to the prosumer cannot be financially compensated by receiving money from the prosumer in the pricing concept design. It can be concluded that the one-way-oriented pricing concept in combination with the mentioned pricing characteristics generally favor participation in positive aFRR services over negative aFRR services.

Table 6: Total power offered, and energy traded through SMT within the scenarios

	HE	*ME*	*LE*
positive aFRR [kW]	42,870	39,420	41,100
negative aFRR [kW]	14,460	15,360	14,310
FCR [kW]	18,810	20,490	19,740
SMT buy [kWh]	3,293	2,667	2,648
SMT sell [kWh]	3,489	2,799	3,393

The difference in profitability and operations between the three scenarios is relatively small. In the HE and LE scenario, a higher participation in positive aFRR is achieved as well as slightly more SMT trades than in the ME scenario. This could be explained by the extreme high or low energy valuation. For high energy valuation, the savings from injecting energy to the grid or directly serving the electrical consumption are considered less valuable compared to the energy value. For low energy valuation, taking energy from the prosumer can be more easily compensated due to a low energy valuation. Hence, the EVA can more freely decide how to use the energy, exploiting the compensations for its operations.

Next, the results are analyzed regarding temporal dependencies. Figure 26 shows the monthly EVA profit as well as the power reserved throughout the year for the HE scenario. The figures for other scenarios can be found in the appendix. A noticeable drop in August is observed. As mentioned earlier, the extremely volatile and abnormal energy market prices during this period caused difficulties in solving certain time steps. To complete the simulation within the available time, certain time steps had to be substituted with V2H-only results when a solution could not

be achieved within a specific timeframe. This issue occurred particularly in August, resulting in a drop in EVA profit for that month. On one hand, it is estimated that the profit for August would be approximately 1,000 € higher for the year 2022 under normal conditions. On the other hand, 2022 was characterized by unusual energy prices, and the overall EVA profit in a typical year would likely be significantly lower.

However, the EVA profit shows a strong correlation with the energy market prices as the profit increased by almost fourth fold from deep in February to peak in September. At the same time, the power provided only increases by up to 32 %. This makes clear that significant share of EVC power is not strongly contested for V2G. This is also evident from the high share of 71 % for 0 €/kW*h power prices the optimization determined, as it will be discussed below.

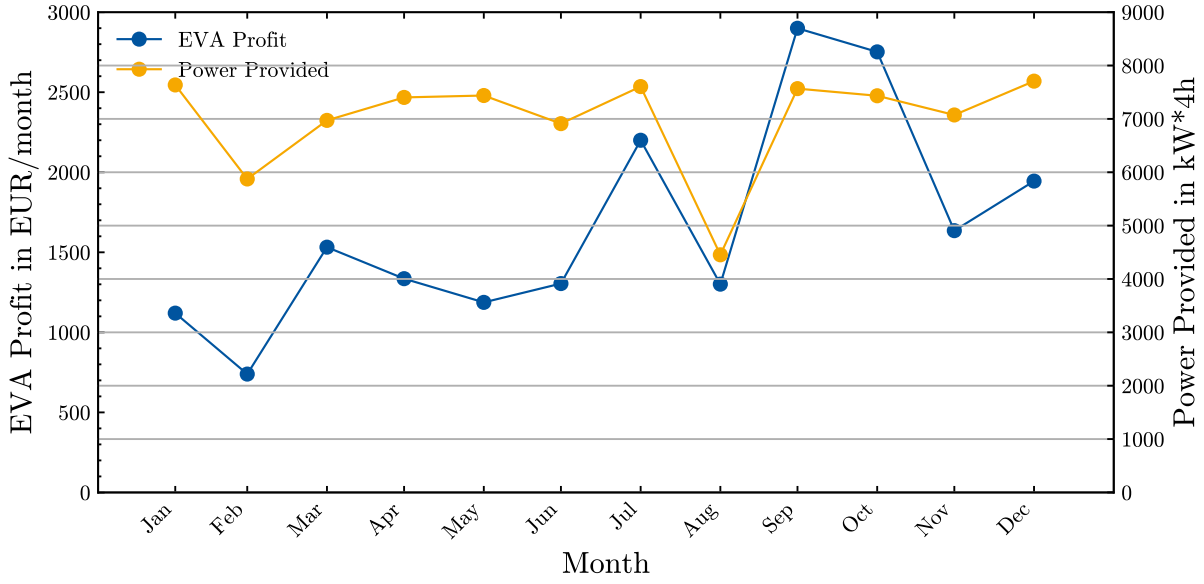

Figure 26: Monthly EVA profit and power reserved in the HE scenario

Since V2H and V2G compete for the limited power of the EVC, it is expected that this competition shifts in favor of V2G during the winter months. In the summer, when the solar PV system generates high amounts of energy, more power is required for storing the surplus energy. However, due to the abnormal changes in energy market prices in 2022, this assumption cannot be validated within this simulation.

Subsequently, the daily distribution of the EVA profit and power price is analyzed. During the yearly simulation, a power price of 0 €/kW*h led to optimal results in 71 % of the decision time steps where V2G was conducted. V2G was conducted in 85 % of the decision time steps. To understand these results, several aspects need to be highlighted. Firstly, the calculated power price is the optimized price for an optimal operation plan and power allocation, resulting in the lowest power prices possible. Translated to real-world conditions, this power price represents the lowest bound, not considering significant benefits for the prosumers or competition with other market participants. Secondly, a significant share of roughly half of the prosumer financial compensation is done through individual cycle costs payments. If only a power price is to be paid, this would increase significantly. Thirdly, the short decision period of 4 hours disadvantages load shifting for V2H and SMT. But the EVA has the attractive option to

participate in balancing services, while load shifting represents a major value stream of V2H. This possibly worsens the attractiveness of V2H for certain decision periods, making lower power prices more often sufficient.

Figure 27 visualizes the statistical analysis results in form of a boxplot diagram of the EVA profit and power price for the different time slots of the day. Only the results for the ME scenario are shown, since the differences between the scenarios are not significant. Results for the other scenarios can be found in the appendix. Only the power prices from decision steps that yielded a minimum profit of 2 € were included to filter out V2H-only and insufficient profitable periods.

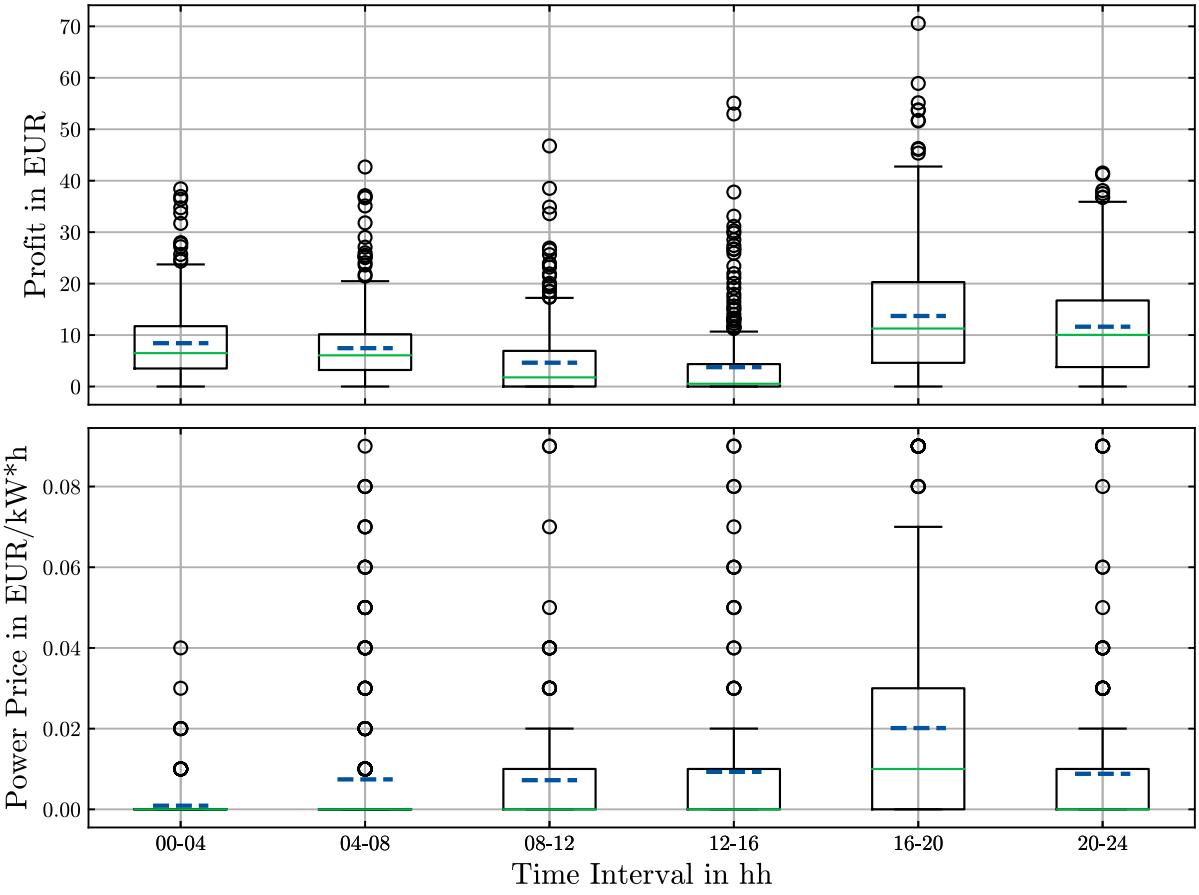

Figure 27: Temporal boxplot of EVA profit and power price for the ME scenario

The EVA profit remains fairly constant during the night, averaging 8-9 €/4h, and then slightly decreases to 5-7 €/4h for the time slots from 8 am to 4 pm, mainly due to the absence of EVs. The time slot from 4 pm to midnight represent the highest profitability for the EVA, with an average of 13-15 €/4h and a high spread. This corresponds to slightly higher aFRR prices and typical consumption peaks in the evening hours as it can be seen in the aFRR price analysis in the appendix. Additionally, the fully charged EV battery after the solar PV production period and the diminishing solar PV production rate encourage V2G services, especially highly economical positive aFRR during that time.

The statistical analysis of the power price shows similar patterns. During the night hours, the availability of the EV is secured and the competition with V2H is constantly low. Hence, the prosumer provides the required power without high power prices, as compensation through cycle costs and energy exchange is sufficient. Because of this, for most decision periods the optimal power price remain zero. During the day, with increased electrical consumption and solar PV production, as well as the need to charge the EV, the competition is generally higher, resulting more often in a higher power price. The average power price from 8 pm to 16 pm is around 0.01 €/kW*h, while the median remains at zero. Particularly between 4 pm and 8 pm, a high average power price of 0.02 €/kW*h and median of 0.01 €/kW*h is met due to typical peaks in the consumption pattern and arrival of EVs. This leads to high competition between V2G and V2H, resulting in higher power prices.

Overall, it can be concluded that a two-shift TOU power price scheme could be appropriate for the power price design. During the night (midnight to 8 am), a low power price 0 €/kW*h is sufficient, while a higher power price of 0.1-0.2 €/kW*h covers most periods during the day (8 am to midnight) in the simulation. As mentioned before, for a real-world application, a generally higher power price by 0.01 €/kW*h could be considered on top in order to encourage prosumers to adapt their behavior and to strengthen the market position. As it was seen in Figure 25 the cycle compensation contributes to a significant amount of the total payments. A pricing concept design without an individual compensation for the battery aging incurred would result in even higher power prices. It is estimated that roughly 0.01 €/kW*h additional power price for every time slot could be added in that case. This estimation does not consider changes in the EVA operations, resulting from such a change in the pricing concept. However, a significant spread of the power price can be seen during the day, indicating that a dynamic pricing scheme is more efficient to cover these variations.

Next, Figure 29 visualizes the average offered power for positive and negative aFRR as well as FCR for different time slots for the ME scenario. It becomes evident that positive aFRR is particularly utilized in the evening hours. As mentioned before, the evening hours offer extremely attractive conditions due to the high aFRR price, the constant availability of the EV, and the stored surplus energy. Even though some EVs are unavailable during the day for storing surplus energy, the aggregation benefits of the EV pool compensate for this. In such cases, the power is provided by all participating prosumers, but the energy is mainly drawn from those with a high SOC. The reduced provided power during the day is due to the absence of EVs. Interestingly, during the night, more power for negative aFRR is offered, representing an economical way to charge EVs that need to depart the next morning. Similarly, FCR is primarily offered during the night, from 8 pm to 8 am. Particularly, most power is used for FCR between midnight and 4 am. This can be explained by higher FCR prices at night and a reduced need to charge or discharge the EV. Additionally, more EVs are available at night, allowing for more bundled energy transfer and reducing conversion losses at low power rates of the EVC.

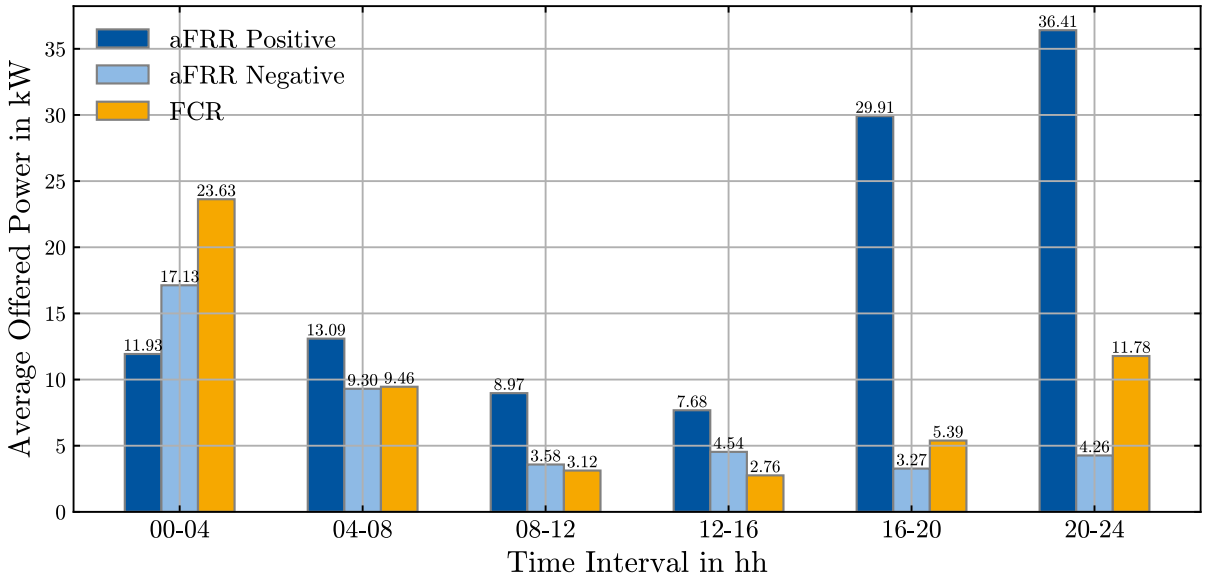

Figure 28: Average offered aFRR and FCR power per time slot for ME scenario

4.3.2 EV owner

In this Chapter, the simulation results from the prosumer perspective are examined, focusing on the resulting costs and customer satisfaction. The three scenarios and prosumer types are therefore compared. To ensure that the model is properly designed and considers the individual needs of the prosumer, an additional comparison with a V2H-only reference scenario is conducted. From the EVA perspective, it is evident that the model generates a positive profit. However, it is necessary to verify whether the model's operation plan benefits the prosumer. This is crucial because the reformulation of the bi-level model into a single-level problem does not directly optimize the prosumer's electricity cost reduction. The reference scenario captures the identical model configuration, input data, and RH setting but do not allow V2G.

First, Figure 29 shows the various power rates for prosumer L2 in the ME scenario for a sample week in July. Driving consumption and electrical consumption are visualized as negative power rates, while EV charging through the grid is represented as positive rates in bright blue. V2H is depicted as positive power rates when charging the EV from the solar PV generator and as negative when discharging the EV to serve electrical consumption. Discharging the EV to inject energy directly into the grid did not occur during this week. The power rates for V2G refer to the positive and negative energy exchange due to aFRR, FCR, and SMT, managed by the EVA.

Naturally, when the EV is driving, no charging or discharging of the EV through the EVC can occur. When the EV is available during the day, V2H is used to charge the EV with surplus energy, though with a limited amount of power. During the afternoon, the EV can be discharged to serve the electrical consumption needs, as seen on the last day. However, relatively low power rates of up to 6 kW are observed for V2H, which can be attributed to a certain share of power reserved for V2G. Higher power rates of up to 11 kW are used for V2G or direct charging of the EV from the grid. Direct charging the EV from the grid is only done before departing for a trip to meet the minimum SOC restrictions, with high charging rates of up to 11 kW observed.

The V2G applications results in many mini cycles of the EV battery, as seen in the second plot, where the SOC of the battery remains always within the 30-80 % SOC range. Most of the time, even smaller cycles between 50-80 % SOC are conducted.

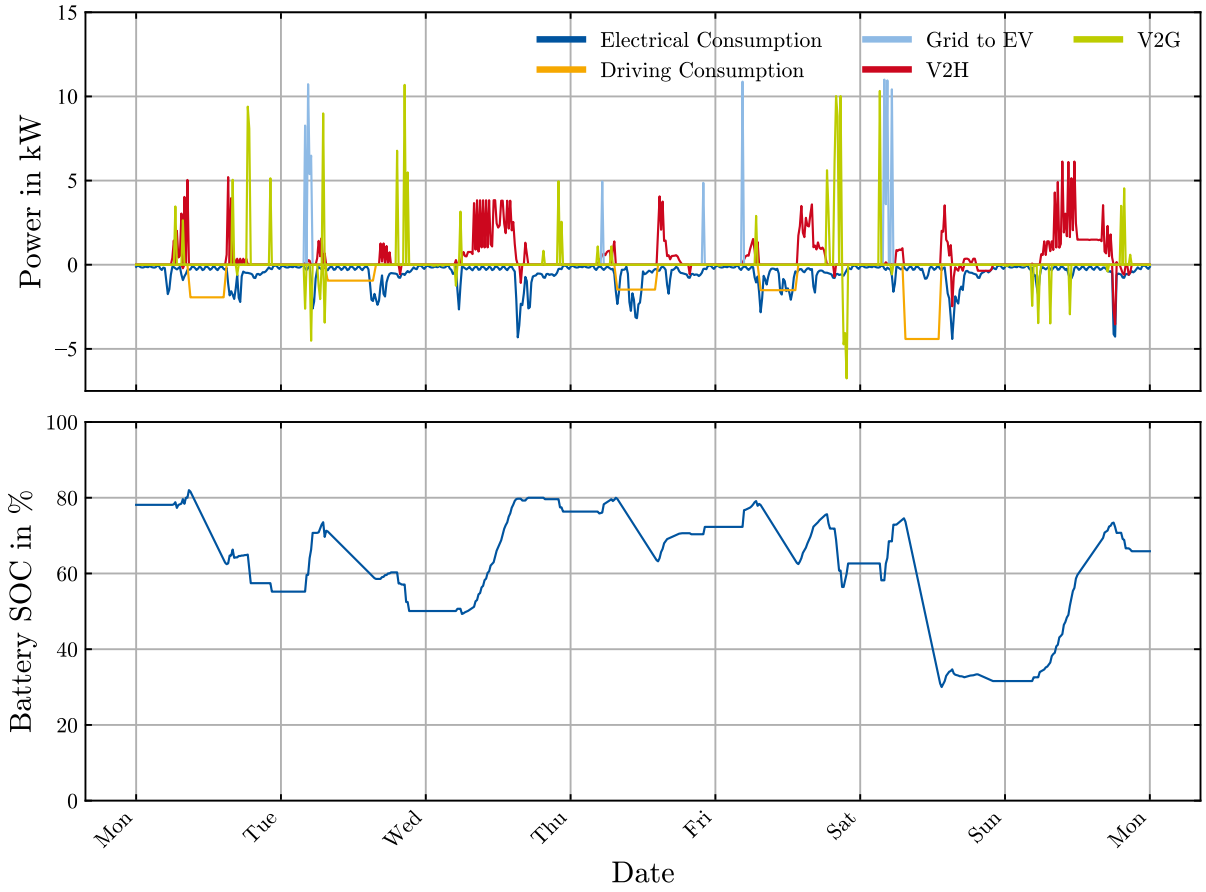

Figure 29: Prosumer L2 power rates and SOC for a sample week in July

Figure 30 compares the average prosumer costs and incomes for each scenario. In the bi-level model, the decision function ensures that the prosumer only accepts the offer if it provides at least a minimal benefit for this decision period. The benefit can be achieved financially or through energy exchange. Considering this, the operations from the bi-level model should result in at least slightly lower costs for the prosumer than in the V2H-only case. As expected, this is observed across all scenarios. The average costs for the prosumer in the V2H scenario are 1,025 €, while in case of EV pool participation the final costs for the prosumer are 834 €, 711 €, and 798 € for the HE, ME, and LE scenarios, respectively. As mentioned in the previous Section, the ME scenario does yield in the lowest profit for the EVA but therefore in the lowest costs for the prosumer. Thus, the ME scenario provides the most appropriate and fair energy valuation, enabling more balanced operations in favor of the prosumers.

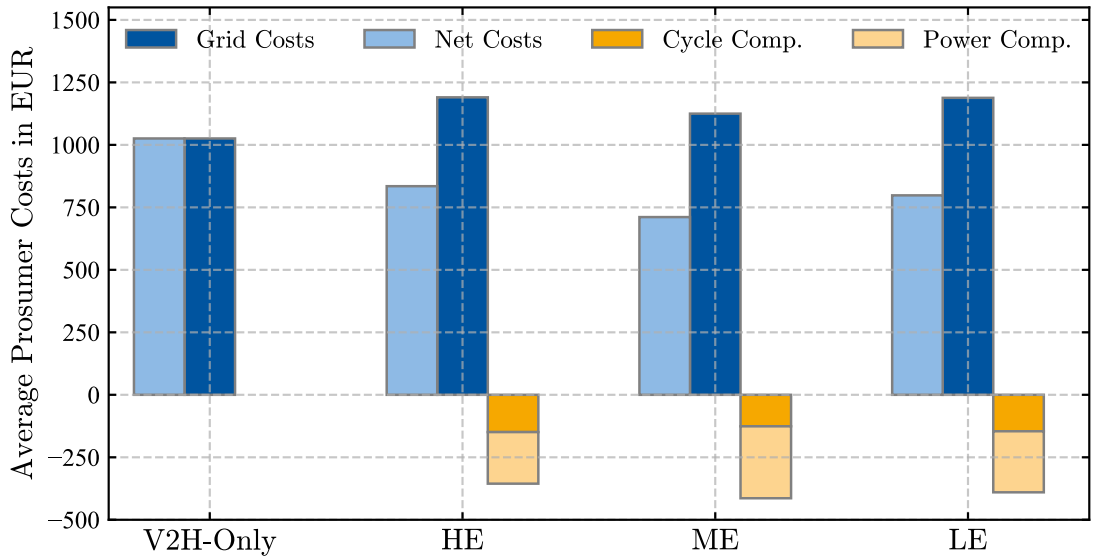

Net Costs	1025.62	834.68	711.13	798.04
Grid Costs	1025.62	1190.20	1125.00	1188.16
Cycle Comp.	0	149.16	126.03	145.83
Power Comp.	0	206.36	287.83	244.29

Figure 30: Average prosumer costs for different scenarios

However, economic benefits are not the only decision criteria for encouraging EV owners to participate in the EV pool. When installing bi-directional charging infrastructure for V2X services, additional criteria for customer satisfaction such as grid-autarky and incurred battery degradation can play a decisive role for the decision. Figure 31 shows the resulting grid-autarky and Equivalent Full Cycles (EFC) for all scenarios. Here, grid-autarky is defined as the total consumption need minus the energy sourced from the local grid connection at the prosumer's electricity tariff conditions in relation to the total consumption need. The total consumption need includes both electrical and driving consumption in order to properly evaluate the V2G impact. In case of V2H-only the grid-autarky match the common definition of self-sufficiency [60]. The EFC refers only to the additional cycles due to bi-directional charging and excludes the driving of the car, which corresponds to roughly 43 cycles a year when driving 13,000 km.

The results show that V2H application alone incurs significantly fewer additional EFC than a combined V2H and V2G strategy. The operation plan of the ME scenario resulted fewest additional EFC with an average of 31. Similar, all three scenarios yielded a lower gird-autarky than the V2H-only reference scenario. This aligns with the high utilization of positive aFRR, suggesting that utilizing surplus energy for balancing services, especially positive aFRR, is often more economical than using it to cover consumption needs. Still the ME scenario results in the highest grid-autarky degree at 34.06 %, compared to the other EV pool scenarios, indicating overall the highest customer satisfaction and economic benefits.

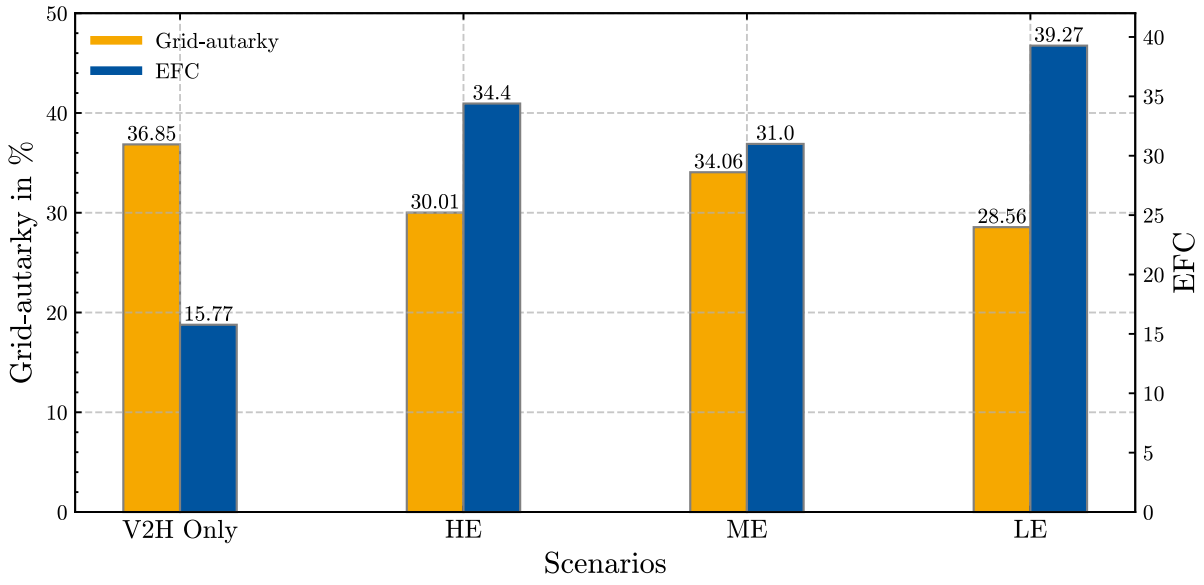

Figure 31: Average prosumer grid-autarky and EFC for different scenarios

Next, a more detailed look into the differences between the prosumer types within the EV pool is given. The focus is set on the ME scenario, as it yields the highest prosumer benefits. Figure 32 shows the average prosumer costs and compensation for the three prosumer types S, M, and L.

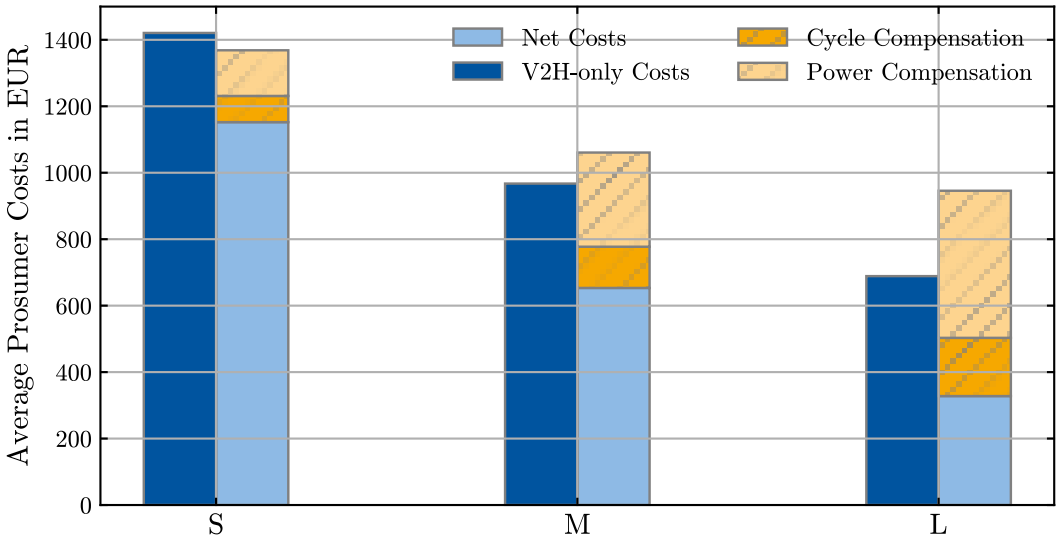

V2H-only Costs	1420.65	967.35	688.85
Grid Costs	1368.48	1060.73	945.77
Cycle Comp.	78.83	124.08	175.18
Power Comp.	137.41	283.39	442.69

Figure 32: Cost comparison of prosumer types for ME scenario

Obviously, larger prosumer sizes lead to lower electricity costs due to increased solar PV production in V2H-only and EV pool scenario. However, it can be observed that both the absolute compensation from the EVA and the relative share of net cost reduction increase with larger prosumer sizes. The net costs are calculated by subtracting the compensation payments from the grid costs. For prosumer type L, financial compensation payments reduce electricity costs by 52 %, whereas for prosumer type M and S, it accounts for only 32 % and 18 %, respectively. This also emphasizes the higher potential for prosumer type L to benefit from an increased power price. The average prosumer L would gain 572 € annually if the power price is raised by 0.01 €/kW*h in every decision period, assuming no change in the EVA's operation plan. In that case the prosumer type L would have reached negative total costs. This allows to conclude, that a larger EVC power size significantly improves the profitability for the prosumer. Notably, prosumer S achieves even without compensation payments lower total costs than in the V2H-only scenario. This can be explained by a higher amount of energy received through the EV pool participation, as it will be seen in the increased grid-autarky rate next.

In the following, the customer satisfaction among different prosumer types is compared. Figure 33 visualizes the participation rate and grid-autarky for the three prosumer types for the ME scenario. The results for the other scenarios can be found in the appendix. The participation rate is defined as the ratio of provided power to total power possible to provide. Here, the absence of the EVs due to their availability is taken into account, theoretically making it possible to reach a 100 % participation rate.

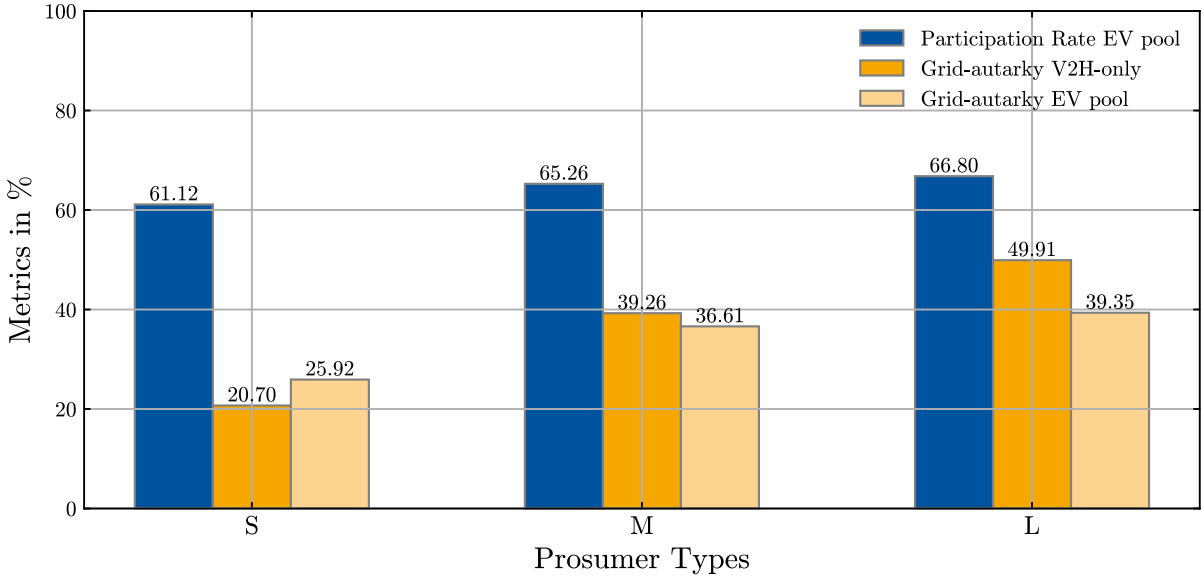

Figure 33: Grid-autarky and participation rate among different prosumer types

As previously observed, prosumer L benefits economically the most from participating in the EV pool. However, this does not apply in terms of customer satisfaction. Through EV pool participation, prosumer type L reduces their grid-autarky degree from 49.91 % to 39.35 %. Conversely, prosumer type S self-sufficiency rate increases from 20.70 % to 25.92 %. It can be assumed that the ratio between electrical consumption and PV production is decisive for this. Prosumer S generally lacks sufficient energy to satisfy their consumption needs, as these remain constant across prosumers, while the production rate increases with larger solar PV

systems. The specific need for prosumer S is indirectly implemented in their decision function, as they are more likely to accept an offer when receiving energy, creating the highest value for them. The model adapts the energy distribution accordingly to the specific needs of the prosumers. Conversely, prosumer L has more cheap surplus energy available, allowing to take energy from them and using it for positive aFRR. In exchange, prosumer type L favors more likely to receive a financial compensation.

Therefore, it can be concluded that the model adapts the operation plan and energy distribution according to the prosumers' needs and situations. This emphasizes the strengths and benefits of EV pool aggregation compared to single flexibility participation. In the end, the slightly lower participation rate for smaller prosumer is observed, which can be explained by higher competition for the limited power with V2H.

Lastly, the additional incurred EFC due to V2X applications are visualized in Figure 34 for the three prosumer types. It is evident that larger prosumers are significantly more utilized for energy exchange than smaller prosumers, since they have generally more surplus energy to provide as explained before. Thus, the battery of larger prosumer is therefore more often discharged and charged than for smaller prosumers, which generally lack of energy. Considering the typical lifespan of an EV, a certain number of additional cycles is acceptable for the EV owner, although this strongly depends on battery characteristics, external conditions, and further product usage.

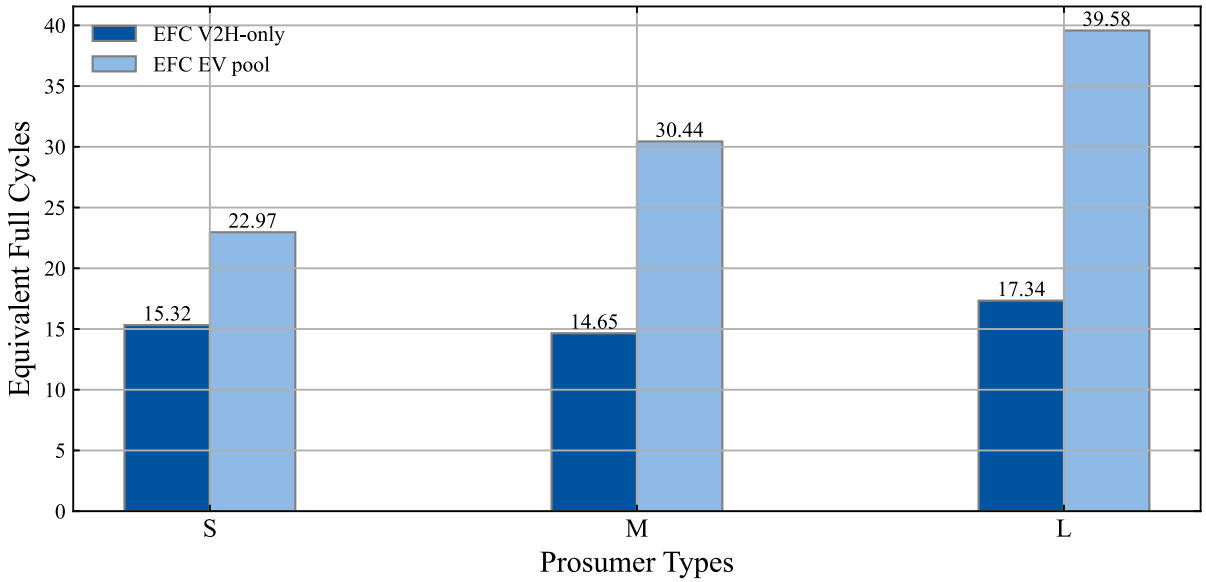

Figure 34: EFC incurred for different prosumer types

Also, additional factors, such as DOD, SOC regime and power rates do also play a decisive role for battery aging [57]. Within the developed model, battery degradation sparing assumptions were applied, limiting the SOC range for V2X applications from 30 % to 80 % SOC. This significantly reduces degradation effects due to cyclic and calendric aging, as shown in [57]. Especially utilizing the advantages of an aggregated EV pool allows compliance with such a tight SOC range without significant performance losses. As it can be observed in Figure 29, the maximal DOD is 50 % of SOC, due to the SOC restriction, while many mini

cycles at a DOD of roughly 30 % are conducted due to V2G. Thus, most of the additional EFC due to V2G are conducted with a sparing DOD within a sparing SOC regime. Nevertheless, for larger prosumers a general higher power rate is observed. It should be validated, if implementing power rate reducing functionalities do significantly impact the V2G services of the EV pool.

Also, it should be validated whether the applied static cycle costs of 0.10 €/kWh are reasonable. With higher cycle cost values, the model would adapt the operation plan to reduce the EFC incurred. Additionally, the size and composition of the EV pool can play a significant role. The configured EV pool with a total size of 66 kW is relatively tight compared to the possible double bid size of two times 30 kW for reserving power at the balancing market. Hence, only 6 kW are available for other value streams in case of two bids offered, which likely limits available EVC power for serving the household electrical consumption need.

5. Conclusion

This Chapter draws a conclusion on the presented framework and analysis for critical reflection of the work. In the end, an outlook for possible future work is given.

5.1 Framework

The EV Aggregator (EVA) serves as an intermediary entity between EV owners and the energy market, facilitating private individuals' access to the energy market and thereby unlocking the flexibility potential of EV batteries. However, the competition with individual prosumers' interests forces the EVA to craft a compelling business model that presents an attractive value proposition, encouraging them to participate in the EV pool rather than opting for individual V2H applications. Depending on the generated price incentives, prosumers adapt their consumption behavior and participation choices, which, in turn, impact the EVA's operations and strategy.

This work presents a bi-level optimization framework to capture this strategic interaction between the EVA and prosumers in a dynamic and competitive Stackelberg game for analyzing pricing and operational concepts. Building on the existing FOCUS-Framework [21,80], the developed framework allows within a customizable EV pool and prosumer configuration to concurrently maximize the EVA profit and minimize prosumers' electricity costs. This framework considers multiple value streams, such as increased PV self-consumption, load shifting, energy arbitrage, aFRR, and FCR participation. Furthermore, the framework enables a dynamic decision-making process to determine an appropriate power price for every decision period offered to the prosumer. To facilitate this dynamic decision process, the rolling horizon method is applied for temporally decomposing the problem into sub optimization problems with one day horizon and a decision period of 4 hours. As a result, optimized operation plans for the EVA’s energy market participation and prosumers' charging schedules are generated.

Within this work, new functionalities and adaptations to existing classes were made to cope with the new strategy of an EVA. Therefore, the EV pool is connected via a new VirtualAggregator class, which strictly reserves the EV charger power share according to the offer. To simulate real conditions for the EV pool, minimum bid size restrictions for balancing services and SOC restrictions are implemented. The resulting non-convex bi-level MILP optimization problem is solved by applying the reformulation method, which reduces the bi-level problem to two dedicated single-level problems. At the heart of this reformulation method, a decision function in the EVA´s Energy Management System decides whether the prosumer accepts the offer based on a predefined benefit for the prosumer. Respective cost-value functions calculate the benefit for each offer by capturing the costs, compensation payments, and deviations in battery SOC for each prosumer and decision period. By this adaptation, the participation choice and energy distribution in the model are optimized according to the needs of the prosumer and EVA profit maximization efforts. By integrating the prosumers' electricity costs in the upper-level model, a precise assessment of all value streams at every moment is achieved. Since battery degradation is a major counter-argument for V2X applications, cycle

costs and a limited SOC range for bi-directional charging are implemented based on recommendations from the literature to reduce battery aging effects [57].

A general hurdle in solving bi-level optimization problems is the resulting high computation time. Several modeling techniques were applied and validated to achieve a user-friendly computation time without significant losses in quality. However, extremely long computation times for certain simulation periods are still encountered, when the energy market data shows enhanced volatility in late summer 2022. While the framework simplifies calculations, it does not fully capture the real-world uncertainties an EVA faces when planning its operations. V2G operations are idealized, excluding complexities such as bidding strategies, which may not fully represent the competitive nature of energy markets. The model also does not account for competition with other EVAs. Additionally, the short decision period of 4 hours disadvantages long-term trades on the spot market. To overcome this, longer decision intervals or an individual financial payment for the energy exchanged should be introduced to fully promote long-term energy trading.

5.2 Simulation Analysis

The analysis of the yearly simulation results provided critical insights into the operations and profitability of the EVA and the impact on prosumers. During model evaluation, three scenarios (HE, ME, LE) with different energy valuations were analyzed to assess the effectiveness of the developed bi-level model. The pricing concept allows compensation through energy exchange and financial payments based on the power provided and battery aging incurred. A heterogeneous EV pool composition is used for all three scenarios, containing nine prosumers (S, M, L) with a total charging power of 66 kW. The prosumer usage patterns were statistically modified to account for the randomness in individual behavior.

For the simulation year 2022, the EVA achieved the highest annual profit of 19,951 € in the HE scenario, followed by 19,632 € and 18,113 € in the LE and ME scenarios, respectively. It can be assumed that the EVA can better exploit the extremely high or low energy valuation, resulting in less benefit for the prosumers. Results show that FCR and SMT contribute only minimally to the revenue, with FCR characterized by high energy exchange rates, which lower profitability due to conversion losses and battery degradation costs. SMT is predominantly used for compensating the prosumer through energy exchange, especially in the HE scenario. Notably, over 85 % of the EVA’s revenue is earned from participating in aFRR, highlighting its major role in the EVA's business model. Positive aFRR is utilized approximately three times more than negative aFRR due to higher associated power and energy prices and the high availability of surplus energy from the participating prosumers. Additionally, the pricing concept design favors positive aFRR since the EVA can compensate the prosumer financially for taking their energy but not the other way around. Temporal analysis indicated that the EVA's profitability closely correlates with spot market and aFRR prices. Up to a fourfold difference in profit between months is observed, raising questions about the stability of the EVA business model. Even at low market prices, considerable high amount of power is provided for balancing services, indicating that a significant share of EVC power is not contested for V2G services.

Further daily analysis of the EVA operations showed that the highest profitability is achieved during evening hours (4 pm to midnight), due to availability of EVs, stored surplus energy and slightly higher aFRR prices. Similar patterns are observed for the analysis of the power price. The simulation results suggested that a two-shift Time-of-Use power price scheme could be appropriate, with low power prices around 0 €/kW*h during the night (midnight – 8am) and higher prices around 0.01 – 0.02 €/kW*h during the day (8 am to midnight). These prices represent the lowest price possible to be offered in optimal conditions. Additionally, roughly half of the compensation payments were invoiced for individual cycle cost payments. If these aspects were included in the power price, it is estimated that roughly 0.01 – 0.02 €/kW*h can be added on top to the power price during the day to account for a higher prosumer benefit, battery aging, and securing market position. However, the high share of 71 % zero power price in combination with a high spread during the day indicates that a dynamic pricing scheme could be more appropriate to capture these dynamics.

From the prosumer's perspective, prosumers do benefit economically from participating in the EV pool. The ME scenario yielded the highest prosumer benefits and customer satisfaction, indicating the most balanced and fair energy valuation. The average prosumer could reduce its electricity costs by a further 31 % compared to the V2H-only scenario, while the large prosumer even gained a 52 % cost reduction. This highlights the larger potential from more EVC power in combination with a larger PV system, which can even lead to negative total costs when power prices were adapted as recommended.

Generally, the grid-autarky is lower in the EV pool scenarios compared to the V2H-only scenario, indicating that at some moments higher earnings from giving surplus energy to the energy market than serving own consumption needs can be achieved. Notably, prosumer S could improve their grid-autarky from 20.70 % to 25.92 % through EV pool participation, while prosumer L’s grid-autarky decreased from 49.91 % to 39.35 %. This highlights that the model adapts operation plans according to energy needs of each prosumer. The additional equivalent full cycles caused for different prosumers sizes, range from 23 to 40 with a maximum DOD of 50%. Even though battery degradation sparing restrictions are considered, these additional cycles could shorten the lifespan of the EV. Also, further investigation should be done to determine a dynamic cycle cost value to account for different EV costs, changing external conditions, and intended uses.

Overall, the bi-level model effectively captures the interactions between the EVA and prosumers for determining a power price, while demonstrating the feasibility and significant economic benefits of aggregated EV pool operations. The findings underscore the importance of tailored pricing schemes to optimize both economic and operational outcomes for all stakeholders involved.

5.3 Outlook

Building upon the work presented, future investigations should aim to further extend the framework functionalities to more efficiently examine EVA operations and pricing concepts in a more realistic environment. Initially, the framework should be used for further simulations with more extended and advanced pricing concepts, considering individual bi-directional

payments. This will provide a more comprehensive understanding of the interaction between the EVA and prosumers in the dynamic Stackelberg game environment.

Future studies should also consider incorporating a more representative modeling of the competitive landscape. Currently, the model simplifies V2G operations and does not completely account for the complexities of bidding strategies, the unpredictability of prosumer behavior, or competition with other EVAs. Introducing these elements could provide a more realistic assessment of the EVA's market dynamics and competitive positioning, which is crucial for prosumer interaction. However, these additional features will likely increase computation time. Therefore, further framework development should aim to implement more time-efficient solving approaches to accommodate these enhancements.

In the author's view, a significant avenue for future work is to evolve the role of the EVA beyond its current scope, positioning it as a more holistic energy manager, which would substitute the current electricity provider. In this more integrated role, the intermediary entity would expand its functionalities beyond flexibility and charging management of EVs towards energy optimization and commercialization for all energy assets of the prosumer within the aggregation pool. By doing so, a cooperative environment between the intermediary entity and the prosumers could be achieved, entirely optimizing benefits for all participants. This approach would fully unlock the aggregation and flexibility potential of private prosumers and offer a major step towards energy transition.

Appendix

1 Workflow

A more detailed examination of the workflow within the individual models is now presented. Figure 35 illustrates the most essential classes and functions for the workflow of the models. Both models share almost the same workflow. The grey-shaded boxes are used specifically for the UL-Model. The process begins with the 'runme' file, which sets up the input files, model parameters, strategy, and creates the `MainProsumer` class. This class is instrumental in generating `Prosumer` objects and accessing their functions. During the initialization of the prosumer object, the component classes are created and linked according to the model configuration. Subsequently, the `optimize_sizing` function calls the `build_model` function, which generates the `OptimizationModel` object by invoking the `add_variables` and `add_constraints` functions of each respective component. It also defines the strategy of the optimization through using `implement_strategy` of the `EMS` class, which sets the optimization objective. In the case of the UL-Model, additionally the function `add_EVA_constraints` is called and the classes `FCR` and `aFRR` are created. After constructing the model, it is solved using the Pyomo function `solve`. The results are then transferred to the `save_results` function to be stored in an Excel file.

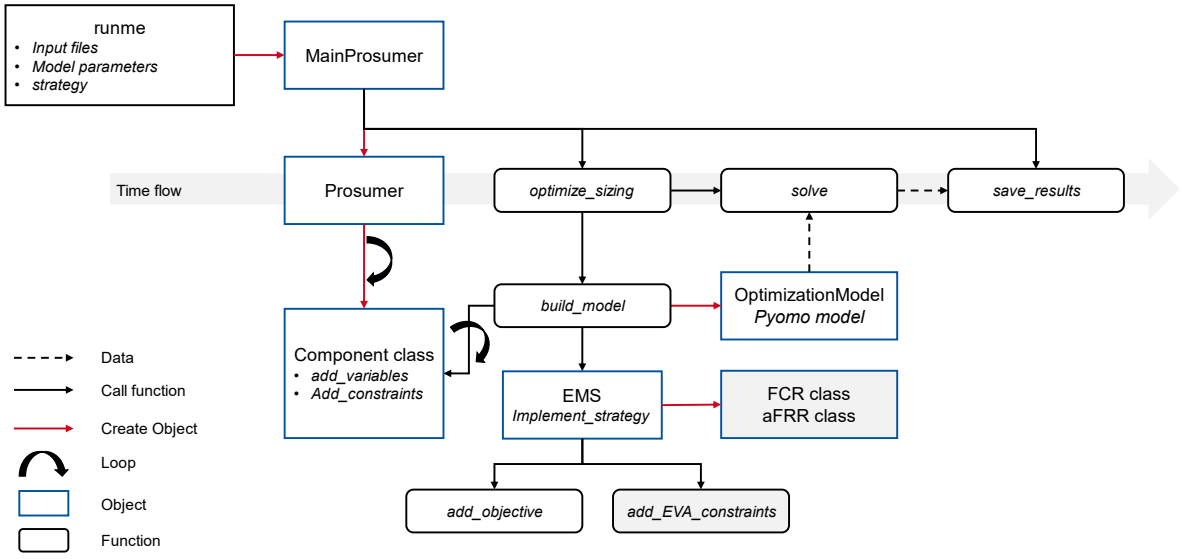

Figure 35: Workflow of the LL and UL-Model

2 Input Data

The table below shows several other input data used in the simulations, which were not explained in detail in the thesis. Among these is especially the efficiency of the PV inverter, EVC and battery system. For the EVC the data for a dynamic bi-directional inverter was used

from the model “STP-7000TL-20” from SMA. The non-linear efficiency curve is characterized by the six parameters below.

Table 7: Efficiency values for PV Invert, EV Battery and EVC

System	***Parameter***	***Value***
PV Inverter	η_{PV-INV}	0.9694
EV Battery	η_{EV}	0.99
EVC	P_1	0.05
	P_2	0.1
	P_3	0.75
	η_1	0.88
	η_2	0.928
	η_3	0.973

3 Analysis

Figure 36 – 44 show the presented analysis results for the remaining scenarios to complement the presented analysis in Chapter 4.

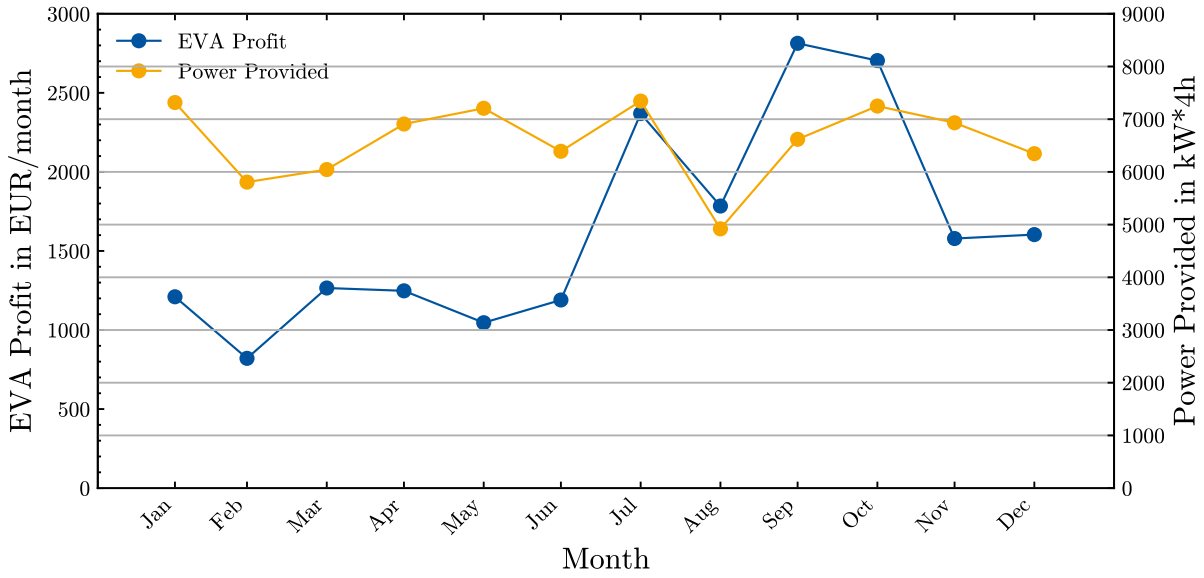

Figure 36: Monthly EVA profit and power reserved in the ME scenario

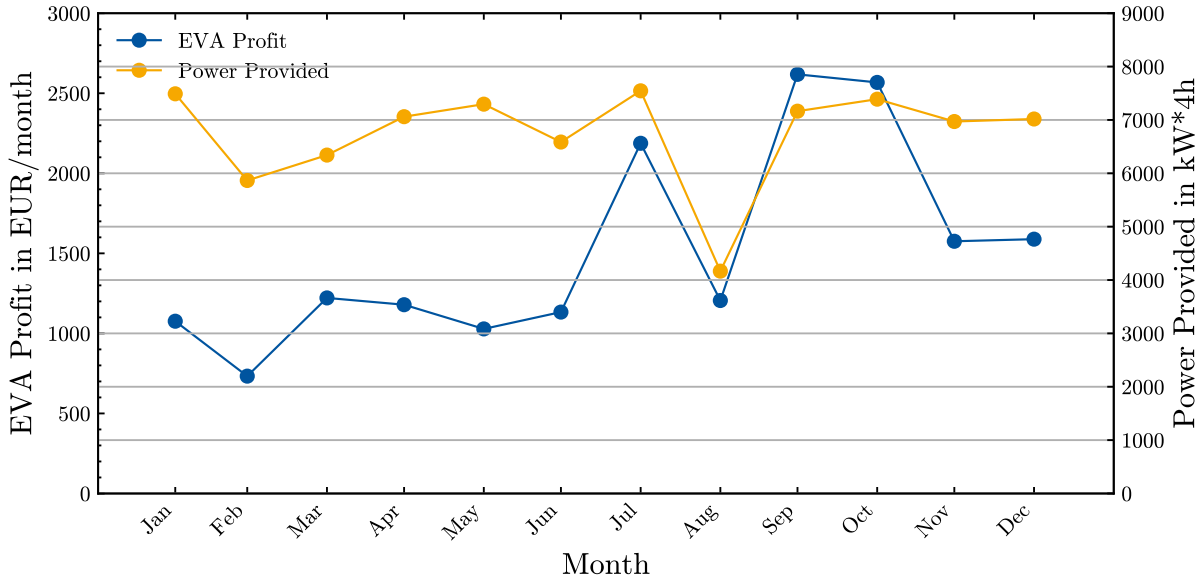

Figure 37: Monthly EVA profit and power reserved in the LE scenario

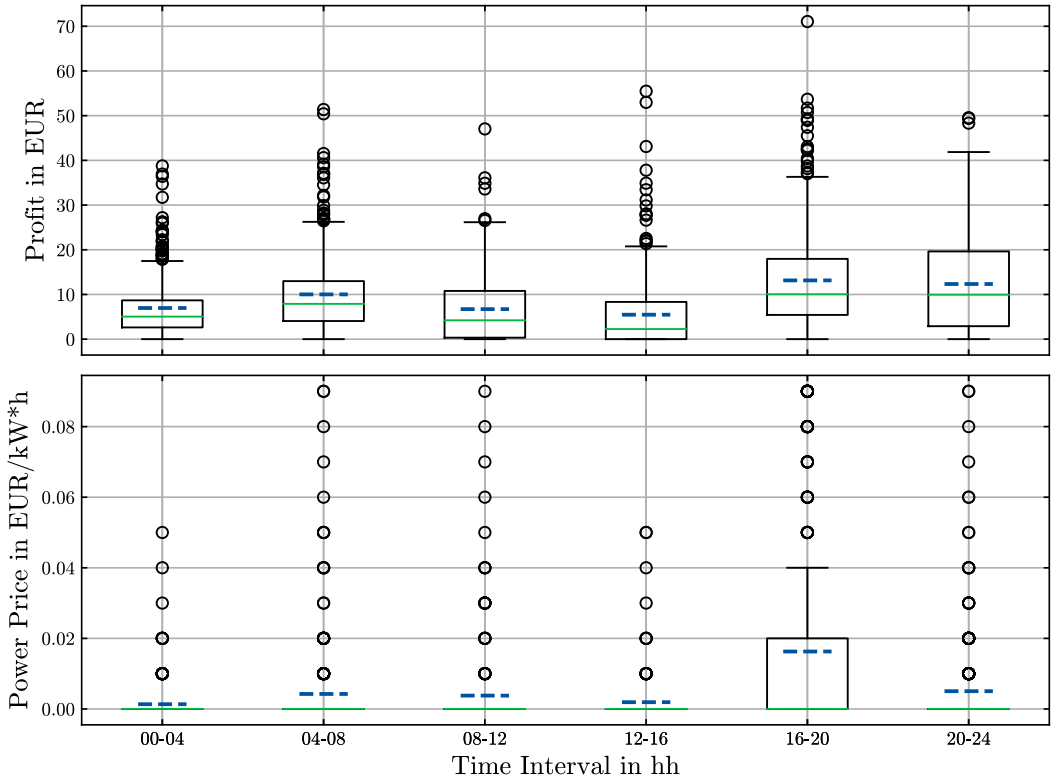

Figure 38: Boxplot of EVA profit and power price for time slots for the HE scenario

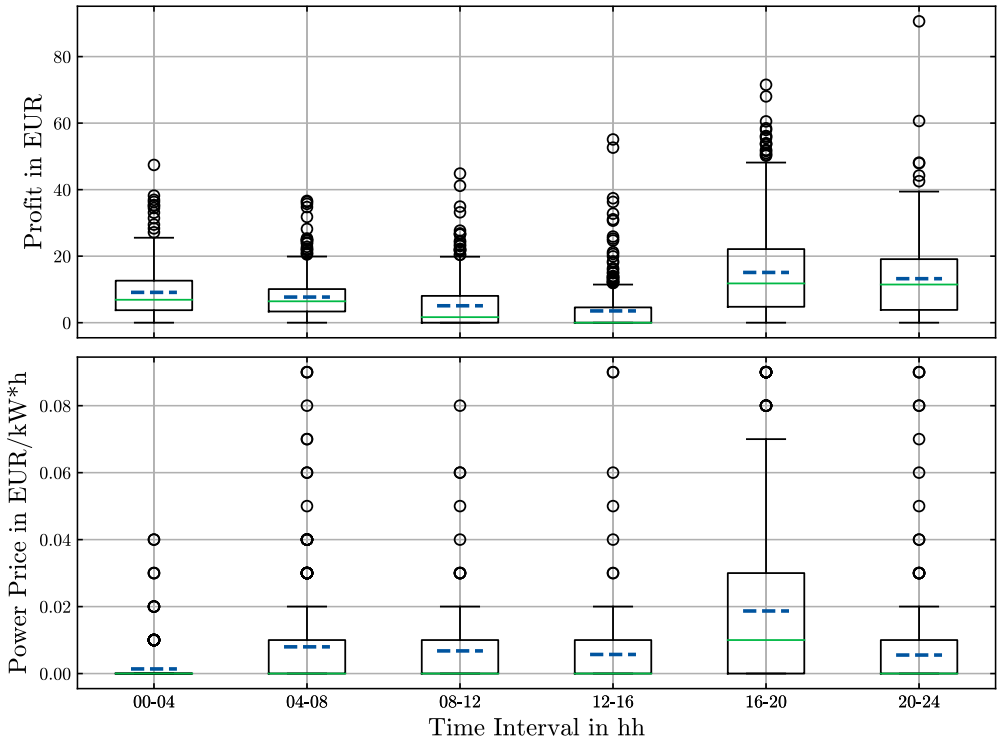

Figure 39: Boxplot of EVA profit and power price for time slots for the LE scenario

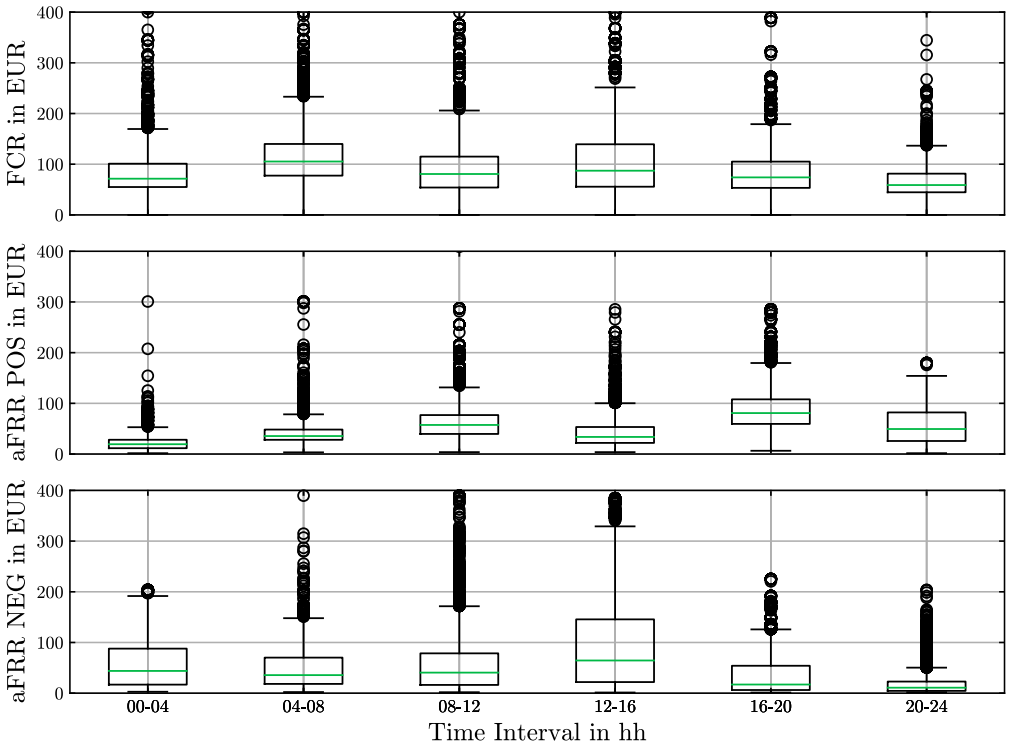

Figure 40: Boxplot of power prices for aFRR and FCR in 2022

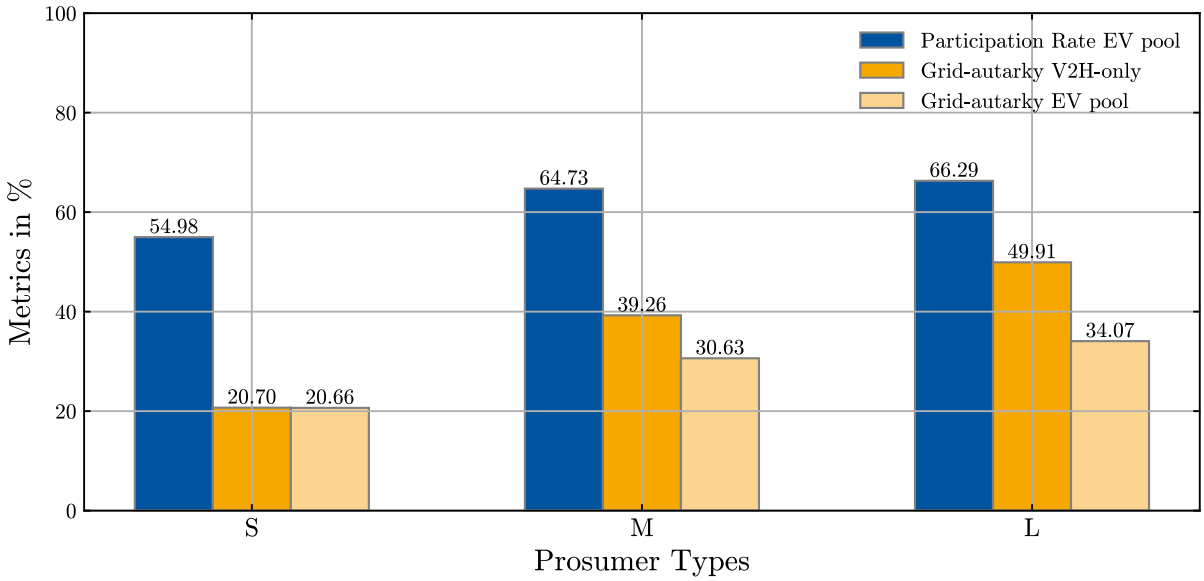

Figure 41: Participation rate and grid-autarky for LE scenario

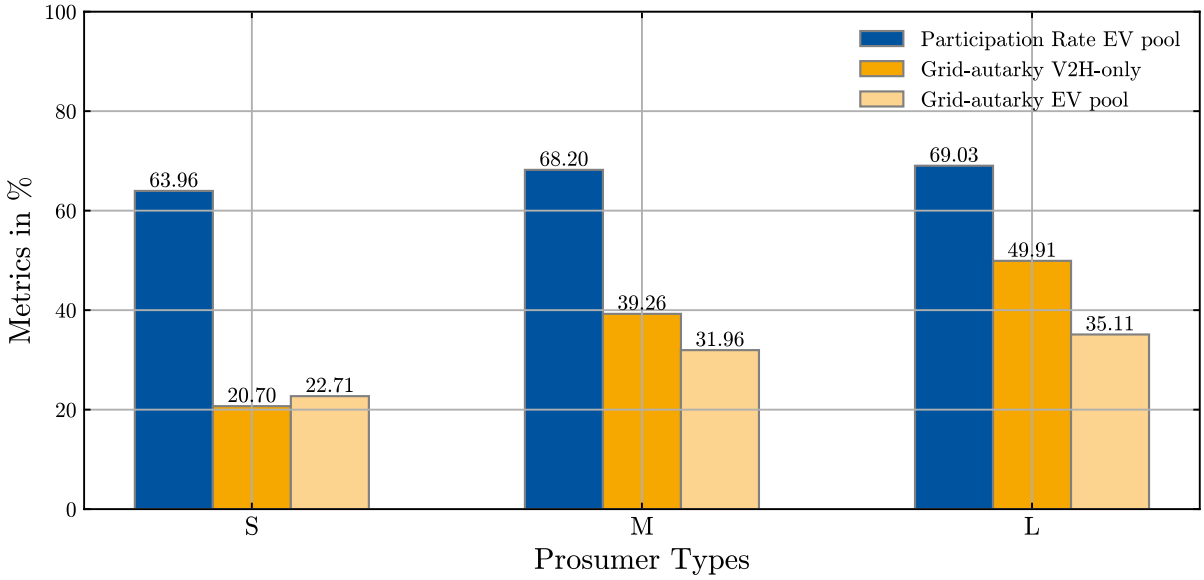

Figure 42: Participation rate and grid-autarky for HE scenario

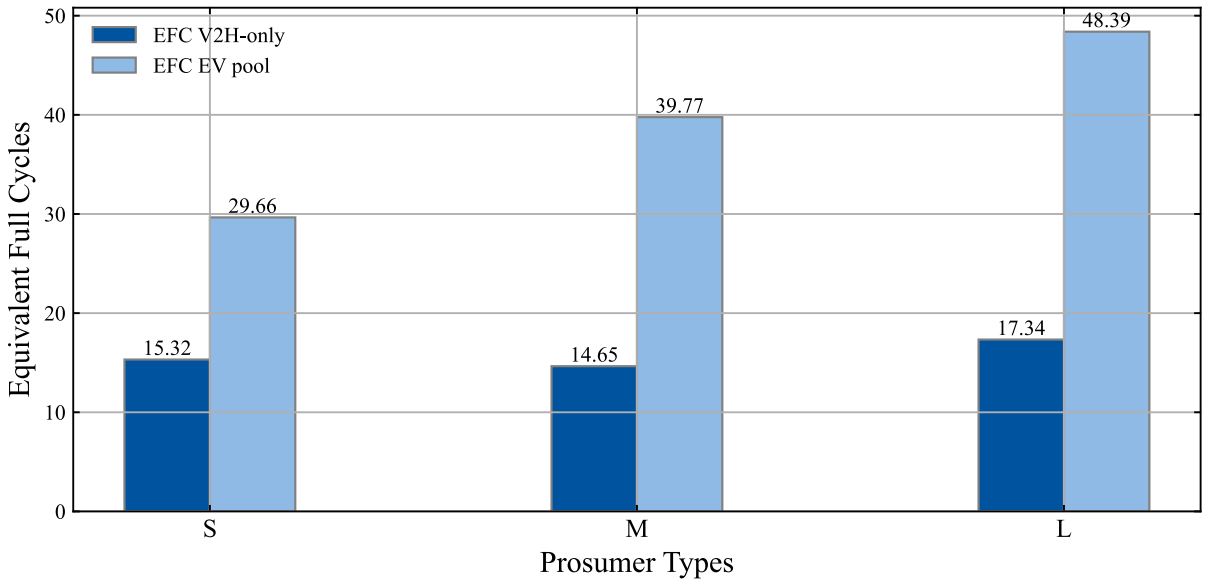

Figure 43: EFC for each prosumer type for LE scenario

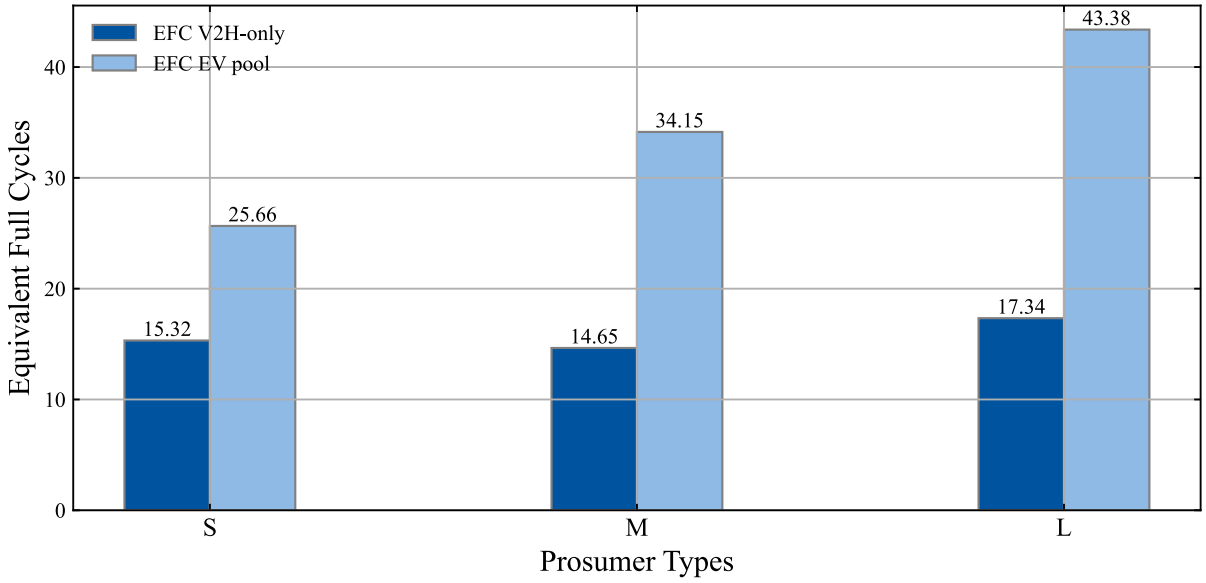

Figure 44: EFC for each prosumer type for LE scenario

Glossary

AFRR	Automatic frequency restoration reserve
BSP	Balancing Service Provider
CET	Central European Time
DSO	Distribution System operator
EFC	Equivalent full cycle
EMS	Energy management system
EV	Electric Vehicle
EVA	Electric Vehicle Aggregator
EVC	Electric Vehicle Charger
FCR	Frequency containment restoration
KKT	Karush-Kuhn-Tucker
LL	Lower Level
LP	Linear Problem
MCP	Market clearing price
MILP	Mixed-Integer-Linear Problem
MOL	Merit Order List
MW	Mega Watt
NLP	Non-Linear Problem
OTC	Over the counter
PDF	Probability density function
PV	Photovoltaic
RH	Rolling Horizon
RR	Restoration reserve
SBG	Stackelberg game
SMT	Spot Market Trading
SOC	State of Charge
ST	Static tariff
TOU	Time-of-Use
TSO	Transmission System operator
UL	Upper Level

V2G	Vehicle-to-Grid
V2H	Vehicle-to-Home
V2X	Vehicle-to-X (everything)
VAT	Value added Taxes
IR	instantaneous reserve
KWP	Kilo watt peak

References

[1] Bundesregierung Deutschland, Generationenvertrag für das Klima, [March 25, 2024], https://www.bundesregierung.de/breg-de/schwerpunkte/klimaschutz/klimaschutzgesetz-2021-1913672.pdf.
[2] Statistisches Bundesamt, Pressemitteilung Nr. 087 vom 7. März 2024, [March 25, 2024], https://www.destatis.de/DE/Presse/Pressemitteilungen/2024/03/PD24_087_43312.html.
[3] Bundesregierung Deutschland, Mehr Energie aus erneuerbaren Quellen, https://www.bundesregierung.de/breg-de/schwerpunkte/klimaschutz/energiewende-beschleunigen-2040310.
[4] Umweltbundesamt, Klimaschutz im Verkehr, [March 25, 2024], https://www.umweltbundesamt.de/themen/verkehr/klimaschutz-im-verkehr#ziele.
[5] FFE, Der Smart Meter Rollout in Deutschland und Europa, https://www.ffe.de/veroeffentlichungen/smart-meter-rollout-in-deutschland-und-europa/.
[6] W. Kempton, J. Tomić, Vehicle-to-grid power fundamentals: Calculating capacity and net revenue, Journal of Power Sources 144 (2005) 268–279.
[7] S. Englberger, K. Abo Gamra, B. Tepe, M. Schreiber, A. Jossen, H. Hesse, Electric vehicle multi-use: Optimizing multiple value streams using mobile storage systems in a vehicle-to-grid context, Applied Energy 304 (2021) 117862.
[8] F. Rücker, M. Merten, J. Gong, R. Villafáfila-Robles, I. Schoeneberger, D.U. Sauer, Evaluation of the Effects of Smart Charging Strategies and Frequency Restoration Reserves Market Participation of an Electric Vehicle, Energies 13 (2020) 3112.
[9] EpexSpot, Become a member, [March 25, 2024], https://www.epexspot.com/en/becomeamember.
[10] M. Nazari-Heris, M. Abapour, B. Mohammadi-Ivatloo, An Updated Review and Outlook on Electric Vehicle Aggregators in Electric Energy Networks, Sustainability 14 (2022) 15747.
[11] Entso-e, Frequency Containment Reserves, [March 25, 2024], https://www.entsoe.eu/network_codes/eb/fcr/.
[12] M. Adil, M.P. Mahmud, A.Z. Kouzani, S. Khoo, Energy trading among electric vehicles based on Stackelberg approaches: A review, Sustainable Cities and Society 75 (2021) 103199.
[13] S.S. Amiri, J.C. do Prado, F.R. Bin Karim, P.C. Lopes Gerum, Participation of Electric Vehicle Aggregators in Wholesale Electricity Markets: Recent Works and Future Directions, in: 2023 IEEE Belgrade PowerTech: June 25-29, 2023, Belgrade, Serbia, Belgrade, Serbia, 2023, pp. 1–6.
[14] W. Liu, S. Chen, Y. Hou, Z. Yang, Optimal Reserve Management of Electric Vehicle Aggregator: Discrete Bilevel Optimization Model and Exact Algorithm, IEEE Trans. Smart Grid 12 (2021) 4003–4015.
[15] J. Vuelvas, F. Ruiz, G. Gruosso, A time-of-use pricing strategy for managing electric vehicle clusters, Sustainable Energy, Grids and Networks 25 (2021) 100411.
[16] S. Sharma, P. Jain, R. Bhakar, P.P. Gupta, Time of Use Price based Vehicle to Grid Scheduling of Electric Vehicle Aggregator for Improved Market Operations, in: International Conference on Innovative Smart Grid Technologies (ISGT Asia 2018): 22-25 May 2018, Singapore, Singapore, 2018, pp. 1114–1119.

[17] D. Liu, W. Wang, L. Wang, H. Jia, M. Shi, Dynamic Pricing Strategy of Electric Vehicle Aggregators Based on DDPG Reinforcement Learning Algorithm, IEEE Access 9 (2021) 21556–21566.
[18] Y. Vardanyan, H. Madsen, Stochastic Bilevel Program for Optimal Coordinated Energy Trading of an EV Aggregator, Energies 12 (2019) 3813.
[19] Q. Wang, C. Huang, C. Wang, K. Li, N. Xie, Joint optimization of bidding and pricing strategy for electric vehicle aggregator considering multi-agent interactions, Applied Energy 360 (2024) 122810.
[20] X. Dong, X. Wei, G. Zu, Y. Ma, X. Yu, Y. Mu, The charge-discharge compensation pricing strategy of electric vehicle aggregator considering users response willingness from the perspective of Stackelberg game, IET Smart Grid (2023).
[21] J. Gong, Y. Nie, J. van Ouwerkerk, F. Wege, M.C. Cortés, C. von Oy et al., FOCUS A framework for energy system optimization from prosumer to district and city scale, 2023.
[22] Bmwk, Ein Stromnetz für die Energiewende, [July 22, 2024], https://www.bmwk.de/Redaktion/EN/Publikationen/whitepaper-electricity-market.pdf?__blob=publicationFile&v=1.
[24] H.-W. Schiffer, Energiemarkt Deutschland: Daten und Fakten zu konventionellen und erneuerbaren Energien, Springer Vieweg, Wiesbaden, 2019.
[25] Müncon, The German Electricity Market - simplified, [March 21, 2024], https://muencon.com/2022/09/20/the-german-electricity-market-simplified/.
[26] Bmwk, Wie funktioniert eigentlich der Strommarkt?, [June 17, 2024], https://www.bmwk-energiewende.de/EWD/Redaktion/Newsletter/2020/06/Meldung/direkt-erklaert.html.
[27] Dr.-Ing. Eglantine Künle, Philipp Theile, Dr.-Ing. Christian Wagner, Entwicklung der Momentanreserve und Abschätzung des Bedarfes an Fast Frequency Response im Europäischen Verbundsystem, [July 22, 2024], https://www.ewi.uni-koeln.de/cms/wp-content/uploads/2019/12/Momentanreserve_und_FFR.pdf.
[28] NextKraftwerke, What are Balancing Services?, [June 19, 2024], https://www.next-kraftwerke.com/knowledge/balancing-services.
[29] Entso-e, Supporting Document for the Network Code on Load-Frequency Control and Reserves, [July 23, 2024], https://www.entsoe.eu/fileadmin/user_upload/_library/resources/LCFR/130628-NC_LFCR-Supporting_Document-Issue1.pdf.
[30] Enefirst, USING TIME-OF-USE TARIFFS TO ENGAGE CUSTOMERS AND BENEFIT THE POWER SYSTEM, https://enefirst.eu/wp-content/uploads/1_Using-ToU-Time-of-Use-tariffs-to-engage-consumers-and-benefit-the-power-system.pdf.
[31] IRENA, Innovation landscape brief: Time-of-use tariffs, Abu Dhabi.
[32] ADAC, Autostromtarife: Das E-Auto günstig zu Hause laden, https://www.adac.de/rund-ums-fahrzeug/elektromobilitaet/laden/autostrom-tarife/#was-genau-ist-ein-autostromtarif.
[33] Bundesnetzagentur, Preisbestandteile und Tarife, https://www.bundesnetzagentur.de/DE/Vportal/Energie/PreiseAbschlaege/Tarife-table.html.
[34] Westnetz GmbH, vorläufige Preisblätter WESTNETZ Strom 2023-01-01, https://www.westnetz.de/content/dam/revu-global/westnetz/documents/ueber-westnetz/unser-netz/netzentgelte-strom/vorl%C3%A4ufige-preisbl%C3%A4tter-strom-2023-01-01-inkl-ka.pdf.
[35] Lanenergie, EEG 2023 - Einspeisevergütung, https://www.maschinenring.de/eeg-2023.

[36] Nationale Leitstelle Ladeinfrastruktur, Bidirektionales Laden diskriminierungsfrei ermöglichen: Handlungsempfehlungen des Beirats der Nationalen Leitstelle Ladeinfrastruktur zur Umsetzung der Maßnahme 47 des Masterplans Ladeinfrastruktur II, https://bmdv.bund.de/SharedDocs/DE/Pressemitteilungen/2024/013-kluckert-elektroautos-als-stromspeicher.html.
[37] Bundesnetzagentur, Großhandelpreise, [March 22, 2024], https://www.smard.de/page/home/wiki-article/446/562.
[38] EpexSpot, Basics of the Power Market, [March 22, 2024], https://www.epexspot.com/en/basicspowermarket.
[39] FFE, German electricity prices on EPEX Spot 2023, [March 22, 2024], https://www.ffe.de/en/publications/german-electricity-prices-on-epex-spot-2023/.
[40] German TSO´s, Regelleistung.net, [July 20, 2024], https://www.regelleistung.net/de-de/.
[41] B. Thormann, W. Purgstaller, T. Kienberger, EVALUATING THE POTENTIAL OF FUTURE E-MOBILITY USE CASES FOR PROVIDING GRID ANCILLARY SERVICES, in: CIRED 2021 - The 26th International Conference and Exhibition on Electricity Distribution, Online Conference, 2021, pp. 1752–1756.
[42] J. Figgener, B. Tepe, F. Rücker, I. Schoeneberger, C. Hecht, A. Jossen et al., The influence of frequency containment reserve flexibilization on the economics of electric vehicle fleet operation, Journal of Energy Storage 53 (2022) 105138.
[43] German TSOs, Frequency Containment Reserve, [April 01, 2024], https://www.regelleistung.net/en-us/General-info/Types-of-control-reserve/Frequency-Containment-Reserve.
[44] Nano energies, Frequency Control Reserve (FCR), [July 23, 2024], https://nanoenergies.eu/knowledge-base/frequency-control-reserve-fcr.
[45] Frequency Containment Reserves, [April 01, 2024], https://www.entsoe.eu/network_codes/eb/fcr/#contacts.
[46] F. Nitsch, M. Deissenroth-Uhrig, C. Schimeczek, V. Bertsch, Economic evaluation of battery storage systems bidding on day-ahead and automatic frequency restoration reserves markets, Applied Energy 298 (2021) 117267.
[47] NextKraftwerke, aFRR, [April 01, 2024], https://www.next-kraftwerke.com/knowledge/afrr.
[48] NextKraftwerke, Sekundarregelleistungen, [August 02, 2024], https://www.next-kraftwerke.de/wissen/sekundaerreserve.
[49] German TSOs, Präqualifikationsverfahren für Regelreserveanbieter (FCR, aFRR, mFRR) in Deutschland, [April 01, 2024], https://www.regelleistung.net/xspproxy/api/staticfiles/regelleistung/pqbedingungen(stand03.06.2022).pdf.
[50] INNOVATION outlook Smart charging for electric vehicles, IRENA, Abu Dhabi, 2019.
[51] Hans de Heer, Marten van der Laan, Aurora Sáez Armenteros, USEF: THE FRAMEWORK EXPLAINED, [April 03, 2024], https://www.usef.energy/app/uploads/2021/05/USEF-The-Framework-Explained-update-2021.pdf.
[52] S. Islam, A. Iqbal, M. Marzband, I. Khan, A.M. Al-Wahedi, State-of-the-art vehicle-to-everything mode of operation of electric vehicles and its future perspectives, Renewable and Sustainable Energy Reviews 166 (2022) 112574.

[53] A. Kampker, H.H. Heimes (Eds.), Elektromobilität: Grundlagen einer Fortschrittstechnologie, 3. Aufl. 2024, Springer Berlin Heidelberg, Berlin, Heidelberg, 2024.
[54] I.A. Umoren, M.Z. Shakir, Electric Vehicle as a Service (EVaaS): Applications, Challenges and Enablers, Energies 15 (2022) 7207.
[55] M.H.S.M. Haram, J.W. Lee, G. Ramasamy, E.E. Ngu, S.P. Thiagarajah, Y.H. Lee, Feasibility of utilising second life EV batteries: Applications, lifespan, economics, environmental impact, assessment, and challenges, Alexandria Engineering Journal 60 (2021) 4517–4536.
[56] R. Korthauer (Ed.), Handbuch Lithium-Ionen-Batterien, Springer Vieweg, Berlin, Heidelberg, 2013.
[57] J. Gong, D. Wasylowski, J. Figgener, S. Bihn, F. Rücker, F. Ringbeck et al., Quantifying the impact of V2X operation on electric vehicle battery degradation: An experimental evaluation, eTransportation 20 (2024) 100316.
[58] M.S. Mastoi, S. Zhuang, H.M. Munir, M. Haris, M. Hassan, M. Usman et al., An in-depth analysis of electric vehicle charging station infrastructure, policy implications, and future trends, Energy Reports 8 (2022) 11504–11529.
[59] ADAC, Elektroauto laden: Das sind die Voraussetzungen zuhause und unterwegs, [April 03, 2024], https://www.adac.de/rund-ums-fahrzeug/elektromobilitaet/laden/faq-elektroauto-laden/.
[60] R. Luthander, J. Widén, D. Nilsson, J. Palm, Photovoltaic self-consumption in buildings: A review, Applied Energy 142 (2015) 80–94.
[61] ADAC, Das Elektroauto als Stromspeicher fürs Haus: So funktioniert bidirektionales Laden, [June 20, 2024], https://www.adac.de/rund-ums-fahrzeug/elektromobilitaet/laden/bidirektionales-laden/.
[62] D.P. Tuttle, R. Baldick, The Evolution of Plug-In Electric Vehicle-Grid Interactions, IEEE Trans. Smart Grid 3 (2012) 500–505.
[63] B. Tepe, J. Figgener, S. Englberger, D.U. Sauer, A. Jossen, H. Hesse, Optimal pool composition of commercial electric vehicles in V2G fleet operation of various electricity markets, Applied Energy 308 (2022) 118351.
[64] M.R. Sarker, Y. Dvorkin, M.A. Ortega-Vazquez, Optimal Participation of an Electric Vehicle Aggregator in Day-Ahead Energy and Reserve Markets, IEEE Trans. Power Syst. 31 (2016) 3506–3515.
[65] M.A. Ortega-Vazquez, Optimal scheduling of electric vehicle charging and vehicle-to-grid services at household level including battery degradation and price uncertainty, IET gener. transm. distrib. 8 (2014) 1007–1016.
[66] Heinrich Von Stackelberg, The Theory of Market Economy, 1952.
[67] D. Fudenberg, J. Tirole, Game theory, 14 [print.], MIT Press, Cambridge, Mass., ca. 2010.
[68] T. Li, S. P. Sethi, A review of dynamic Stackelberg game models, Discrete & Continuous Dynamical Systems - B 22 (2017) 125–159.
[69] Y. Wang, W. Saad, Z. Han, H.V. Poor, T. Basar, A Game-Theoretic Approach to Energy Trading in the Smart Grid, IEEE Trans. Smart Grid 5 (2014) 1439–1450.
[70] A. Sinha, P. Malo, K. Deb, A Review on Bilevel Optimization: From Classical to Evolutionary Approaches and Applications, 2017.

[71] S. Dempe, A.B. Zemkoho (Eds.), Bilevel optimization: Advances and next challenges, Springer, Cham, Switzerland, 2020.
[72] J.F. Bard, Practical Bilevel Optimization: Algorithms and Applications, Springer, Boston, MA, 1998.
[73] Visual Studio Code, Python in Visual Studio Code, [June 17, 2024], https://code.visualstudio.com/docs/languages/python.
[74] M. Lutz, Learning Python: Powerful object-oriented programming; covers Python 2.6 and 3.x, 4. ed., O'Reilly, Beijing, Köln, 2009.
[75] PYOMO, Pyomo Documentation 6.7.3, https://pyomo.readthedocs.io/en/stable/index.html.
[76] Gurobi Optimization, Gurobi Optimizer - The worlds fastest Solver, https://www.gurobi.com/solutions/gurobi-optimizer/.
[77] J.F. Marquant, R. Evins, J. Carmeliet, Reducing Computation Time with a Rolling Horizon Approach Applied to a MILP Formulation of Multiple Urban Energy Hub System, Procedia Computer Science 51 (2015) 2137–2146.
[78] Martin Schmidt, Yasmine Beck, A Gentle and Incomplete Introduction to Bilevel Optimization, 2023.
[79] BDEW, Standardlastprofile Strom, [July 20, 2024], https://www.bdew.de/energie/standardlastprofile-strom/.
[80] F. Jiayin, Identifying the potential of EV batteries with the multi-use operation, Master thesis at the ISEA RWTH, 2023.
[81] M. Cococcioni, L. Fiaschi, The Big-M method with the numerical infinite M, Optim Lett 15 (2021) 2455–2468.
[82] Thomas L. Paez, Introduction to Model Validation: citation from (ASME, 2006, U.S. DOE, 2000, AIAA, 1998), [July 20, 2024], https://www.osti.gov/servlets/purl/1142730.
[83] X. Li, Y. Tan, X. Liu, Q. Liao, B. Sun, G. Cao et al., A cost-benefit analysis of V2G electric vehicles supporting peak shaving in Shanghai, Electric Power Systems Research 179 (2020) 106058.
[84] Dr. Gudrun Valerius, Photovoltaik und 10-kWp-Grenze, [July 31, 2024], https://www.solaranlage-ratgeber.de/photovoltaik/photovoltaik-planung/photovoltaik-und-10-kwp-grenze.
[85] Lichtblick, Grüner ÖkoStrom für eure Nachtspeicherheizung, [July 20, 2024], https://www.lichtblick.de/waermestrom/oekostrom-nachtspeicherheizung/.
[86] EWI Cologne, Energy crisis 2022: Gas price drives electricity price to record levels, https://www.ewi.uni-koeln.de/en/aktuelles/mo-tool-2022-update/.
[87] E. Parzen, On Estimation of a Probability Density Function and Mode, vol. 33, The Annals of Mathematical Statistics, 1962.
[88] Y. Iwafune, T. Kawai, Data analysis and estimation of the conversion efficiency of bidirectional EV chargers using home energy management systems data, Smart Energy 15 (2024) 100145.